SAND2005-42364236
Unlimited Release
Printed mm 2005

Determination of the Porosity Surfaces of the Disposal Room Containing Various Waste Inventories for WIPP PA

Byoung Yoon Park
Performance Assessment and Decision Analysis Department

Francis D. Hansen
Carlsbad Programs Group

Sandia National Laboratories
P.O. Box 5800
Albuquerque, NM 87185-1395

Abstract

This report develops a series of porosity surfaces for the Waste Isolation Pilot Plant. The concept of a porosity surface was developed for performance assessment and comprises calculation of room closure as salt creep processes are mitigated by gas generation and back stress created by the waste packages within the rooms. The physical and mechanical characteristics of the waste packaging that has already been disposed--such as the pipe overpack--and new waste packaging--such as the advanced mixed waste compaction--are appreciably different than the waste form upon which the original compliance was based and approved. This report provides structural analyses of room closure with various waste inventories. All of the underlying assumptions pertaining to the original compliance certification including the same finite element code are implemented; only the material parameters describing the more robust waste packages are changed from the certified baseline. As modeled, the more rigid waste tends to hold open the rooms and create relatively more void space in the underground than identical calculations run on the standard waste packages, which underpin the compliance certification. The several porosity surfaces quantified within this report provide possible ranges of pressure and porosity for performance assessment analyses.

Intentionally blank

Acknowledgements

This research is funded by WIPP programs administered by the U.S. Department of Energy. The authors would like to acknowledge the valuable contributions to this work provided by others. Dr. Joshua S. Stein helped explain the hand off between these finite element porosity surfaces and implementation in the performance calculations. Dr. Leo L. Van Sambeek of RESPEC Inc. helped us understand the concepts of room closure under the circumstances created by a rigid waste inventory. Dr. T. William Thompson and Tom W. Pfeifle provided technical review and Mario J. Chavez provided a Quality Assurance review. The paper has been improved by these individuals.

Sandia is a multiprogram laboratory operated by Sandia Corporation, a Lockheed Martin Company, for the United States Department of Energy under Contract DE-AC04-94Al85000

Intentionally Blank

TABLE OF CONTENTS

1 INTRODUCTION 5

1.1 Objective 5
1.2 Background 5
1.3 Report Organization 5

2 ANALYSIS MODELS 5

2.1 Initial porosity 5
2.1.1 Standard waste 5
2.1.2 Pipe overpack waste 5
2.1.3 AMWTP Supercompacted waste 5
2.1.4 Combined cases 5
2.2 Gas generation potential and production rate 5
2.3 Geomechanical Models 5
2.3.1 Stratigraphy and constitutive models 5
2.3.2 Waste constitutive model 5

3 MESH GENERATION 5

3.1 Disposal Room 5
3.2 Standard waste and POP waste 5
3.3 AMWTP Waste 5
3.3.1 All AMWTP case 5
3.3.2 Combined Case I (2/3 AMWTP + 1/3 Standard Waste) 5
3.3.3 Combined Case II (1/3 AMWTP + 2/3 Standard Waste) 5

4 CALCULATION FLOW AND FILE NAMING CONVENTION 5

4.1 Computer Codes and Calculation Flow 5
4.2 File Naming Convention 5

5 ANALYSES RESULTS 5

5.1 Disposal Room Creep Closure 5
5.2 Pressure Histories 5
5.3 Porosity Histories 5
5.4 Porosity History Comparisons 5
5.5 Porosity Surface 5

6 DISCUSSION AND CONCLUDING REMARKS 5

7 REFERENCES 5

APPENDIX A: CALCULATION SHEET TO COMPUTE THE VOLUME OF EACH COMPONENT IN THE WASTE DRUM 5

A-1 12 inch-POP 5
A-2 6-inch POP 5
A-3 AMWTP Debris Waste 5

APPENDIX B: CALCULATION SHEET FOR THE INITIAL POROSITY OF THE UNDEFORMED DISPOSAL ROOM 5

B-1 12-inch POP 5
B-2 6-inch POP 5
B-3 All AMWTP waste 5
B-4 1/3 AMWTP waste and 2/3 Standard waste 5
B-5 2/3 AMWTP waste and 1/3 Standard waste 5

APPENDIX C: GAS GENERATION POTENTIAL AND RATE 5

C-1 Standard Waste and POP Waste 5
C-2 1/3 AMWTP and 2/3 Standard Waste 5
C-3 2/3 AMWTP and 1/3 Standard Waste 5
C-4 All AMWTP Waste 5

APPENDIX D: HEIGHT OF THE AMWTP MODEL IN THE DISPOSAL ROOM 5

APPENDIX E: MODIFIED WIDTH AND LENGTH OF THE WASTE 5

E-1 All AMWTP Waste Case 5
E-2 2/3 AMWTP + 1/3 Standard Waste Case 5
E-3 1/3 AMWTP and 2/3 Standard Waste Case 5

APPENDIX F: POROSITY CALCULATION FOR THE PUCK PART 5

APPENDIX G: SAMPLE FASTQ FILE (2/3 AMWTP+1/3STANDARD CASE) 5

APPENDIX H: SAMPLE AWK SCRIPT TO CALCULATE THE POROSITY CHANGE IN THE ROOM WITH TIME (ALL AMWTP CASE) 5

APPENDIX I: SAMPLE SANTOS INPUT FILE 5

I-1: 12-inch POP 5
I-2: All AMWTP 5

APPENDIX J: SAMPLE USER SUBROUTINES (ALL AMWTP WITH F=0.1) 5

J-1 Initial Stress State 5
J-2 Adaptive Pressure Boundary Condition 5

APPENDIX K: COMPARISON BETWEEN POROSITY HISTORIES FOR THE DISPOSAL ROOM CONTAINING VARIOUS WASTE INVENTORIES 5

APPENDIX L: CALCULATION OF POROSITY SURFACES USED IN THE AMW PA 5

L-1 Overview 5
L-2 File Naming Convention 5
L-3 Results 5

LIST OF TABLES

Table 1: WIPP CH-TRU Waste Material Parameter Disposal Inventory (Butcher, 1997) .5
Table 2: The available data for characterizing the waste in the 12-inch pipe over pack.....5
Table 3: Material properties of each component for the 12-inch POP 5
Table 4: Material properties of each component for the 6-inch POP 5
Table 5: Material properties of each component for AMWTP waste 5
Table 6: Total gas potential and gas production rates for each waste configuration. 5
Table 7: SANTOS input constants for POP waste constitutive model (Park and Hansen, 2004) 5
Table 8: Directory descriptions for porosity surface calculations 5
Table 9: File naming convention for porosity surface calculations (* means wild card) 5

LIST OF FIGURES

Figure 1: Various waste packages 5
Figure 2: AMWTP pucks produced by supercompaction of 55-gallon drums of debris waste 5
Figure 3: Illustration of waste containers and waste configuration 5
Figure 4: Simplified outline drawing of the 100-gallon container and supercompacted waste 5
Figure 5: Combined cases included supercompacted waste 5
Figure 6: Histories of gas generation potential used for the disposal room analyses, f=1.0 5
Figure 7: Stratigraphic model for the current level of the disposal room 5
Figure 8: Simulated volumetric strain for POP compared to the standard 55-gal drum (Park and Hansen, 2004) 5
Figure 9: Mesh discretization and boundary conditions around the disposal room 5
Figure 10: Meshes for various waste package inventories in the disposal room 5
Figure 11: Ideal packing of 100-gallon containers in rooms 5
Figure 12: Rearrangement of containers for all AMWTP waste by the inward movement of the walls 5
Figure 13: Concept separating pucks and container for mesh generation 5
Figure 14: Representation of pucks and containers for a room filled with supercompacted AMWTP. 5
Figure 15: 2/3 AMWTP and 1/3 Standard waste are placed in the room 5
Figure 16: The AMWTP containers are rearranged by the inward movement of the walls 5
Figure 17: Representation of pucks and containers for a room containing 2/3 AMWTP and 1/3 standard waste packages. 5
Figure 18: Emplacement of 1/3 AMWTP and 2/3 Standard waste in the disposal room 5
Figure 19: The AMWTP containers are rearranged by the inward movement of the walls 5
Figure 20: Idealized array separating incompressible and compressible materials for mesh generation 5
Figure 21: Computational flowchart to determine the porosity surface 5
Figure 22: Close-up views of the deformed disposal room containing the standard waste for f=0.0 5
Figure 23: Close-up views of the deformed disposal room containing the 6-inch POP waste for f=0.0 5
Figure 24: Close-up views of the deformed disposal room containing the 12-inch POP waste for f=0.0 5
Figure 25: Close-up views of the deformed disposal room containing the 1/3 AMWTP + 2/3 Standard waste for f=0.0 5
Figure 26: Close-up views of the deformed disposal room containing the 2/3 AMWTP + 1/3 Standard waste for f=0.0 5
Figure 27: Close-up views of the deformed disposal room containing the All AMWTP waste for f=0.0 5
Figure 28: Pressure histories for a disposal room containing the standard waste 5
Figure 29: Pressure histories for a disposal room containing the 6-inch POP waste 5
Figure 30: Pressure histories for a disposal room containing the 12-inch POP waste 5

Figure 31: Pressure histories for disposal room a containing the 1/3 AMWTP + 2/3 Standard waste 5
Figure 32: Pressure histories for disposal room a containing the 2/3 AMWTP + 1/3 Standard waste 5
Figure 33: Pressure histories for a disposal room containing the AMWTP waste 5
Figure 34: Porosity histories for a disposal room containing the standard waste 5
Figure 35: Porosity histories for a disposal room containing the 6-inch POP waste 5
Figure 36: Porosity histories for a disposal room containing the 12-inch POP waste 5
Figure 37: Porosity histories for a disposal room containing 1/3 AMWTP+2/3 standard waste 5
Figure 38: Porosity histories for a disposal room containing 2/3 AMWTP+1/3 Standard waste 5
Figure 39: Porosity histories for a disposal room containing all AMWTP waste 5
Figure 40: Comparison between porosity histories for the disposal room containing various waste inventories, f=0.0 5
Figure 41: Comparison between porosity histories for the disposal room containing various waste inventories, f=0.4 5
Figure 42: Comparison between porosity histories for the disposal room containing various waste inventories, *f*=1.0 5
Figure 43: Comparison between porosity histories for the disposal room containing various waste inventories, f=2.0 5
Figure 44: Porosity surface for the room containing the standard waste 5
Figure 45: Porosity surface for the room containing the 12-inch POP waste 5
Figure 46: Porosity surface for the room containing the 6-inch POP waste 5
Figure 47: Porosity surface for the room containing the AMWTP waste 5
Figure 48: Porosity surface for the room containing 2/3 AMWTP + 1/3 standard waste ...5
Figure 49: Porosity surface for the room containing 1/3 AMWTP + 2/3 standard waste ...5

ACRONYMS

AMWTP	Advanced Mixed Waste Treatment Project
BRAGFLO	Brine And Gas FLOw (a numerical model)
CCA	Compliance Certification Application
CFR	Code of Federal Regulations
CPR	Cellulosics, Plastics, and Rubber
CRA	Compliance Recertification Application
CH-TRU	Contact-Handled Transuranic
DOE	U.S. Department of Energy
EPA	U.S. Environmental Protection Agency
FEM	Finite Element Method
FEPs	Feature, Events, and Processes
INEEL	Idaho National Environmental Engineering Laboratory
PA	Performance Assessment
PAVT	Performance Assessment Verification Test
POP	Pipe OverPack
SNL	Sandia National Laboratories
TDOP	Ten Drum Over Pack
TRU	Transuranic Waste
TWBID	TRU Waste Baseline Inventory Database
WIPP	Waste Isolation Pilot Plant
WTS	Washington TRU Solutions
WWIS	WIPP Waste Information System

1 INTRODUCTION

Objective

In 1996, the U.S. Department of Energy (DOE) completed a performance assessment (PA) for the Waste Isolation Pilot Plant (WIPP). The performance assessment was part of the Compliance Certification Application (CCA) (DOE, 1996) submitted to the U.S. Environmental Protection Agency (EPA) to demonstrate compliance with the long-term disposal regulations in 40 Code of Federal Regulations (CFR) 191 (Subparts B and C) and the compliance criteria in 40 CFR 194. In 1997, EPA required a verification of the calculations performed for the CCA, termed the Performance Assessment Verification Test (PAVT). On the basis of these submittals, WIPP was certified for operations. Since March 1999 the DOE has disposed of radioactive waste at WIPP in accordance with provisions of compliance certification.

One provision of the certification itself is a requirement for recertification on a five-year interval. The compliance recertification application (CRA) includes analyses of conditions that depart from the bases underlying the original certification. This requirement was imposed in recognition that operations of the repository are likely to change from the baseline conditions underpinning the original certification. In fact, this provision was prescient, as several features of operations have changed from the original certification. Performance assessment is charged with the responsibility of evaluating the consequences of these changes. One example is implementation of the Option D panel closure system in PA and evaluating the performance impact of panel closures that are less permeable than the panel closure modeled for the original compliance certification. This document examines other actual and potential changes in disposal operations that are substantially different from the compliance basis: These are the structural/mechanical impacts to room closure and porosity surfaces created by the waste packages actually placed in the underground as well as waste packaging proposed for delivery to the WIPP for disposal. The planning basis for the analysis of these changes was provided in earlier documentation (Hansen et al., 2003b).

The compliance certification of WIPP was predicated on many assumptions, including mechanical properties of the waste. In the original compliance calculations the *standard waste form* comprised a 55-gallon drum filled with waste, as illustrated in Figure 1A. In practice, the actual inventory disposed in Panel 1 includes a significant proportion of 55-gallon drums containing an interior stainless steel pipe, illustrated in Figure 1B. This packaging is called the pipe overpack or POP. The POP waste package has been shown to be much more rigid than the baseline waste package (Park and Hansen, 2004). From the WIPP waste information system (WWIS) dated July 29, 2003, there are 39,415 total containers in Panel 1, of which 16,989 are POPs. It is also anticipated that very few, if any, additional POPs will be shipped in the future. Another notable example of a possible future waste package includes super-compacted wastes from the Advanced Mixed Waste Treatment Project (AMWTP), illustrated schematically in Figure 1C. The AMWTP supercompacted waste includes highly compressed 55-gallon drums, which are subsequently placed in a 100-gallon drum. The supercompacted drums are called "pucks" because they are dense disks compressed to stress levels approaching 60 MPa, a

factor of four times greater than lithostatic stresses extant in the WIPP salt (15 MPa). Another waste form that has been received at WIPP is the ten drum overpack (TDOP), illustrated in Figure 1D. It is anticipated that additional forms of packaging will eventuate over the disposal operational life of the repository. In this analysis, focus is given to the POP and AMWTP waste packages, as they represent the most significant structural differences to the standard package. It is estimated that the TDOP response would also be more rigid than the standard drums, but less rigid than the POP or AMWTP packages. To capture the maximal variation in possible porosity surfaces, emphasis is given here to the POP and AMWTP supercompacted waste packages.

Both waste package configurations--POPs and AMWTP--are structurally more rigid than a typical 55-gallon waste drum, and may affect repository processes. If groups of the super-compacted AMWTP waste or the wastes in POPs are stored in the rooms they would create stiff columns and influence creep closure. This effect would be reflected in the porosity surface look-up table accessed for performance assessment calculations. An evaluation of the porosity surfaces resulting from placement of these waste forms is the subject of this report.

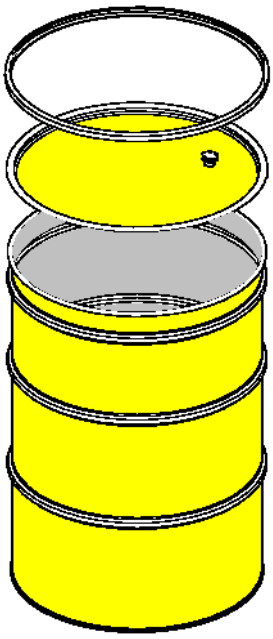

A. 55-Gallon Drum

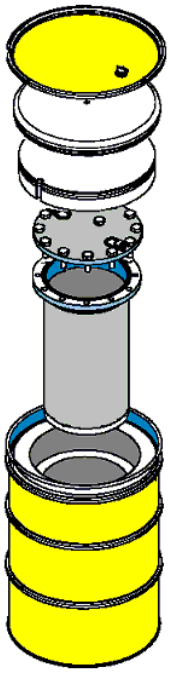

B. Pipe Overpack within a 55-Gallon Drum

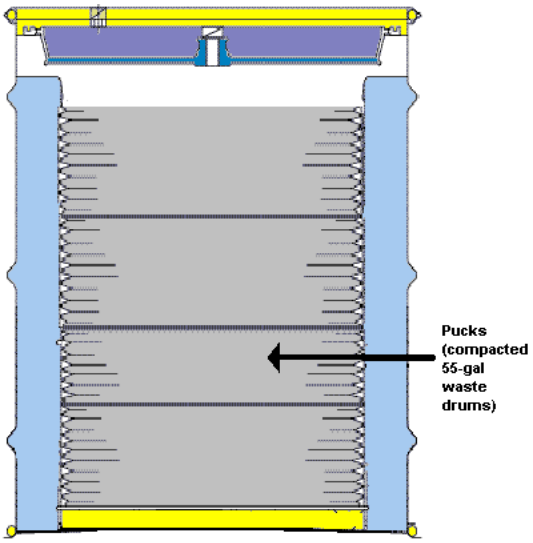

C. AMWTP Compressed Pucks in 100-Gallon Drum

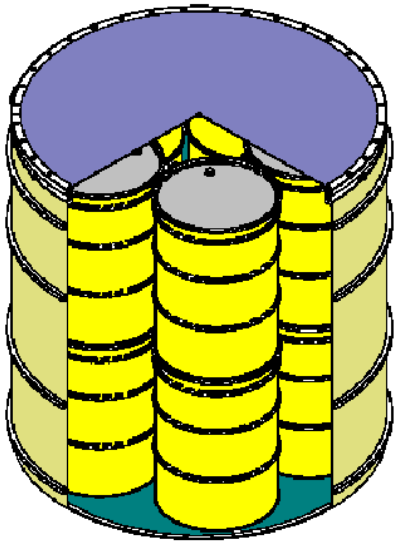

D. Ten Drum Overpack (TDOP)

Figure 1: Various waste packages

Background

The structural response of the WIPP underground setting has been modeled many times over the years. The conceptual model for room closure describes salt creep into a disposal room, in which the rock salt impinges on the waste and compresses the waste until stress equilibrium is approached. The geomechanical response of the WIPP salt and other lithologies in proximity to the rooms is well understood and validated by decades of full-scale experiments as well as continuous monitoring during the emplacement period. Thus, the essential elements of disposal room behavior and closure modeling that are different today than at the time of the original certification involve the constitutive properties of the inventory residing within the rooms.

Geomechanical response of the underground is coupled with waste deformation. Prior to submittal of the original certification application, an empirical model was developed from stress-deformation experiments on surrogate waste in 55-gallon drums (Butcher et al., 1991). From the laboratory data, a volumetric plasticity representation was developed and used for room closure calculations and subsequent creation of the porosity surfaces, which are accessed as a look-up table in performance assessment calculations. Because the actual waste placed in WIPP to date and proposed future shipments of waste to WIPP include packaging that differs appreciably from the standard 55-gallon drums, new analyses are required to assess the impact of possibly more robust and durable waste forms. No laboratory experiments were conducted on the new waste forms as had been conducted on 55-gallon drums. However, sufficient engineering information is available to develop credible response models for the POP and AMWTP waste packages.

Volumetric plasticity model parameters for the POP waste packages were developed in a series of finite element simulations (Park and Hansen, 2004). Design drawings of the POP had exact dimensions and material properties of the composite elements were known precisely. The pipe overpack within the 55-gallon drum and the other packing material were accurately represented in axisymmetry using the finite strain code called SANTOS (Stone, 1997b). Laboratory tests for uniaxial, triaxial and hydrostatic stress conditions were simulated to compute model parameters for the POP waste configurations. Parameters for the waste constitutive model, such as shear modulus, bulk modulus, deviatoric yield surface constants, and a pressure-volumetric strain function were determined (Park and Hansen, 2004). Essentially, the POP is approximately ten times stiffer than the standard waste packages.

The model for the supercompacted AMWTP waste package will be described in detail in the analysis of Section 3.3. Basically, the model of an individual AMWTP package comprises three components: pucks, outer drum, and an annulus. The annular space and the 100-gallon drum lining offer little resistance to room closure. On the other hand, the compressed pucks resting inside the drum are very rigid and dense. The supercompaction process applies approximately 60 MPa (9,000 psi) to compress the initially 55-gallon drums into the so-called pucks. The maximal *in situ* stress at WIPP is 15 MPa (2,150 psi). Even accounting for tributary loading, which could load rigid waste columns above 15 MPa, it is not probable that the supercompacted waste will be further deformed by salt

compaction. Although it is a minor consideration for the calculation of initial porosity in the room, the pucks are assumed to have zero porosity.

In performance assessment calculations, room closure initially proceeds as if the room were open. The free air space is eliminated early by creep closure without resistance from the waste packages. Eventually the salt contacts the top of the waste stacks and deforms the room inventory. Modeling room closure onward from the moment the country rock contacts the waste packages requires implementation of an appropriate response model for the waste. Simultaneously, the conceptual models for corrosion and gas generation allow internal pressure to build within the room. It should be noted that waste mechanical properties are not adjusted to account for degradation or other processes. The room closure owing to salt creep is modified by the structural response of the waste and by gas generation. These competing conditions (creep closure, waste package rigidity, gas generation) yield porosity histories for each waste package configuration, which are compiled into a porosity surface.

The uncertainty in the future placement of the waste requires structural calculations for a variety of waste configurations. Waste configurations were chosen to capture a wide range of combinations of porosity and waste rigidity. Based on analyses completed prior to the current work (Stone, 1997a; Park and Hansen, 2004) general characteristics of the waste packages can be summarized in terms of rigidity and porosity. The standard 55-gallon drums have high porosity and little rigidity, the POPs have high porosity and high rigidity and the AMWTP packages have low porosity and high rigidity. To ensure models evaluated here cover the full range of possibilities, room closure calculations are conducted for six configurations of waste:

1. All standard waste (55-gallon drums)
2. All 6-inch POPs
3. All 12-inch POPs
4. A mix of 1/3 supercompacted waste and 2/3 standard waste
5. A mix of 2/3 supercompacted waste and 1/3 standard waste
6. All supercompacted waste

Since the time of the CCA, the response of the standard waste configuration was calculated and reported as part of the assessment of the effects of raising the repository to Clay Seam G (Park and Holland, 2003). Initial calculations for the other five cases were reported by Hansen et al. (2003a) and have been modified to improve model details for the calculations in this report.

For each waste package configuration, 13 separate calculations were conducted in which the gas generation rate is varied from the base rate by factors (f) ranging from 0.0 (no gas generation) to 2.0 (twice the base rate). For a gas generation rate of zero, porosity histories for various waste package configurations reflect the mechanical effects unambiguously. Gas generation initiates immediately, so for most analyses, creep closure is counterbalanced by various pressure levels caused by internal gas pressure. The response surfaces are developed in terms of porosity as a function of time at various levels of f.

Report Organization

The remainder of this report describes implementation details. Section 2 summarizes basic information involved with the analyses, such as calculation of initial porosity. It turns out that initial porosity for a room full of waste does not vary greatly, despite the noted significant differences in the packaging. This similarity occurs because the volume of solids (waste and containers) is relatively small compared to the room volume. The MgO engineered barrier material, for example, contributes 5% to the initial porosity calculations. Gas generation potential and gas production rates are described and related to the performance assessment utilization. Section 2 also provides an overview of the stratigraphy and mechanical models, including the POP volumetric plasticity model and the AMWTP treatment. The detailed development of the POP constitutive model is described in a separate report (Park and Hansen, 2004).

Section 3 describes the mesh generation, especially as regards treatment of the AMWTP wastes. The AMWTP supercompacted pucks are treated as rigid inclusions, and the air annulus and outer container are simulated using the standard waste model developed for the 55-gallon drums. The proportioning of rigid elements and compliant elements is described in Section 3. Section 4 documents the computer codes, files and documentation of the multiple runs executed for this study.

Section 5 presents the results of the calculations, making ample use of figures. Pressure and porosity histories from the SANTOS calculations are provided and comparisons are made for the various waste packages modeled. Section 6 provides discussion of the phenomenon observed for the stiff wastes, which tend to prop the rooms open and reduce creep into the rooms. Section 6 provides some additional perspective on these calculations and some concluding remarks. References are provided in Section 7.

2 ANALYSIS MODELS

The analysis involves the familiar underground setting of the WIPP repository. Disposal rooms are mined at 655-m depth in bedded salt formations in southeastern New Mexico and are designed to store waste drums containing transuranic waste for a regulatory period of 10,000 years. The rooms are rectangular and the model represents a plane-strain two-dimensional slice perpendicular to a typical room. Geotechnical components include the constitutive models for salt and anhydrite, which are unchanged from the CCA and identical to those described by Park and Holland (2003). Calculations of initial porosity are completed for rooms filled entirely with standard waste drums, POPs or AMWTP waste packages and for two combinations of these inventories.

Initial porosity

The solid volume of MgO amounts to 5% of the total volume of a room (see Appendix B-3). Although the MgO does not affect structural response, its inclusion or exclusion in these analyses is inconsistent and warrants explanation. This report will compare results from earlier analyses (Stone, 1997a; Park and Holland, 2003) with the current analyses of POP and AMWTP. The early calculations that replicated the CCA did not include MgO in the original porosity surface because it was necessary to replicate calculations identical to the baseline in the CCA (Park and Holland, 2003). Calculations of the porosity surface for the CCA did not include MgO. The POP analyses, which were calculated first in this series also did not include MgO, which thereby yields a porosity surface that is slightly higher than it would be with MgO, because including MgO would reduce porosity by 5%. The last in the series of calculations run on AMWTP included MgO as part of the initial porosity. MgO was included in the AMWTP calculations by placing a standard 1 m^3 supersack above all waste stacks regardless of the proportion of AMWTP waste filling the room. The authors recognize this inconsistency, but choose to explain its impact rather than re-run all the analyses. The important mechanical response and overall results and conclusions are not changed.

2.1.1 Standard waste

The standard waste configuration comprises 6,804 55-gallon drums uniformly distributed in the disposal room in 7-pack units. There are 972 of these units stacked three high. The initial porosity does not include MgO to ensure consistency with earlier analyses by Stone (1997a), which constitute the compliance baseline. The corresponding volume occupied by the waste and the drums is 1,728 m^3.

The standard transuranic waste is a combination of metallics, sorbents, cellulose, rubber and plastics, and sludges. Table 1 summarizes the available data for characterizing the waste. The initial waste density, ρ_0, is 559.5 kg/m^3 and the solid waste density, ρ_s, is 1,757 kg/ m^3. The initial waste density is the sum of the densities of the constituent waste forms. Using the following definition of porosity, $\phi = 1 - \rho_0 / \rho_s$ (Park and Holland, 2003), the initial waste porosity, ϕ_0, is calculated to be 0.681 resulting in an initial solid volume of 551.2 m^3. Using the difference of the undeformed disposal room volume and

the initial solid volume to calculate the total void volume of the room, the initial porosity of the undeformed disposal room is determined to be 0.849, which is exactly the number underpinning the CCA calculations (Park and Holland, 2003).

Table 1: WIPP CH-TRU Waste Material Parameter Disposal Inventory (Butcher, 1997)

Waste Form	Waste Density (kg/m^3)	Volume Fraction
Metallic	122.	0.218
Sorbents	40.	0.071
Cellulose	170.	0.304
Rubber & Plastics	84.	0.150
Sludges	143.5	0.256
Sum	*559.5*	*0.999*

2.1.2 Pipe overpack waste

Pipe overpacks (POP) are used to ship TRU wastes contaminated with concentrations of plutonium and americium. The stainless steel hollow cylinder is surrounded by an impact limiter and placed inside a 55-gallon drum as standard waste. The impact limiter is typically fabricated from polyethylene or a dense fiberboard. A report by Park and Hansen (2003) provides extensive detail of the POP, including engineering design drawings and the finite-element grid used to model the composite waste package.

The transuranic waste form is a combination of cellulose, iron-base metal/alloys, solidified inorganic matrix, plastics, solidified organic matrix, rubber, aluminum base metal/alloys, other inorganic materials, and other metal/alloys. Characteristics of the waste within the pipe listed in Table 2 were extracted from the Transuranic Waste Baseline Inventory Database (TWBID) 2.1, which consisted of the volume fraction information (Leigh, 2003). The density data are therefore assumed the same as the CCA inventory data from SAND97-0796 (Butcher, 1997). The waste volume of the 12-inch POP is calculated as 0.05006 m^3. The porosity of waste, ϕ_w, is assumed 0.681 as the case of CCA (Butcher, 1997). The volume of waste is multiplied by $(1-\phi_w)$ to calculate the matrix volume of waste (0.01592 m^3). The matrix volume of all combined waste is multiplied by the volume fraction of each material to calculate the matrix volume of each individual waste material. The weights of each material are obtained by multiplying the matrix volume of each material by its density. The initial waste density is the sum of the densities of the constituent waste forms. Thus, the initial waste density, ρ_0, is 594.08 kg/m^3 as shown Table 2.

Table 2: The available data for characterizing the waste in the 12-inch pipe over pack

	Volume Fraction	Density (kg/m^3)	Matrix Volume (m^3)	Weight (kg)	Weight Density (kg/m^3)
Cellulosics	73.27%	1100	0.011664	12.83	256
Other Inorganic Materials	13.70%	2200	0.002181	4.80	96
Iron-Base Metal/Alloys	6.66%	7830	0.001060	8.30	166
Solidified, Inorganic Matrix	2.64%	2200	0.000420	0.92	18
Other Metal/Alloys	2.04%	7830	0.000325	2.54	51
Plastics	1.57%	1200	0.000250	0.30	6
Solidified, Organic Matrix	0.08%	1100	0.000013	0.01	0
Rubber	0.02%	1200	0.000003	0.00	0
Aluminum-Base Metal/Alloys	0.02%	7830	0.000003	0.02	0
Soils	0.00%	2200	0.000000	-	-
SUM	100.00%		0.01592	29.74	594.08

The volume of each component in the 12-inch POP is listed in Table 3. The calculation sheet to compute the volume of each component in the 12-inch POP is provided in Appendix A-1. It is assumed that the porosity of impact limiter is 0.670 (Smith and Blanton, 2001) and the porosity of plywood is 0.5. The densities of each component in the 12-inch POP, which is obtained from the linear hardening materials models by Ludwigsen et al. (1998), are listed in Table 3. The volume of a 55-gal drum is 0.2539 m^3 (Sandia WIPP Project, 1992) while the volume calculated by summing components is 0.18879 m^3 (Appendix A-1). The difference (0.06512 m^3) between the nominal volume and the volume calculated from drawing dimensions is assumed occupied by the impact limiter material.

Table 3: Material properties of each component for the 12-inch POP

	Volume (m^3)	Porosity of Material	Matrix Volume (m^3)	Volume Fraction	Density (kg/m^3)	Weight (kg)
Impact Limiter	0.12267	0.670	0.040481	44.74%	256.49	31.463
Pipe	0.00847	0.000	0.008470	9.36%	7908.00	66.981
Plywood	0.00312	0.500	0.001560	1.72%	427.48	1.334
Waste	0.05006	0.682	0.015919	17.59%	594.08	29.740
Drum Shell	0.00257	0.000	0.002570	2.84%	7908.00	20.324
Space	0.00189	1.000	0.000000	0.00%	0.00	0.000
Space with Impact Limiter	0.06512	0.670	0.021490	23.75%	256.49	16.702
Sum	0.25390		0.090490	100.00%		166.543
					Solid Density (kg/m^3) =	1840.46
					Drum Density (kg/m^3) =	655.94

The volumes of each component are multiplied by the density of each component to produce the weight of each component. Thus, the total weight of the drum and 12-inch POP is 166.543 kg. The matrix (solid) volume of each component, V_m, is determined by the following equation,

$$V_m = V_c(1-\phi_c) \quad (1)$$

where, V_c = The volume of each component

ϕ_c = The porosity of each component

Then, the matrix volumes of each component are calculated as listed in Table 3. The sum of the matrix volumes is 0.09049 m^3. The total weight of the drum and POP is divided by the total matrix volume to produce the matrix density, which is also called the solid waste density. The solid waste density of the drum and 12-inch POP, ρ_s, is 1840.46 kg/m^3. The total weight is divided by the true volume of a 55-gallon drum to produce the initial waste density. The initial waste density, ρ_0, is 655.94 kg/m^3.

Using the following definition of porosity, $\phi = 1 - \rho_0 / \rho_s$, the initial waste porosity, ϕ_0, is calculated to be 0.644 resulting in an initial solid volume of 615.69 m^3. Using the difference of the undeformed disposal room volume and the initial solid volume to calculate the total void volume of the room, the initial porosity of the undeformed disposal room is determined to be 0.831. The calculation sheet for the initial porosity for the case of the 12-inch POP is provided in Appendix B-1. As can be appreciated, the initial room porosity, when occupied entirely with POPs is essentially the same as when the room is filled with the standard waste configurations comprising 55-gallon drums.

Following the same line of reasoning, the waste volume of the 6-inch POP is calculated as 0.01278 m^3. Porosity of waste, ϕ_w, is assumed 0.681. The volume of waste is multiplied by $(1-\phi_w)$ to calculate the matrix volume of waste (0.00406 m^3). A summary of each component is given in Table 4. The calculation sheets for the volume of each component of the 6-inch POP are provided in Appendix A-2. The densities of each component of the 6-inch POP are the same as the 12-inch POP, while the volume of the drum as calculated in Appendix A-2 is 0.18877 m^3. The volumes of each component are multiplied by the density of each component to produce the weight of each component. Thus, the total weight of the 6-inch POP is 124.163 kg. The matrix volume of each component, V_m, is determined (Equation 1) and listed in Table 4. The amount of matrix volume is 0.08838 m^3. The solid waste density of the 6-inch POP, ρ_s, is 1404.82 kg/m^3. The total weight is divided by the true volume of a 55-gallon drum to produce the initial waste density, ρ_0, of 489.02 kg/m^3.

Table 4: Material properties of each component for the 6-inch POP

	Volume (m^3)	Porosity of Material	Matrix Volume (m^3)	Volume Fraction	Density (kg/m^3)	Weight (kg)
Impact Limiter	0.16402	0.670	0.054127	61.24%	256.49	42.069
Pipe	0.00457	0.000	0.004570	5.17%	7908.00	36.140
Plywood	0.00312	0.500	0.001560	1.77%	427.48	1.334
Waste	0.01278	0.682	0.004064	4.60%	594.08	7.592
Drum Shell	0.00257	0.000	0.002570	2.91%	7908.00	20.324
Space	0.00171	1.000	0.000000	0.00%	0.00	0.000
Space with Impact Limiter	0.06513	0.670	0.021493	24.32%	256.49	16.705
Total	0.2539		0.088384	100.00%		124.163
					Solid Density (kg/m^3) =	1404.82
					Drum Density (kg/m^3) =	489.02

The initial waste porosity, ϕ_0, is calculated to be 0.652 resulting in an initial solid volume of 601.385 m^3. The initial porosity of the undeformed disposal room is determined to be 0.835, nearly identical to the porosity of the 12-inch POP. The calculation sheet to compute the initial porosity for the case of the 6-inch POP is provided in Appendix B-2.

As noted in the introduction to this section, the initial porosity of the rooms containing POPs does not include MgO. If MgO were included, the initial porosity would be reduced by 5%. The calculation result plots porosity as a function of time, which would simply be offset by an equivalent 5% if MgO material were included in the calculations.

2.1.3 AMWTP Supercompacted waste

The AMWTP is designed to retrieve, characterize, prepare and package 65,000 m^3 of contact-handled transuranic (CH-TRU) waste at the INEEL for shipment to the WIPP. The CH-TRU wastes at INEEL consist of non-debris and debris wastes. The non-debris wastes constitute approximately 30% of the total stored volume at INEEL and will not be supercompacted. The debris wastes constitute about 70% of the total stored volume at INEEL and will be sorted and supercompacted. The AMWTP will compact 55-gallon drums of debris waste and place the compacted drums into 100-gallon drums before shipment to the WIPP. The compacted 55-gallon drums are referred to as "pucks" (see Figure 2). Each puck has a final volume of 15 gallons to 35 gallons, and each 100-gallon container is anticipated to contain from three to five pucks, with an average of four pucks per container, as illustrated in Figure 1-C.



Figure 2: AMWTP pucks produced by supercompaction of 55-gallon drums of debris waste

The basis of this calculation assumes that an entire waste room is filled with waste from the AMWTP. The compressed pucks have a minimal porosity, which is assumed zero. The AMWTP waste is compressed to 60 MPa prior to being placed in the container. The supercompaction stress is far greater than the waste will experience in the underground from the room closure (maximal compression of ~15 MPa). As before, a typical room can be filled with 972 seven-packs of 55-gallon drums in a hexagonal configuration. A three-pack of 100-gallon containers will occupy the same footprint as the standard seven-pack, as shown in Figure 3(A). Figure 3(B) also shows what might be considered random disposal room inventory. It is highly unlikely that any room would be completely filled with a single type of waste package. The three-pack and seven-pack pallets are identical in size (WTS, 2003). Thus, number of containers in a disposal room is 972 packs × 3 containers/pack = 2,916 containers.

The outer dimensions of the 100-gallon containers are 0.8897 m (35 inches) in height and 0.790 m (31 inches) in diameter as shown Figure 4. The volume of the container is calculated to be 0.436 m^3. The volume of the all containers in a room is 0.436 m^3/container × 2,916 containers = 1,272.3 m^3. Each container has an inner lid 0.0366 m (1.5 inches) below the outer lid. For purposes of these calculations, a void space between the inner lid and the top of the supercompacted waste (pucks) is assumed to be 5% of the outer height, or 0.044 m. Then, the height of the pucks on the inside is 0.805 m (31.75 inches). The diameter of the pucks is 0.635 m (25 inches). The pucks are guided into the 100-gallon drums with longitudinal spacers, which create a 0.076 m (3 inches) annulus between the waste and the outer wall. The incompressible volume of one container (i.e. pucks in the container) is calculated to be 0.255 m^3. Using these values, the total volume of pucks is 0.255 m^3/container × 2,916 containers = 743.6 m^3.

As noted, the previous porosity calculations for rooms full of standard waste packages (i.e., the compliance baseline) and for rooms full of POPs did not include MgO. When investigations into the impact of AMWTP supercompacted waste were undertaken, MgO was included in the calculation of the initial porosity. This has no structural effect, as the

MgO adds nothing to the resistance to creep closure. However, its inclusion for the AMWTP case reduces the initial porosity by 5%. With the addition of 324 supersacks of MgO with a volume of 1 m^3 atop each stack, the total volume of containers and MgO sacks in a room is 1,596 m^3.

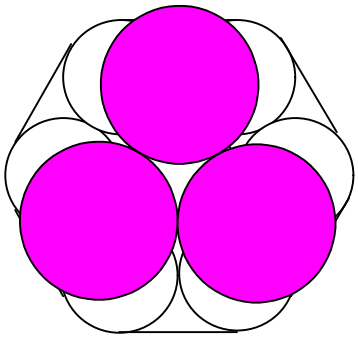

(A) Footprints of three-pack of 100-gallon containers and seven-pack of 55-gallon drums

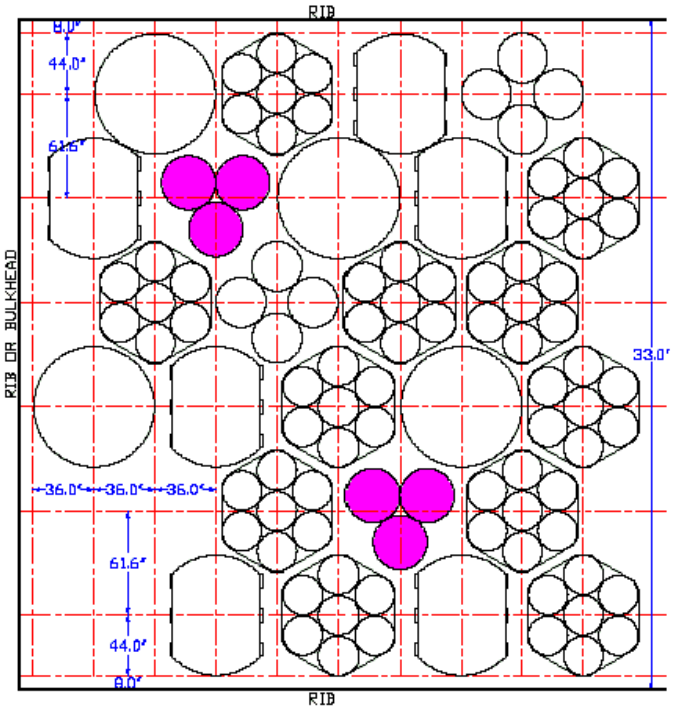

(B) Arrangement of waste containers in the repository

Figure 3: Illustration of waste containers and waste configuration

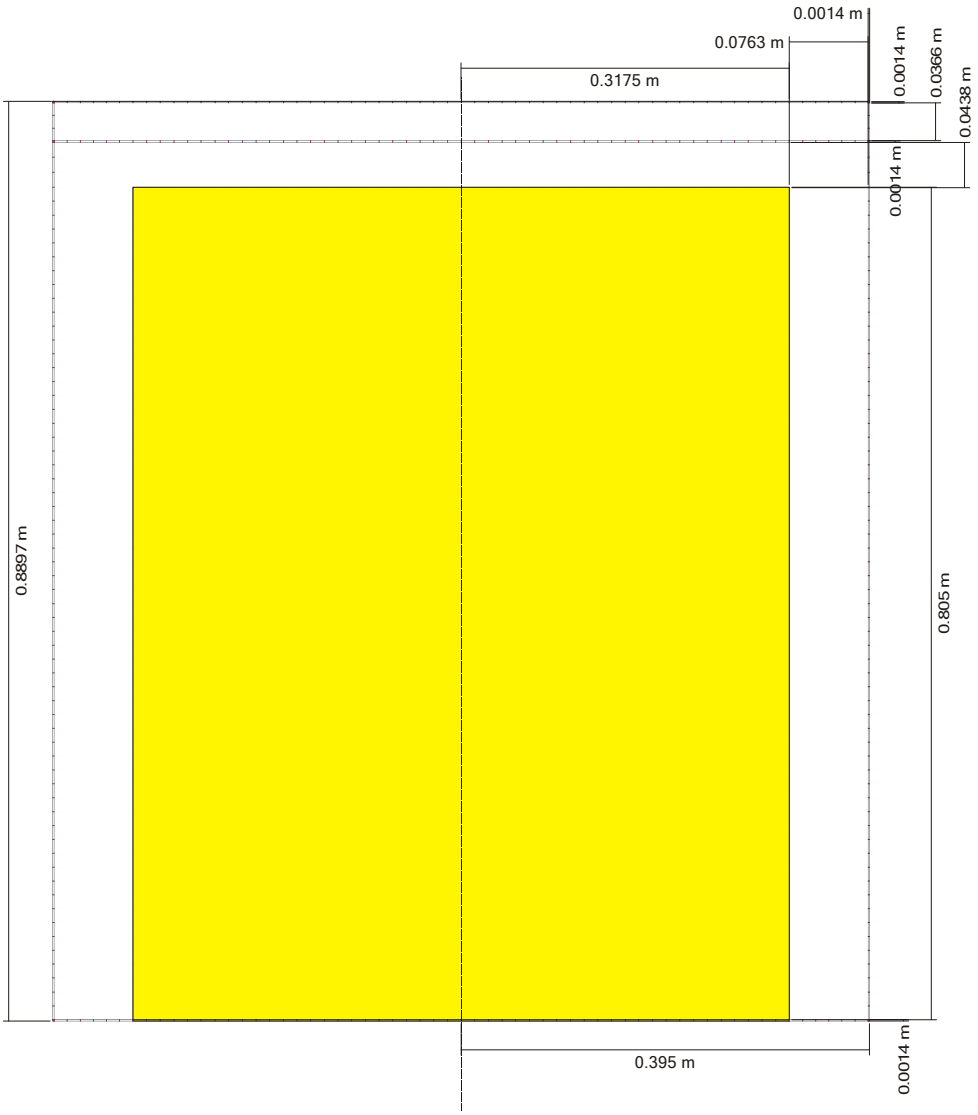

Figure 4: Simplified outline drawing of the 100-gallon container and supercompacted waste

From above, the porosity of a single AMWTP container is calculated to be 41% (= (0.436 m^3 – 0.255 m^3) / 0.436 m^3). There is a sack of MgO atop each stack of containers, for which the porosity is assumed to equal 41%, a nominal value for loose aggregate. Using these values the volume of solid of MgO sacks is 324 m^3 × (1-0.41) = 191.2 m^3. Then, the total volume of incompressible solid in a room is calculated to be 935.9 m^3 (total volume of pucks + total volume of MgO solid). The total volume of the container shells is calculated to be 14.9 m^3 (see Appendix B-3) and the total incompressible solid is 949.5 m^3.

The initial porosity of the room can then be calculated using the following formula:

$$Room\ Porosity = 1 - \frac{949.5}{3642.8} = 0.739$$

The calculation sheet is provided in Appendix B-3. If MgO were not included the initial porosity would be approximately 0.79.

The volume of pucks, drum shell, and the free space (including upper, lower, and annular space) in a container are calculated to be 0.255 m^3, 0.005 m^3, 0.176 m^3, respectively (Appendix A-3). The volume of MgO per container is calculated to be 0.111 m^3/container (= 324 m^3 / 2916 containers). The backfill material (MgO sacks) shall have a minimum loose bulk density of 87 lb/ft^3 (1,394 kg/m^3) (Griswold, 2002). Waste (puck) density is assumed to be 2,238 kg/m^3 based on an assumption that a standard drum is supercompacted to one fourth its original volume. The density of standard waste is 559.5 kg/m3 (Stone, 1997a). The steel drum shell density is assumed 7,908 kg/m^3, typical values for high strength and mild carbon steels.

Table 5: Material properties of each component for AMWTP waste

	Volume (m^3)	Porosity of Material	Matrix Volume (m^3)	Volume Fraction	Density (kg/m^3)	Weight (kg)
MgO	0.111	0.41	0.0655	20.12%	1394.0	154.73
Waste (Pucks)	0.255	0.00	0.2550	78.31%	2238.0	570.58
Container Shell	0.005	0.00	0.0051	1.57%	7908.0	40.49
Space	0.176	1.00	0.0000	0.00%	0.0	0.00
Sum	0.547		0.3256	100.00%		765.80
					Solid Density (kg/m^3) =	2352.26
					Drum Density (kg/m^3) =	1399.21

The volumes of each component are multiplied by the density of each component to produce the weight of each component. The total weight of an AMWTP container with an MgO sack is 766 kg. The matrix volumes of each component are calculated as shown in Table 5. The amount of matrix volume is 0.3256 m^3. The solid waste density of a container with an MgO sack, ρ_s, is 2,352 kg/m^3. The total weight is divided by the actual volume of a container with an MgO sack to determine an initial waste density, ρ_0, equaling 1,399 kg/m^3.

2.1.4 Combined cases

The uncertainty in future placement of waste packages in the disposal rooms and in the waste package response models requires structural calculations for a variety of waste package configurations. Waste package configurations were chosen to cover a range of combinations of porosity and waste package structural characteristics (rigidity). To ensure that these configurations covered the range of possibilities, intermediate cases representing combinations of standard and supercompacted waste packages in various ratios were examined. Recall that the case of a room filled entirely with POP would provide high initial porosity and the rigidity of the POPs would retain the highest porosity surface in cases without gas generation. On the other extreme, rooms filled with standard waste containers continue to close with relatively small backstresses to the lowest

porosity surface, again in the case without gas generation. The variations examined here involve combinations of the standard waste model with AMWTP waste. These intermediate cases are described as follows:

- A mix of 1/3 supercompacted waste and 2/3 standard waste (1/3 AMWTP)
- A mix of 2/3 supercompacted waste and 1/3 standard waste (2/3 AMWTP)

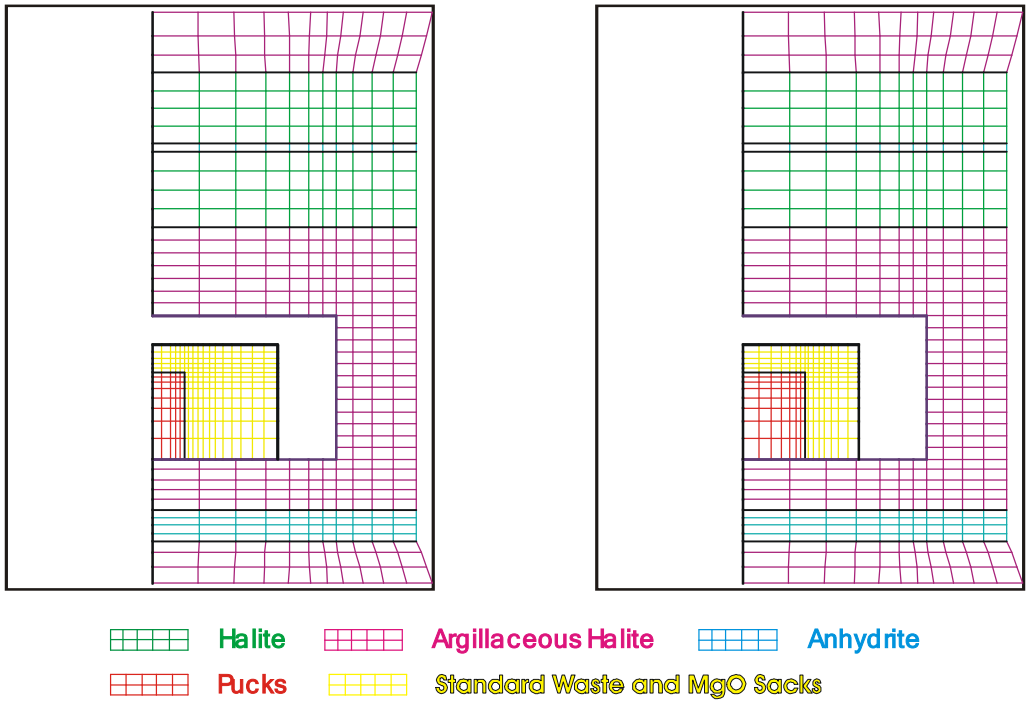

Figure 5: Combined cases included supercompacted waste

As shown in Figure 5, combined cases include supercompacted waste in proportions of 1/3 and 2/3 with standard waste to represent intermediate conditions. More detailed descriptions of these arrangements will be shown subsequently (Figures 15 and 18). The response models for each waste form were applied to the respective columns of waste in the computational grid. The analysis also considered a room filled with supercompacted waste to capture the case of low initial porosity and high rigidity. Note that these calculations simulate the waste somewhat differently than represented in the report by Hansen et al. (2003a). This refinement allows the compliant annular space to be modeled explicitly, a feature not captured in the comparable analysis conducted prior to the Hansen et al. (2003a) report. As will be seen later, this refinement created only a small difference in the porosity surface results.

The initial porosities of the undeformed disposal room filled with 1/3 AMWTP and 2/3 AMWTP are calculated to be 0.802 and 0.767, respectively. The calculation sheets of the initial porosities are provided in Appendix B-4 and B-5, respectively. Treatment of the AMWTP package will be discussed in detail in Section 3.3, but suffice it to say at this

time, that the rigid pucks are pushed together at the beginning and the annular space including the vertical spacer bars are simulated using the standard waste model.

Gas generation potential and production rate

Gas production is a significant component of the room closure model and is unique for each waste package combination examined. A gas production potential and a base gas generation rate were estimated for each waste package. The gas generation methodology was implemented exactly as it was for calculations supporting the original certification (Stone, 1997a). The base gas generation rate was varied by factors ranging from 0.0 (no gas generation) to 2.0 (twice the base rate), to capture uncertainty in actual gas generation from the waste materials.

For the standard waste, the base gas production potential from anoxic corrosion of iron-containing metals was estimated at 1,050 moles/drum, with a base production rate of one mole/drum/year. The gas production potential from microbial activity was estimated to be 550 moles/drum, with a production rate of one mole/drum/year. Gas production ceases after 1050 years. The total amount of gas generated in a disposal room for the standard waste case was based on 6,804 waste drums per room (Stone, 1997a). For this analysis, the base gas generation potential and gas production rate for the pipe overpack configuration are assumed to equal the standard waste package configuration in terms of gas generation potential.

The amount of gas generated from a single supercompacted puck is assumed equal to the amount generated from an uncompacted 55-gallon drum (1 mole/drum/year). Since an average of four pucks are placed in each 100-gallon container, and three 100-gallon containers fill the same space occupied by a seven-pack arrangement of 55-gallon drums, the supercompacted waste has a gas production potential and base gas generation rate 12/7 larger than the potential and rate for the standard waste.

For the 1/3 supercompacted and 2/3 standard waste configuration, the total amount of gas generated in a disposal room is based on 3,888 pucks and 4,536 standard drums per room. For the 2/3 supercompacted and 1/3 standard waste configuration, the total amount of gas generated in a disposal room is based on 7,776 pucks and 2,268 standard drums per room. Rooms completely filled with supercompacted waste contain a total of 11,664 waste pucks. Table 6 summarizes the total potential for gas production, in moles, and the gas production rates for the six waste loading schemes. The total gas potential for each reference case is shown in Figure 6. The gas generation potential assumes that no gas bleeds off through the surrounding lithologies. The calculation sheets of the gas generation potential and rate are provided in Appendix C.

The gas pressure in the disposal room is computed from the ideal gas law based on the current free volume in the room. Specifically, the gas pressure, p_g, utilizes the following relationship:

$$p_g = f \cdot \frac{NRT}{V} \tag{2}$$

where N, R and T are the mass of gas in g-moles for the baseline case, the universal gas constant, and the absolute temperature in degrees Kelvin (300 ºK), respectively. The variable, V, is the current free volume of the room. For each iteration in the analysis, the current room volume is calculated based on the displaced positions of the nodes on the boundary of the room. The free room volume, V, is computed by subtracting the solid volume of the waste from the current room volume. The gas generation variable, f, is a multiplier used in the analyses to scale the pressure by varying the amount of gas generation. A value of f=1 corresponds to an analysis incorporating full gas generation, while a value of f=0 corresponds to an analysis incorporating no internal pressure increase due to gas generation. This portion of the analysis is identical to that implemented by Stone (1997a). It should be noted, however, that the product $f \times N$ in Equation 2 represents different gas potentials depending on the type of waste package configuration assigned to a disposal room. For example, if the entire room is filled with AMWTP waste, then $f \times N$ represents a gas potential that is 12/7 of the gas potential of a standard waste configuration. The differences in gas potential for $f=1$ are shown graphically in Figure 6. These differences need to be considered when model results are compared in Section 5.

The porosity surface defines the relationship between disposal room porosity, amount of gas present in that porosity, and time. The porosity can be computed directly from the disposal room deformed shape. The concept of the porosity surface comes from the observation that the disposal room closure is directly influenced by gas generation. This observation allows a surface to be constructed incorporating the closure results for various values of f, which is a convenient way to express the amount of gas generation.

Table 6: Total gas potential and gas production rates for each waste configuration.

Parameter	Standard	6" POP	12" POP	1/3 AMWTP	2/3 AMWTP	All AMWTP
Total gas potential from 0 yr to 550 yrs (mol)	7.484×10^{6}	7.484×10^{6}	7.484×10^{6}	9.266×10^{6}	1.105×10^{7}	1.283×10^{7}
Total gas potential from 550 yrs to 1050 yrs (mol)	3.402×10^{6}	3.402×10^{6}	3.402×10^{6}	4.212×10^{6}	5.022×10^{6}	5.832×10^{6}
Gas production rate from 0 yr to 550 yrs (mol/s)	4.312×10^{-4}	4.312×10^{-4}	4.312×10^{-4}	5.339×10^{-4}	6.366×10^{-4}	7.392×10^{-4}
Gas production rate from 550 yrs to 1050 yrs (mol/s)	2.156×10^{-4}	2.156×10^{-4}	2.156×10^{-4}	2.669×10^{-4}	3.183×10^{-4}	3.696×10^{-4}

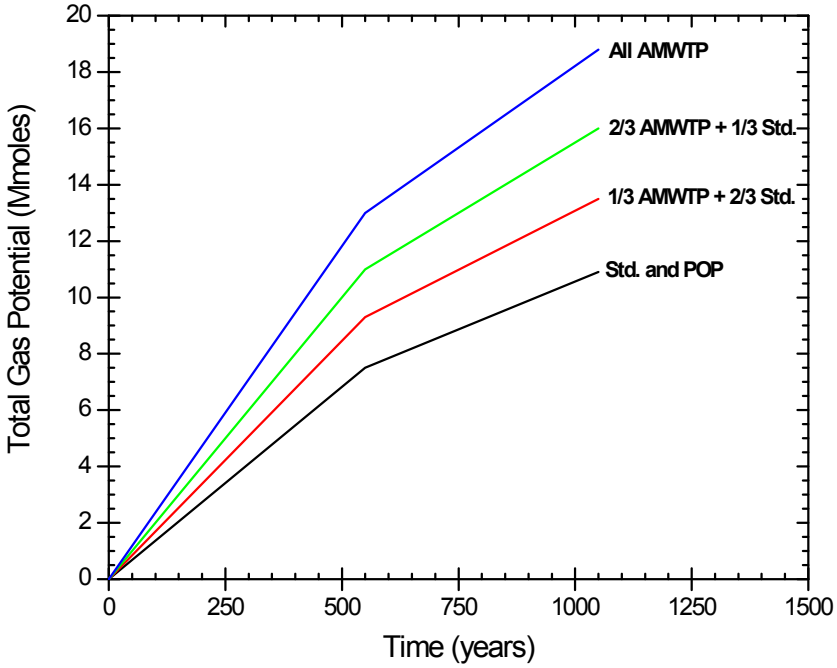

Figure 6: Histories of gas generation potential used for the disposal room analyses, f=1.0

2.1.5 Stratigraphy and constitutive models

The idealized stratigraphy for the WIPP underground, which derives from Munson et al. (1989), has been described recently (Park and Holland, 2003). Only a brief review will be given here. Calculations were conducted using a grid representation on the original disposal level. Park and Holland (2003) showed that minor structural effects could be expected when the repository horizon is raised 2.43 m to Clay Seam G. Because room closure modeled for the raised repository differed almost imperceptibly from the compliance baseline results, the stratigraphic model used here is identical to that used for compliance calculations, as shown in Figure 7.

The traditional (e.g., see Park and Holland, 2003) multi-mechanism deformation model is implemented in SANTOS to model the creep behavior of rock salt. This is exactly the same model used by Stone (1997a) and others for calculations supporting the original compliance certification. As before, the anhydrites are modeled using the Drucker-Prager criterion and a nonassociative flow rule to determine the plastic strain components.

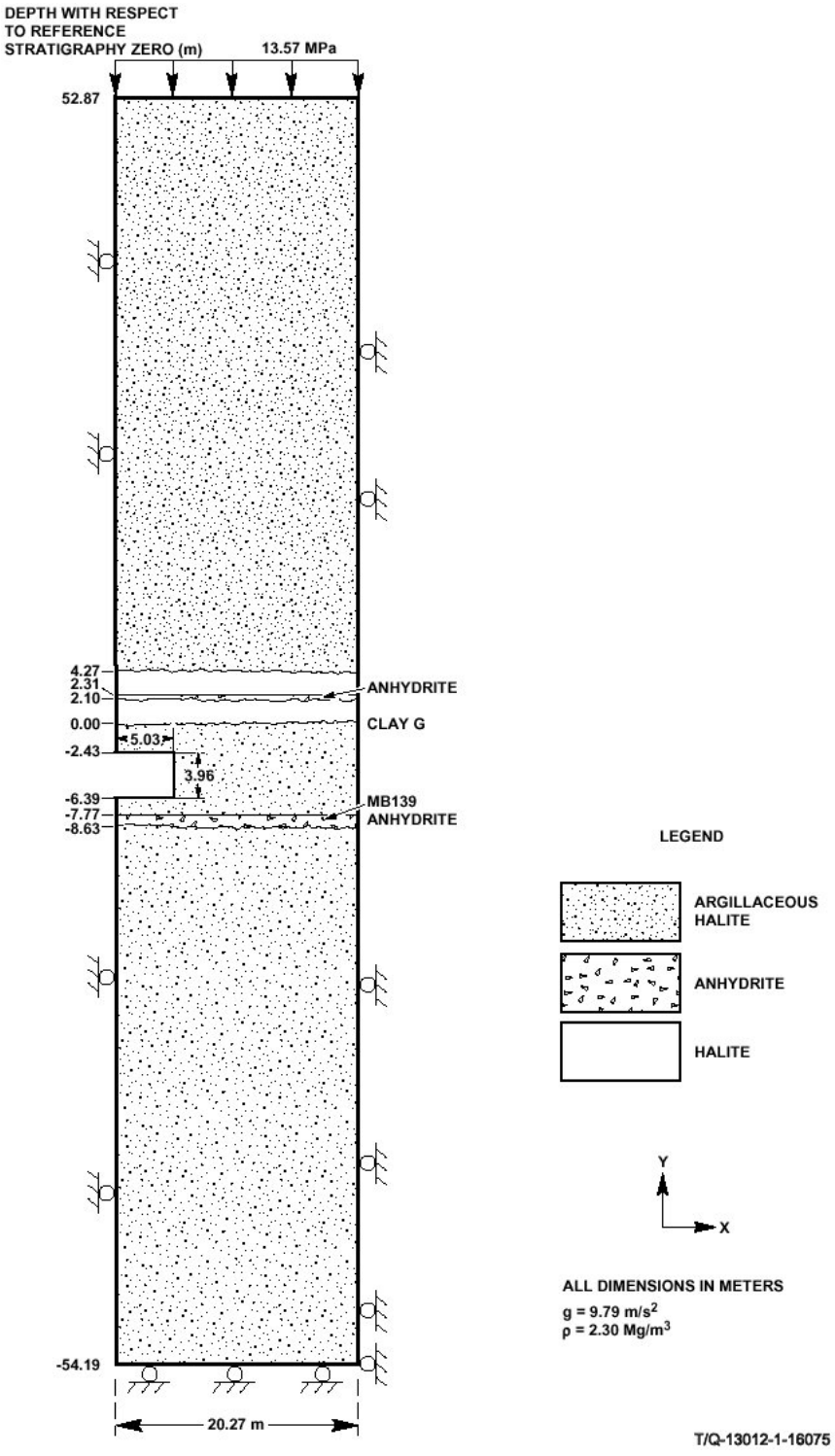

Figure 7: Stratigraphic model for the current level of the disposal room

2.1.6 Waste constitutive model

2.1.6.1 Standard waste

The stress-strain behavior of the standard waste 55-gallon drum was represented by a volumetric plasticity model (Stone, 1997a) with a piecewise linear function defining the relationship between the mean stress and the volumetric strain. Compaction experiments on simulated waste were used to develop this relationship. The deviatoric response of the waste material has not been characterized. It is anticipated that when a drum filled with loosely compacted waste is compressed axially, the drum will not undergo significant lateral expansion until most of the void space inside the drum has been eliminated. The volumetric plasticity relationship consistent with Stone's (1997a) original work and recent calculations supporting WIPP recertification (Park and Holland, 2003) is applied here for standard waste packages.

2.1.6.2 Pipe overpack waste

The material model for standard wastes implemented in the initial compliance certification calculations was based on laboratory testing of 55-gal drums containing surrogate wastes. Similar laboratory tests have not been conducted on the POP, but the composite material properties and geometries are known accurately, thus allowing deformational characteristics to be modeled readily using finite elements. Park and Hansen (2003) presented the details of the several specific analyses used to develop model parameters for the POP. The finite element code called SANTOS was used for these calculations.

The SANTOS analyses allowed determination of shear modulus, bulk modulus, deviatoric yield surface constants, and a pressure-volumetric strain function. Simulations were run for 6-inch and 12-inch interior pipes and included uniaxial, triaxial, and hydrostatic stress applications.

Uniaxial Test Simulation The input to the soil and crushable foams model in the SANTOS code requires a shear modulus and the bulk modulus. These values are derived from Young's modulus and Poisson's ratio of the POP drum simulations.

Triaxial Test Simulation The POP waste package is considered isotropic and elastic until yield occurs. Yield is assumed governed by the Drucker-Prager criterion. The model within SANTOS requires input constants for the deviatoric yield surface.

Hydrostatic Test Simulation To express the volumetric hardening of the POP, the data points defining the volumetric plasticity model are determined from calculating the volume change of the POP drum with hydrostatic pressure. The pressure-volumetric strain curves show the 12-inch POP is slightly more rigid than the 6-inch POP.

SANTOS input constants obtained from test simulations are listed in Table 7. The volumetric strain calculated for the 12-in and 6-in POPs is plotted along with the experimental volumetric strain data for the standard waste 55-gal drum in Figure 8. The volumetric strain of the POP package is calculated to be much less than the standard

waste drum. Park and Hansen (2003) examined the mechanical response of the pipe-overpack waste package under possible stresses in the WIPP disposal room. The response of the POP is dramatically stiffer and stronger than the standard waste. The waste in pipe overpacks could create stiff columns within the disposal rooms and influence room closure. It is possible that rigid waste columns would maintain an overall waste porosity by shielding adjacent standard waste from compaction.

Table 7: SANTOS input constants for POP waste constitutive model (Park and Hansen, 2004)

	12-inch POP	6-inch POP
G (Two Mu) [MPa]	1442.0	1364.0
K [MPa]	1561.0	1690.0
A_0 [MPa]	8.473	6.712
A_1	0.0	0.0
A_2	0.0	0.0

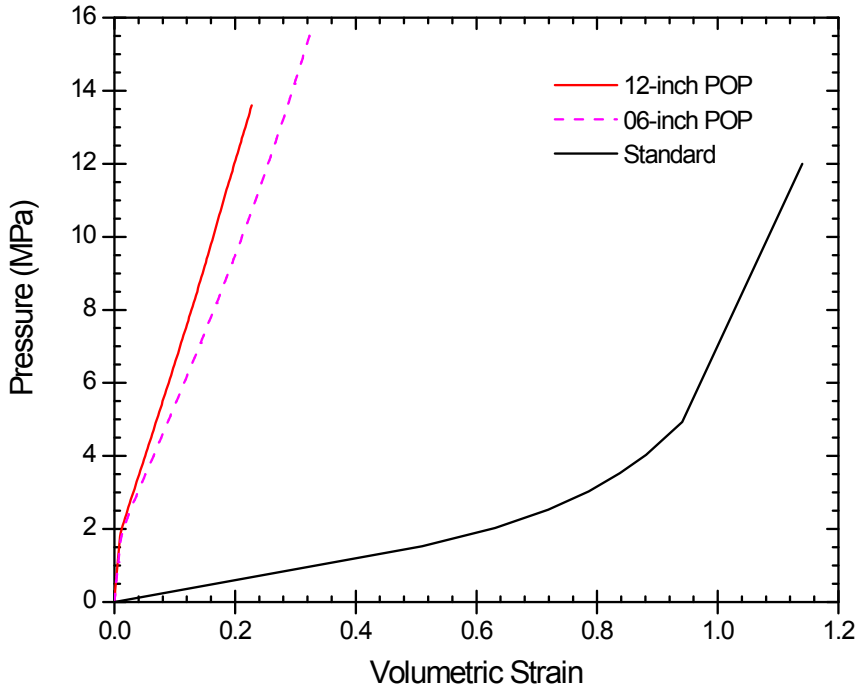

Figure 8: Simulated volumetric strain for POP compared to the standard 55-gal drum (Park and Hansen, 2004).

2.1.6.3 AMWTP waste

The model for AMWTP is developed from engineering judgment based on the supercompaction information. The pucks in the AMWTP containers are compressed to 60 MPa prior to being placed in the 100-gallon container. Because the compaction pressure is much higher than the stresses that develop in the WIPP setting, the AMWTP pucks will retain high density and exhibit relatively high modulus when compared to the standard waste form and POPs. As an approximation, the soil and foams model applied to anhydrite in the SANTOS code is used for the pucks. The modulus thus assumed for the pucks is more than an order of magnitude greater than the POP (75 GPa versus about 2 GPa). In terms of modeling results, this assumption simply means the pucks are undeformable relative to standard waste packages.

The material properties of the container surrounding the pucks are assumed equivalent to the standard waste. The annular space surrounding the pucks is protected by the outer steel of the drum and the vertical positioning brackets. Therefore, the deformation behavior of the 100-gallon container is similar to the standard waste drum until room closure impinges on the pucks themselves.

3 MESH GENERATION

Disposal Room

A two-dimensional plane-strain disposal room model is used to replicate the stratigraphy and the waste room as shown in Figure 9. The model grid represents a cross-section of a typical room in two dimensions. Invoking symmetry, only half of the room is modeled. The left and right boundaries are both planes of symmetry implying that the modeled room represents an infinite series of parallel rooms. The upper and lower boundaries are located approximately 50 m from the room. A lithostatic stress ($\sigma_x = \sigma_y = \sigma_z$) that varies with depth is used as the initial stress boundary conditions and gravity forces are included. A zero-displacement boundary condition in the horizontal direction ($U_x = 0.0$) was applied on both the left and right boundaries of the model to represent the symmetrical nature of a disposal room in an infinite array of rooms. A prescribed normal traction of 13.57 MPa was applied on the upper boundary and a vertical zero-displacement boundary condition ($U_y = 0.0$) was applied on the lower boundary to react to the overburden load. An adaptive internal pressure, p_g, was applied around the boundary of the disposal room. The basic half-symmetry disposal room dimensions are 3.96 m high by 5.03 m wide. This mesh and boundary conditions are identical to those used in Stone's analysis (1997a).

Contact surfaces were defined between the waste and room boundaries to model possible contact and sliding that occurs as the room deforms and contacts the waste. Specifically, contact surfaces were defined between the waste and floor of the room, the waste and room rib, and the waste and ceiling. The contact surfaces allow separation if the forces between the surfaces become tensile. This feature allows the room to reopen due to gas generation within the disposal room.

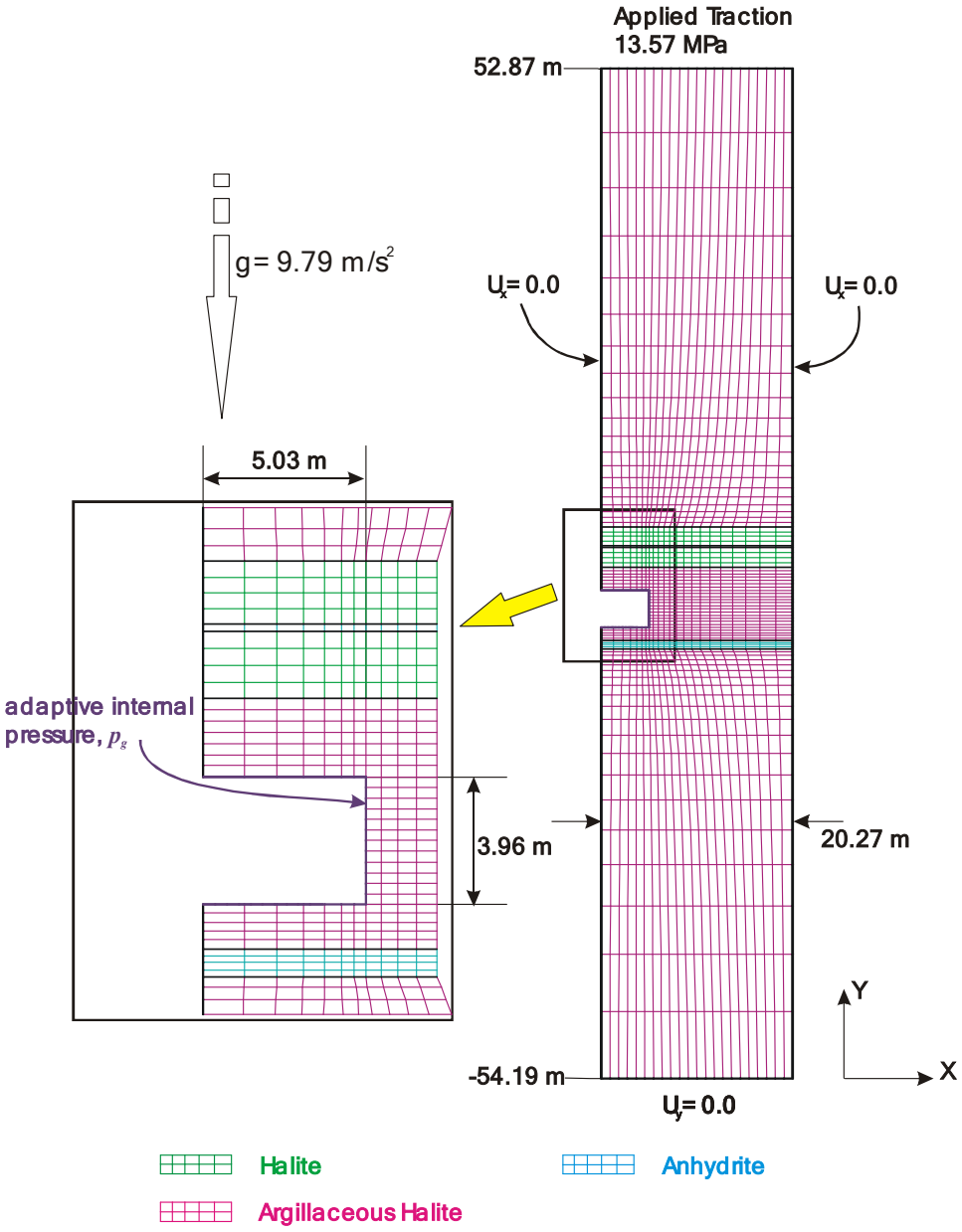

Figure 9: Mesh discretization and boundary conditions around the disposal room

Standard waste and POP waste

Rooms filled completely with POP waste packages and standard waste packages have the same descretized grid. The constitutive model for the waste is changed to appropriate parameters for the soil and foams algorithm in SANTOS. Drums are configured in the standard 7-packs and stacked three high along the drift with a height of 2.676 m. This storage configuration contains a large amount of void volume. To obtain the waste volume dimensions used in the calculations, the assumption is made that each waste drum

will contact its neighbor laterally. Underlying this assumption is the notion that inward movement of the walls of the disposal room is sufficient to eliminate space between the drums early in the closure process and at low stress levels. In other words, the lateral deformation of the disposal room rib compresses the 7-packs causing the void space between the drums to be removed with little or no resistance by the waste drums themselves. This assumption allows calculation of an effective lateral dimension for the waste after lateral displacement eliminates the space between the drums. This idealization was conceived by Stone (1997a) and has been implemented in several additional calculations supporting WIPP recertification. Park and Holland (2003) provide a calculation sheet regarding the dimensions. The grid for the pipe overpack waste package follows the same logic. Of course, the constitutive models for these waste packages differ as the POPs are far more rigid than the standard waste containers. The meshes of the waste contained in the disposal room are shown in Figure 10.

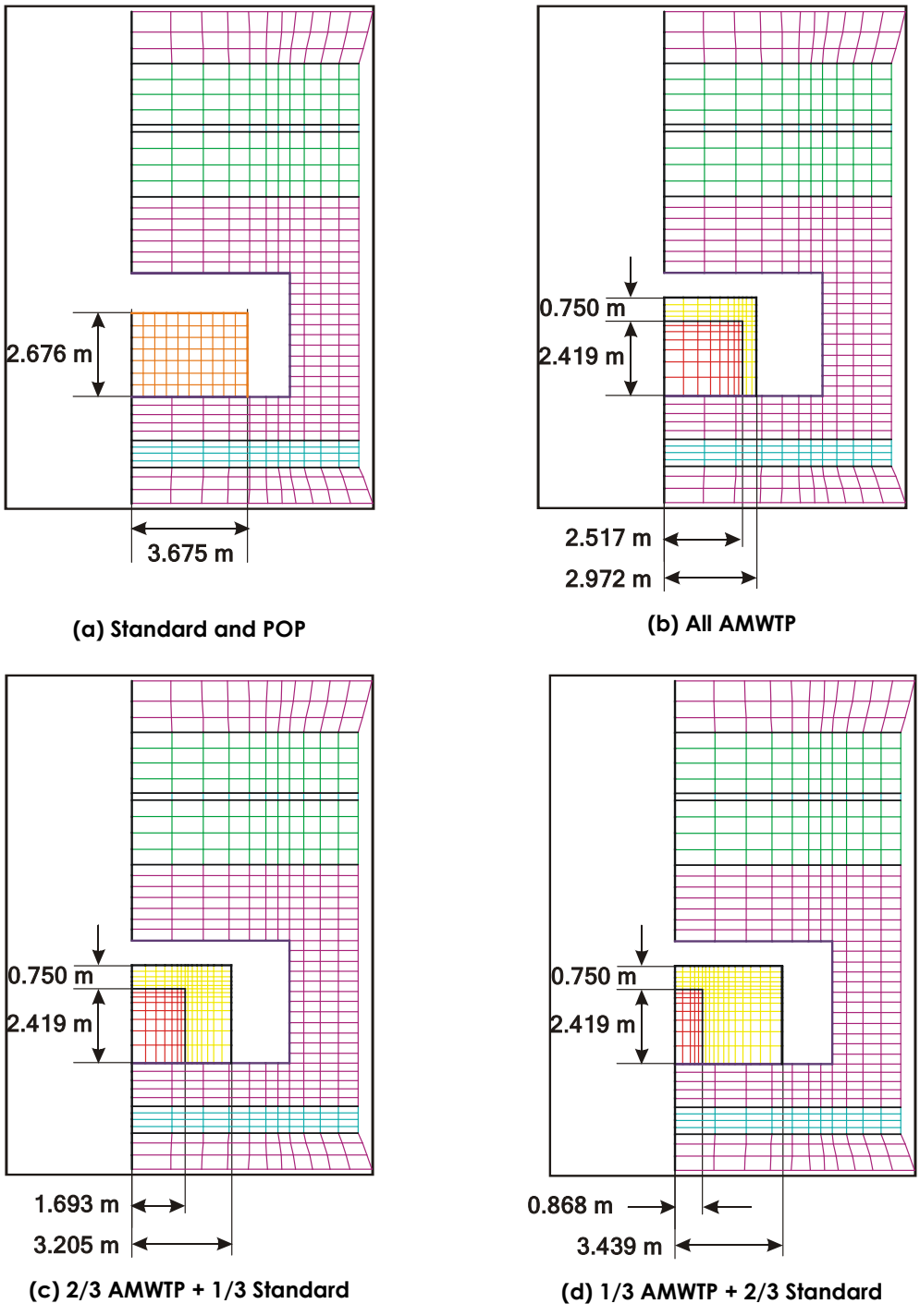

Figure 10: Meshes for various waste package inventories in the disposal room

AMWTP Waste

3.1.1 All AMWTP case

Treatment of the AMWTP waste packages has received attention recently because of the intent by INEEL to ship such containers to WIPP (Hansen et al., 2003). The supercompacted waste package is substantially different from the standard waste considered in the original compliance calculations. Therefore, the AMWTP waste packages represent changes to the certification baseline. One of the main purposes for these calculations is to conduct an assessment of these changes.

The calculations made for the AMWTP 100-gallon waste packages represent a case where it is assumed that an entire room is filled with this dense waste form. Figure 11 illustrates the room-wide configuration of the three-packs of AMWTP superimposed on the footprint of the seven-packs of standard waste. These packages (3-containers) are stacked 3 high and 6 wide across the room. In the ideal packing configuration, a total of 2,916 containers can be placed in one panel. As noted previously, a 0.5-m thick MgO super-sack exists above each stack and the height of a container is 0.889 m. Thus, the height of a stack including a MgO sack is 3.169 m (Appendix D).

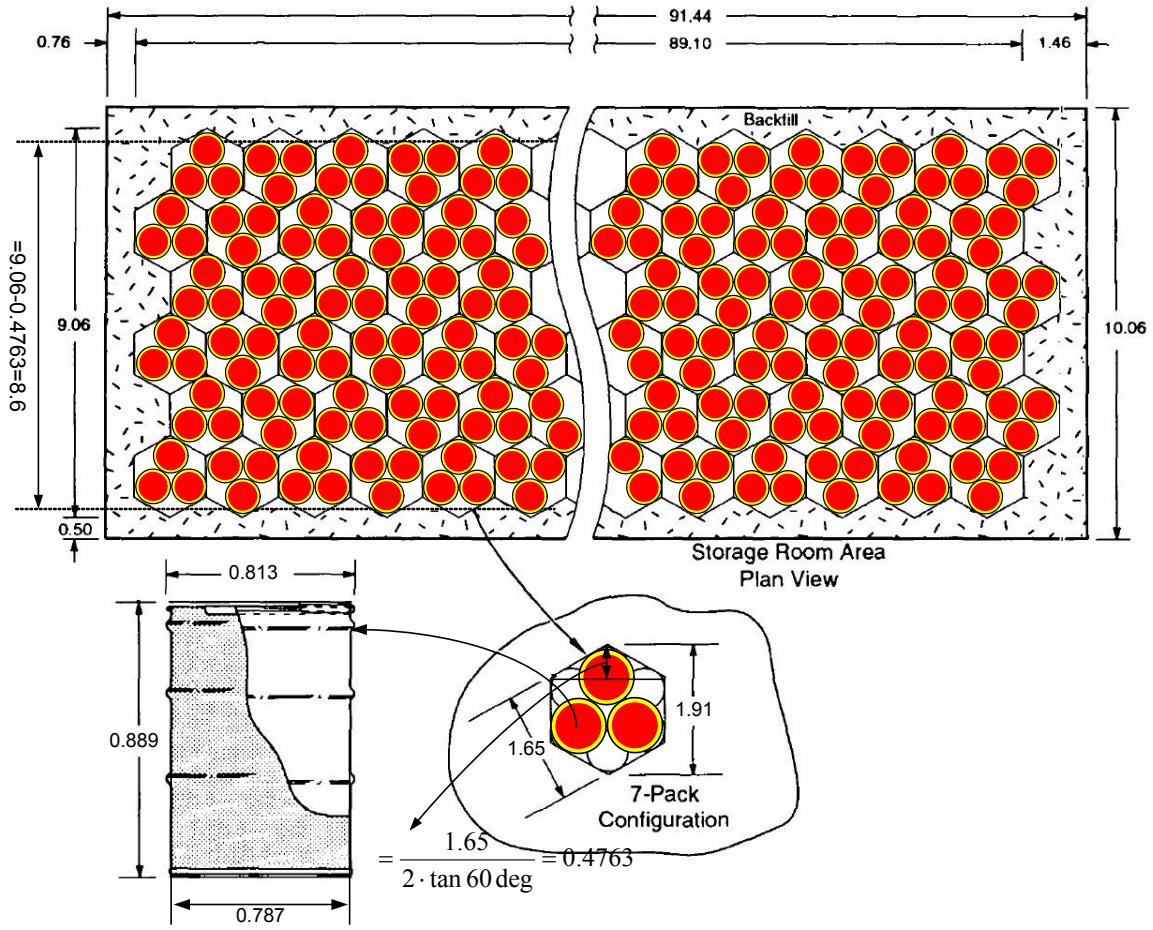

Figure 11: Ideal packing of 100-gallon containers in rooms

The containers are assumed rearranged to remove the void between the containers by the inward movement of the walls, as was assumed for the standard waste and the POP packages. To obtain the waste volume dimensions used in the mesh, each waste container is assumed to move laterally and deform independently. The void space between containers is eliminated in order to have an accurate continuum representation of the waste response. To eliminate the void space between containers, the assumption is made that the lateral deformation of a configuration of containers caused by the inward movement of the walls is sufficient to eliminate space between the containers early in the closure process at low stress levels. This concept is illustrated in Figure 12.

The nominal uncompressed width and length of the stored waste in the disposal room are the same as standard waste, 8.6 m and 89.1 m, respectively as shown in Figure 11.

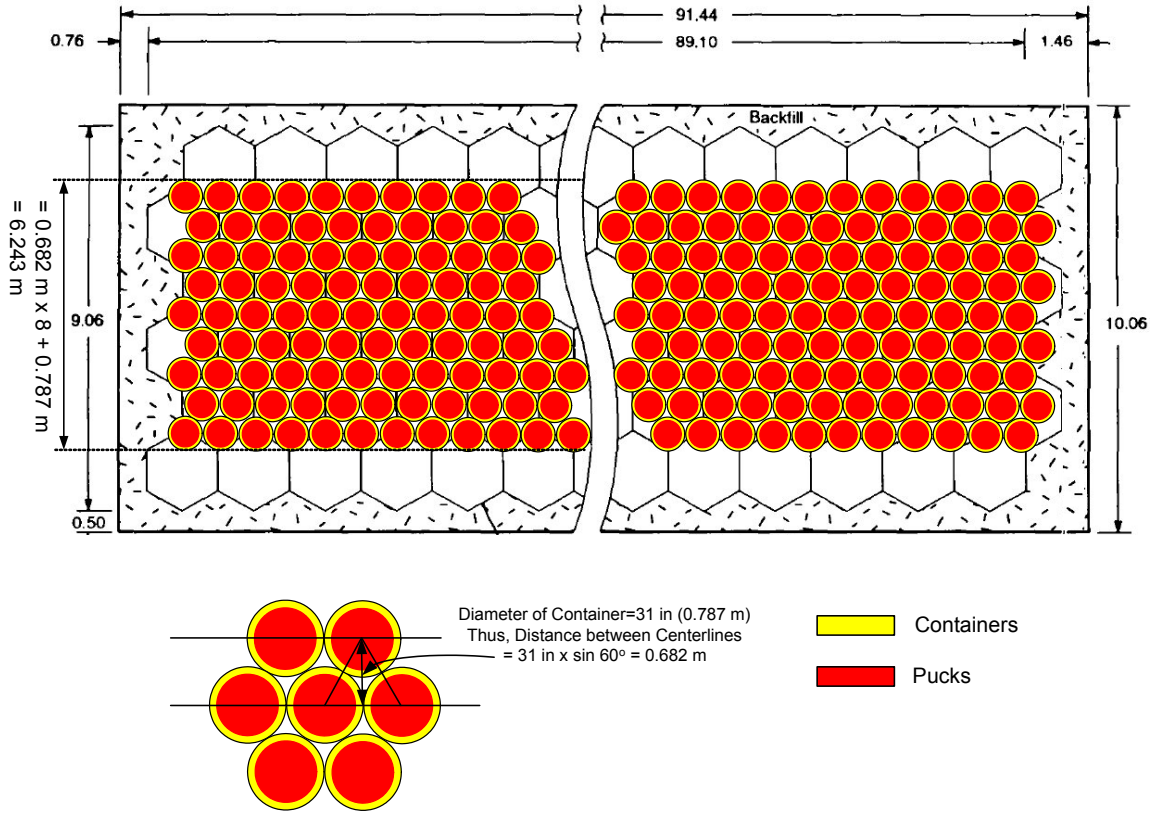

Figure 12: Rearrangement of containers for all AMWTP waste by the inward movement of the walls

To calculate the porosity surface of the disposal room, the deformation of the waste caused by room closure must be determined first. The pucks within the containers are assumed incompressible cylinders. The material properties of the container, the vertical guide rods and annular air space surrounding the pucks are similar to the standard waste model. Therefore, the pucks and the outer container are further separated into two material types, as shown in Figure 13 (a-c). The concept sketched in Figure 13 considers a group of containers in intimate contact. When inward radial pressure is applied on each

container, the container parts are compressed as shown Figure 13-(b). Assuming the container has standard waste material properties, it would compress to a minimum porosity of 0.234 (i.e., the minimum porosity obtained for standard waste containers caused by the room closure with no gas generation in 10,000 years (Park and Holland, 2003)). In addition, an interstitial void remains between the three pucks as shown Figure 13-(c).

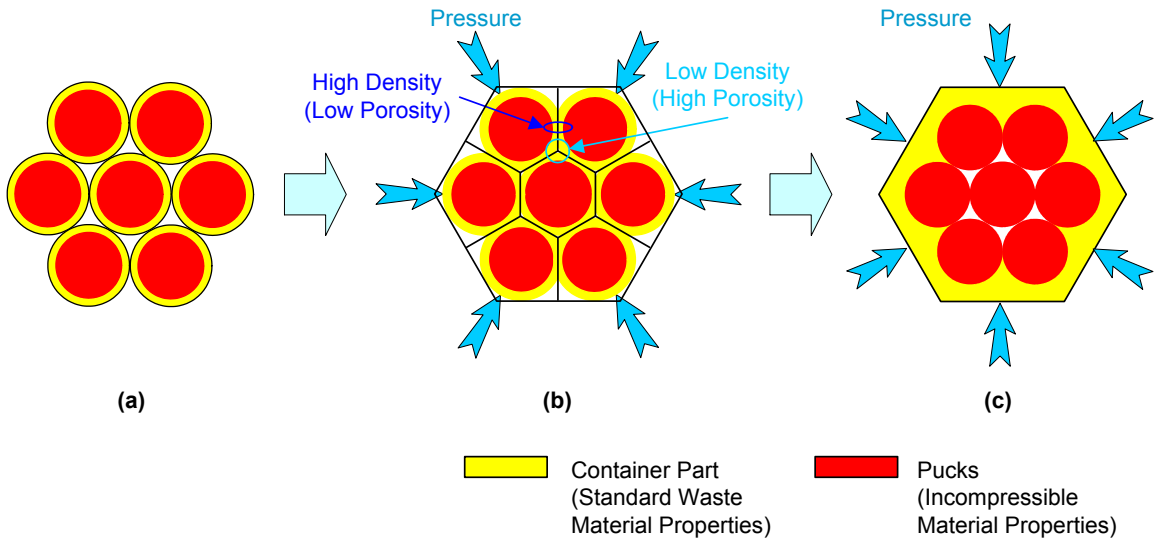

Figure 13: Concept separating pucks and container for mesh generation

Expanding the concept to the model at a room scale, the puck constituents are separated from the compressed container as shown Figure 14. The pucks are represented by rigid material—still possessing the 11% interstitial porosity (Appendix F)—while the compliant material is modeled by an appropriate region comprising elements modeled as standard waste containers. This simplification is felt necessary to capture the possible end-state conditions of a room filled with supercompacted waste packages. In addition, the length and width of the waste inventory is modified as described in Appendix E-1. The width of the mesh consisting of pucks is calculated to be 5.034 m. The height of the puck elements is calculated to be 2.419 m (Appendix D). The widths of the compliant container portions surrounding the pucks are calculated to be 0.455 m (=(5.943-5.034)/2) each. Figure 10-(b) shows the close-up view of the mesh of the disposal room containing AMWTP, as well as the other meshes for comparison.

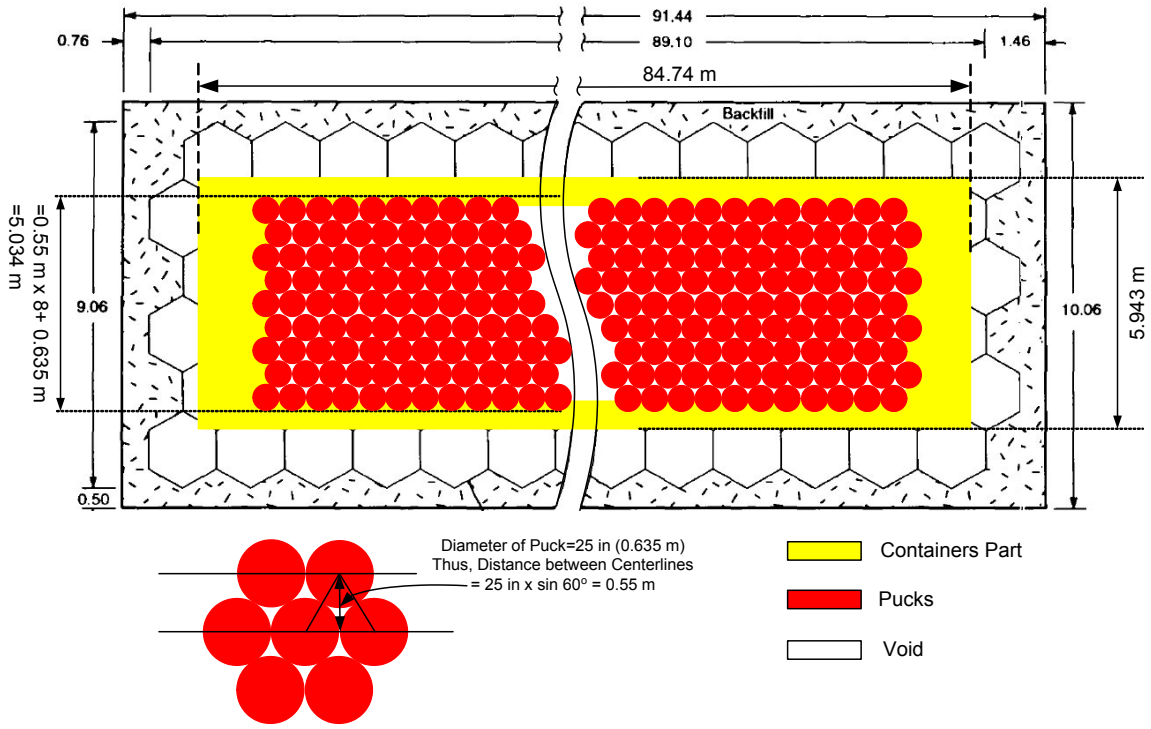

Figure 14: Representation of pucks and containers for a room filled with supercompacted AMWTP.

3.1.2 Combined Case I (2/3 AMWTP + 1/3 Standard Waste)

The line of reasoning above is modified for the combined cases. Simply stated, one third of the pucks are replaced with standard waste elements. For this combined case, the supercompacted AMWTP waste packages are placed in the central portion of the room as shown in Figure 15, compressed as shown in Figure 16 and modeled as shown in Figure 17. Similar to the all-AMWTP case, the effective lateral dimension of the AMWTP containers within the disposal room is determined. The total initial waste volume (V_0) for the all-AMWTP case including the MgO sacks , i.e., 1,596 m^3, is multiplied by 2/3 (1,064 m^3). Dimensional calculations are documented in Appendix E-2.

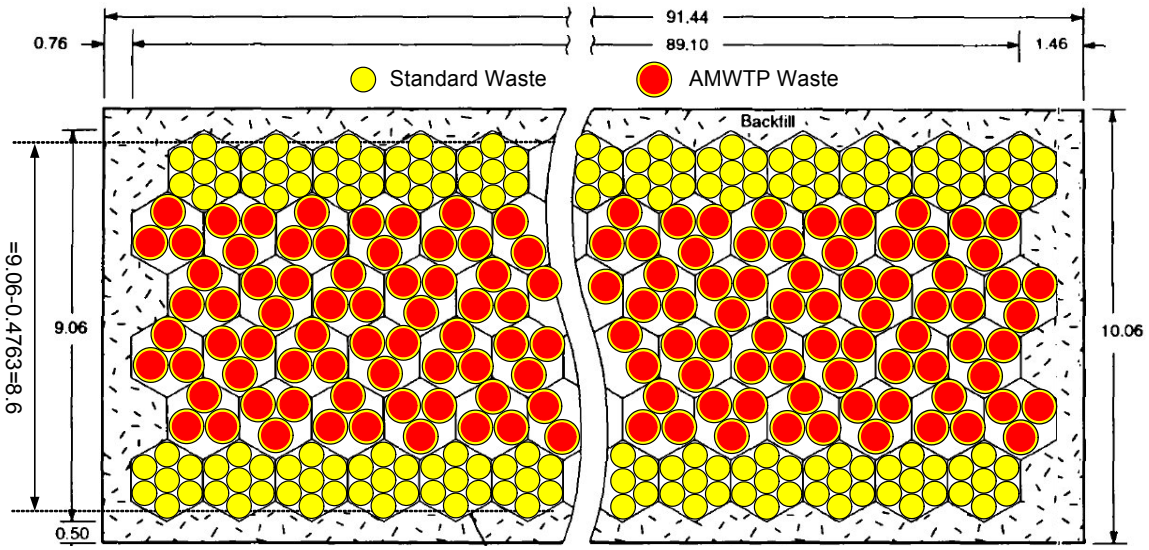

Figure 15: 2/3 AMWTP and 1/3 Standard waste are placed in the room

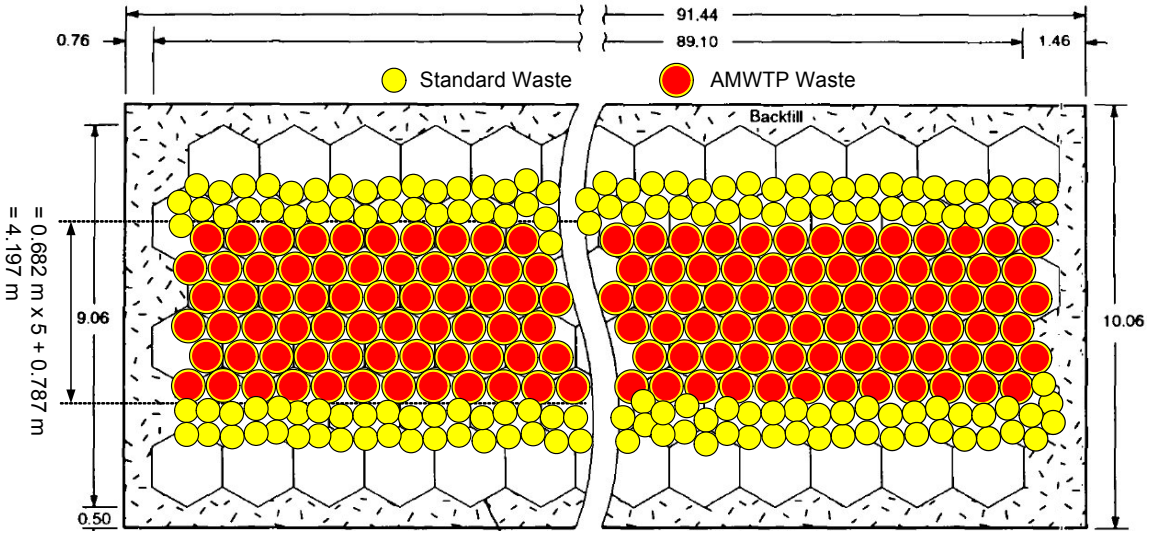

Figure 16: The AMWTP containers are rearranged by the inward movement of the walls

As mentioned in Section 3.3.1, the pucks within the containers are represented by incompressible elements. Figure 17 shows the conceptual drawing used to visualize the width of puck elements of the mesh as separated from the container fraction. The void between incompressible pucks will remain throughout the analysis. The width of the puck elements is calculated to be 3.385 m as shown in Figure 17. The height of the puck elements is 2.419 m, the same as the all AMWTP case. For modeling purposes, the widths of the container elements on both sides of the pucks are calculated to be 0.287 m (= (3.959-3.385)/2)) each. The widths of the standard waste elements, which are modeled on both sides of the AMWTP elements are calculated to be 1.225 ($= 7.35 \cdot \frac{1}{3} \cdot \frac{1}{2}$) m each.

The modified width of the standard waste for mesh generation was calculated to be 7.35 m (Stone, 1997a). The container elements above the stacks represent the compressible materials and MgO and are the same as the all-AMWTP cases (0.75 m). The height of the standard waste elements is assumed equal to the AMWTP plus the complaint material on its top, for modeling simplicity. In actuality, the heights are slightly different (2.676 m versus 3.169 m as shown in Figure 10).

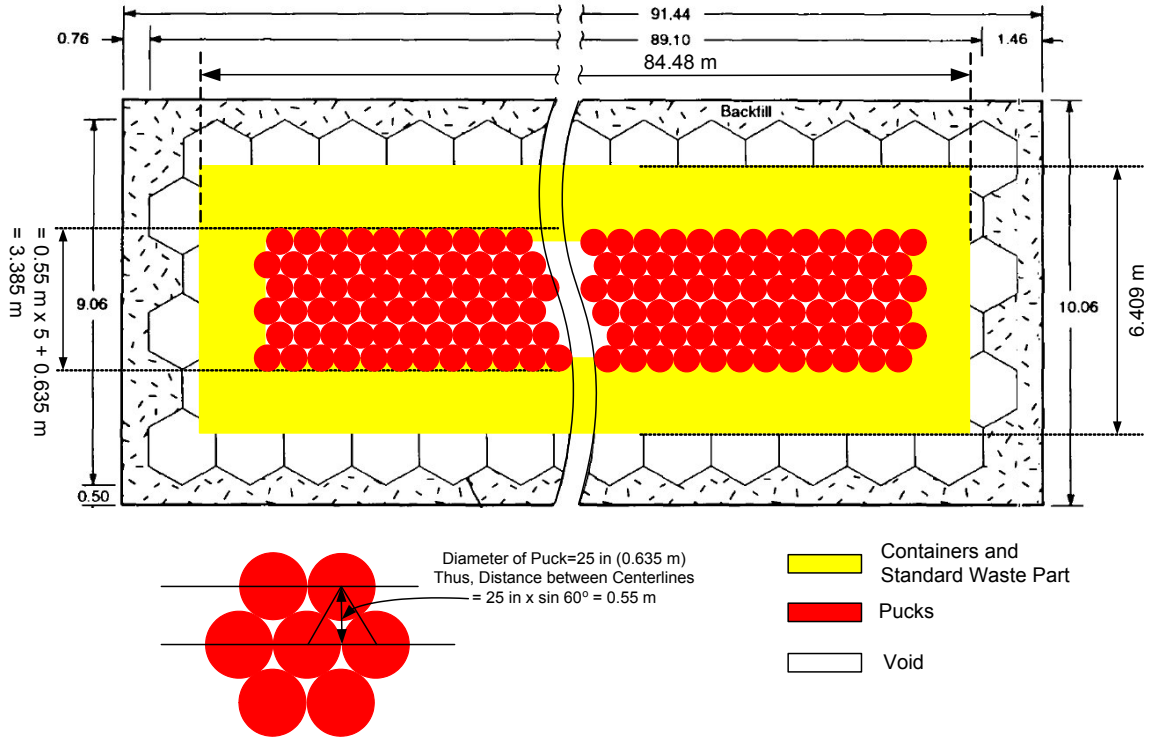

Figure 17: Representation of pucks and containers for a room containing 2/3 AMWTP and 1/3 standard waste packages.

3.1.3 Combined Case II (1/3 AMWTP + 2/3 Standard Waste)

Modeling assumptions begin with two rows of AMWTP packages placed in the center of the room and two rows of standard waste packages rest on either side, as shown in Figure 18. The rows are then compressed together as shown in Figure 19, implementing the same line of assumptions discussed earlier. The nominal uncompressed width of the AMWTP (W_0) is calculated to be 2.151 m (Figure 19). The nominal uncompressed length of the AMWTP (L_0) is calculated to be 85.04 m (Appendix E-3).

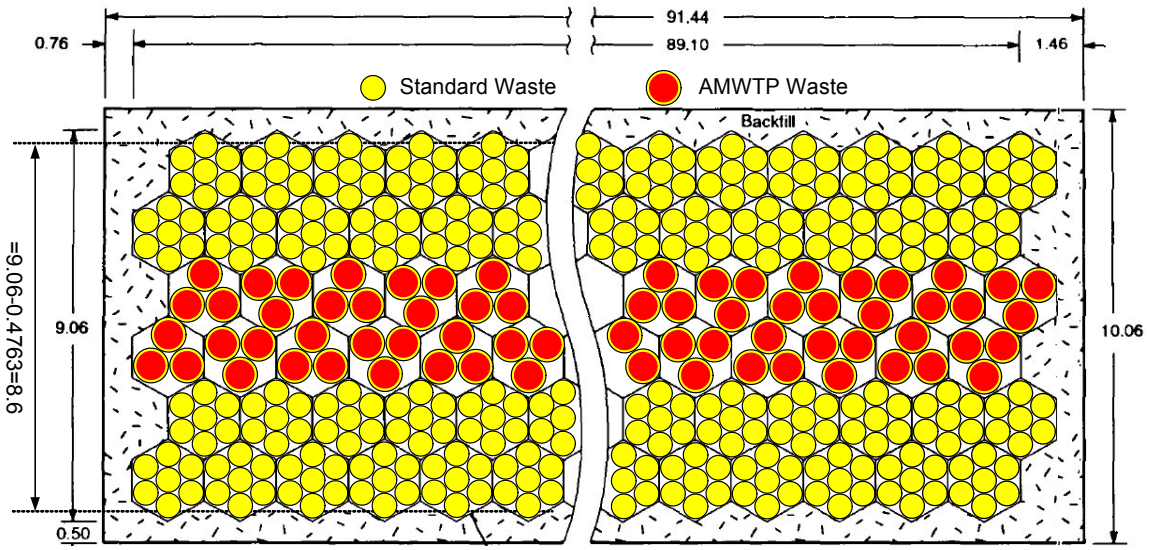

Figure 18: Emplacement of 1/3 AMWTP and 2/3 Standard waste in the disposal room

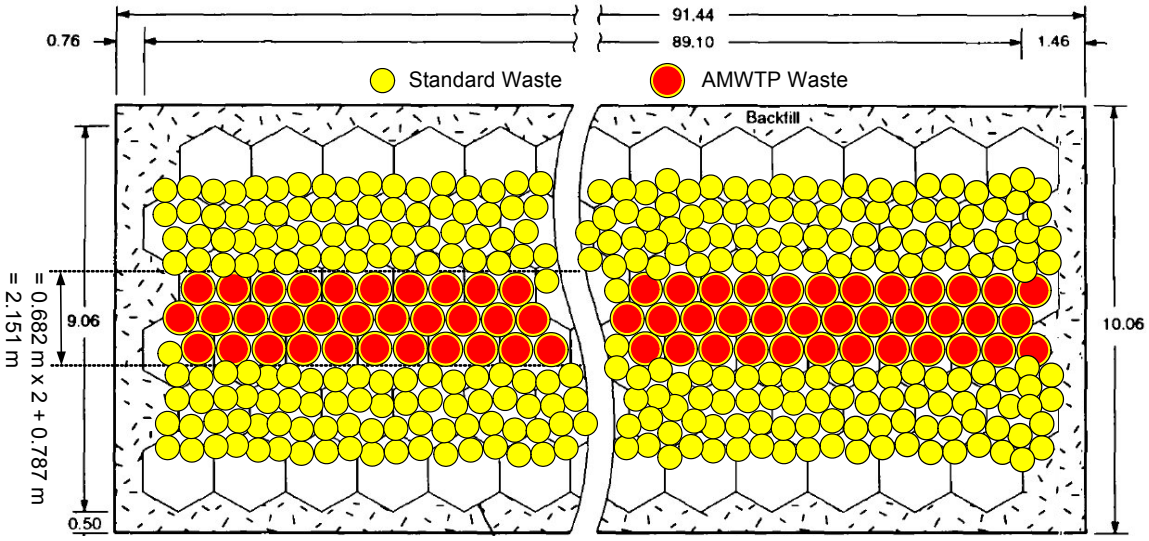

Figure 19: The AMWTP containers are rearranged by the inward movement of the walls

Similar to the previous combined case, the width of the puck elements is calculated to be 1.735 m, as shown in Figure 20. The widths of the container material simulated on either side of the pucks are calculated to be 0.122 m (= (1.978-1.735) / 2) each. The widths of the standard waste elements on both sides are calculated to be 2.45 m ($= 7.35 \cdot \frac{2}{3} \cdot \frac{1}{2}$) each. The container and MgO simulated above the pucks remains the same. Figure 10-(d) shows the close-up view of the mesh of the disposal room containing 1/3 AMWTP and 2/3 standard waste.

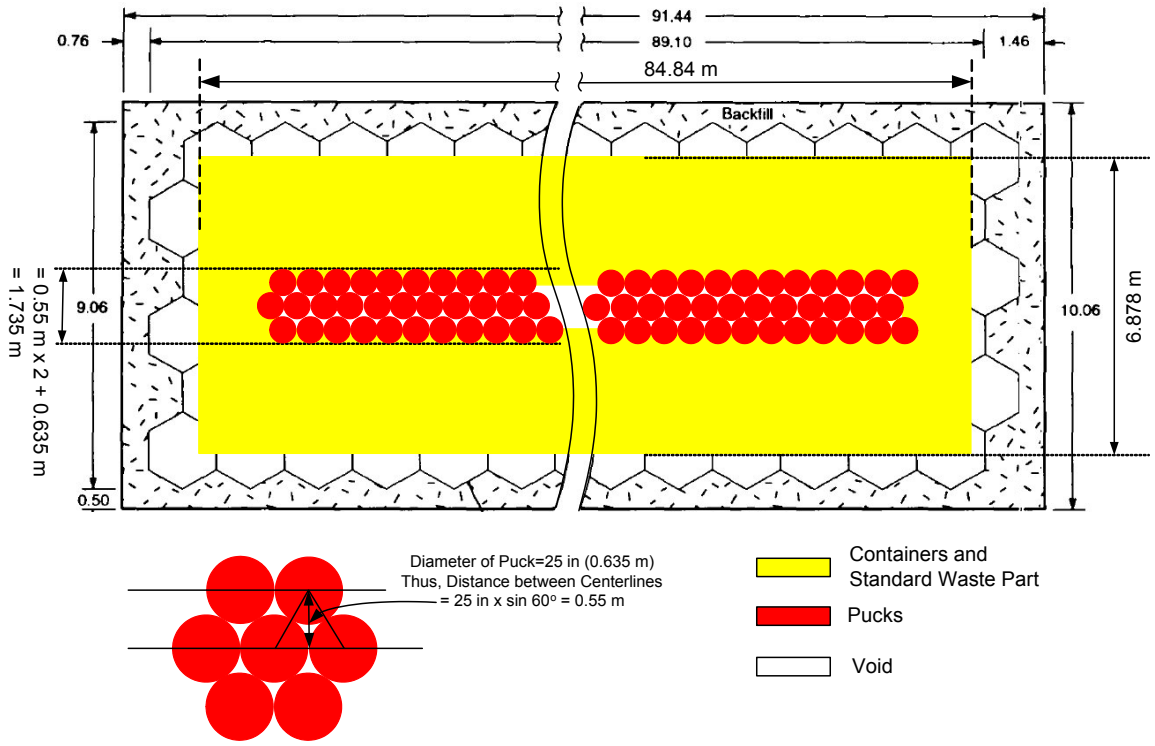

Figure 20: Idealized array separating incompressible and compressible materials for mesh generation

4 CALCULATION FLOW AND FILE NAMING CONVENTION

This section summarizes by name and function the codes used to implement the calculations.

Computer Codes and Calculation Flow

FASTQ version 3.12 is used for the mesh generation. A sample input file for the FASTQ mesh generation is provided in Appendix G. The FASTQ code is an interactive two-dimensional finite element mesh generation program. It is designed to provide a powerful and efficient tool to both reduce the time required of an analyst to generate a mesh, and to improve the capacity to generate good meshes in arbitrary geometries. It has a number of meshing techniques available. FASTQ has been designed to allow user flexibility and control. The user interface is built on a layered command level structure. Multiple utilities are provided for input, manipulation, and display of the geometric information, as well as for direct control, adjustment, and display of the generated mesh. Enhanced boundary flagging has been incorporated and multiple element types and output formats are supported. FASTQ includes adaptive meshing capabilities with error estimation, deformed and undeformed remeshing according to the error, element variable remapping, and some basic post-processing plotting.

SANTOS version 2.1.7 is used for the solver in this analysis. The quasistatic, large-deformation finite element code SANTOS is capable of representing 2D planar or axisymmetric solids (Stone, 1997b). The solution strategy, used to obtain the equilibrium states, is based on a self-adaptive, dynamic-relaxation solution scheme incorporating proportional damping. The explicit nature of the code means that no stiffness matrix is formed or factorized which results in a reduction in the amount of computer storage necessary for execution. The element used in SANTOS is a uniform-strain, 4-node, quadrilateral element with an hourglass control scheme to minimize the effects of spurious deformation modes. Finite strain constitutive models for many common engineering materials are available within the code. A robust master-slave contact algorithm for modeling arbitrary sliding contact is implemented. SANTOS version 2.1.7 was installed on the Compaq Tru64 (BOC) with UNIX V5.1B. All of the verification and qualification test problems were exercised and documented in accordance with QA requirements (WIPP PA, 2003b).

BLOTII2 version 1.39 is used as the final post-processor to plot disposal room creep closure and von Mises stress contours. BLOT is a graphics program for post-processing of finite element analyses output in the EXODUS database format. It is command driven with free-format input and can drive any graphics device supported by the Sandia Virtual Device Interface. BLOT produces mesh plots with various representations of the analysis output variables. The major mesh plot capabilities are deformed mesh plots, line contours, filled (painted) contours, vector plots of two/three variables (e.g., velocity vectors), and symbol plots of scalar variables (e.g., discrete cracks). Path lines of analysis variables can also be drawn on the mesh. BLOT's features include element selection by material, element birth and death, multiple views for combining several displays on each plot, symmetry mirroring, and node and element numbering. BLOT can also produce X-

Y curve plots of the analysis variables. BLOT generates time-versus-variable plots or variable-versus-variable plots. It also generates distance-versus-variable plots at selected time steps where the distance is the accumulated distance between pairs of nodes or element centers. (Gilkey and Glick, 1988).

To calculate the volume change of the disposal room with time, NUMBERS version 1.19 is used. NUMBERS is a shell program that reads and stores data from a finite element model described in the EXODUS database format. Within this program are several utility routines that generate information about the finite element model. The utilities currently implemented in NUMBERS allow the analyst to determine information such as: (1) the volume and coordinate limits of each of the materials in the model; (2) the mass properties of the model; (3) the minimum, maximum, and average element volumes for each material; (4) the volume and change in volume of a cavity; (5) the nodes or elements that are within a specified distance from a user-defined point, line, or plane; (6) an estimate of the explicit central-difference time step for each material; (7) the validity of contact surfaces or slide lines, that is, whether two surfaces overlap at any point; and (8) the distance between two surfaces. (Sjaardema, 1989).

These pre- and post-processing utilities are considered systems software and not subject to the requirements of NP 19-1 (Chavez, 2003).

To calculate the porosity change in the room as a function of time, GNU AWK version 3.1.0 is used. The AWK converts the volume change of the disposal room into the porosity change with time. A sample AWK script is provided in App. H.

The code (n-dimensional Statistical Inverse Graphical Hydraulic Test Simulator) version 1.00 is used for plotting the three-dimensional porosity surface and is only used for visualization, not for any quality-affecting analyses. nSIGHTS was developed as a comprehensive well test analysis software package. It provides a user-interface, a well test analysis model and many tools to analyze both field and simulated data. The well test analysis model simulates a single-phase, one-dimensional, radial/non-radial flow regime, with a borehole at the center of the modeled flow system (Sandia National Laboratories, 2002). In this report, the function of plotting a 3D surface is the only feature used.

Figure 21 shows the computational flowchart to determine the porosity surface of the disposal room containing various waste inventories for WIPP PA.

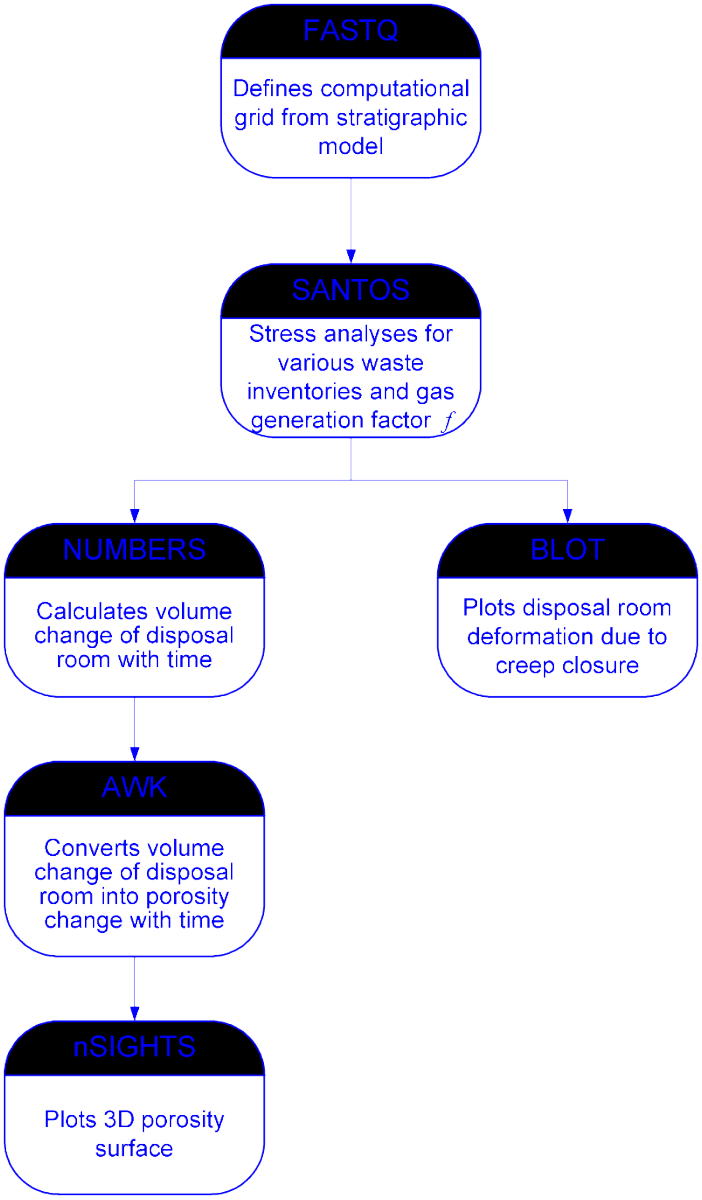

Figure 21: Computational flowchart to determine the porosity surface

File Naming Convention

All files related to porosity surface calculations are stored on BOC, which is a workstation for WIPP project. The general path for any of these subdirectories is /.../waste/poro/. All files related to the analyses for the disposal room containing 12-inch POPs are in the subdirectory /…/waste/poro/pop12/. Similarly, the subdirectory /…/waste/poro/pop06/ is for the 6-inch POP analyses, /…/waste/poro/1puck/ is for the combined cases of 1/3 AMWTP and 2/3 standard waste, /…/waste/poro/2puck/ is for the combined cases of 2/3 AMWTP and 1/3 standard waste, and /…/waste/poro/3puck/ is for

the disposal room containing all AMWTP waste. The detail descriptions of each dictionary on BOC are listed in Table 8.

Table 8: Directory descriptions for porosity surface calculations

Directories	Descriptions of stored files
/data1/bypark/waste/poro/pop06	Related to the porosity surface calculation for 6-inch POPs
/data1/bypark/waste/poro/pop12	Related to the porosity surface calculation for 12-inch POPs
/data2/bypark/waste/poro/2puck	Related to the porosity surface calculation for Combined Case I (2/3 AMWTP + 1/3 standard Waste)
/data3/bypark/waste/poro/3puck	Related to the porosity surface calculation for all AMWTP case
/data3/bypark/waste/poro/report	Related to the report for this analysis
/data3/bypark/waste/poro/calc_sheet	Related to the calculation sheets
/data5/bypark/waste/poro/1puck	Related to the porosity surface calculation for Combined Case II (1/3 AMWTP + 2/3 Standard Waste)

All the files stored in each subdirectory are listed and described in Table 9. The file suffixes, 0p0, 0p025, 0p05, 0p1, …, etc. express the gas generation factors. For examples, the 0p0 means the gas generation factor is f=0.0, 0p1 means f=0.1, 1p2 means f=1.2, and so forth.

The FASTQ file names are 0.00up.fsq, 1puck.fsq, 2puck.fsq and 3puck.fsq. The 0.00up means the current disposal room containing the standard waste or the POP waste, and the 1puck.fsq means the disposal room containing 1/3 AMWTP and 2/3 standard waste.

Table 9: File naming convention for porosity surface calculations (* means wild card)

File Prefix/Suffix	File Definition
*.fsq	The FASTQ input files for the mesh generation
*.g	The FASTQ output files that will be used for the mesh file of SANTOS
*.i	The SANTOS input files
*.e	The SANTOS output files in the EXODUS database format
*.o	The SANTOS output files in the ASCII format
initst_*.f	The user-supplied subroutine INITST to provide an initial stress state and the FPRES to provide the gas generation parameter, *f*, to SANTOS
initst_*.o	The object files from compiling the *.f
porosity.awk	This AWK script computes the porosity change in the room as a function of time
num_curr.inp	The NUMBERS input script file to calculate the room volume change
*.num	The NUMBERS output file in the ASCII format to calculate the volume change of the disposal room with time from the SANTOS output files, *.e
normal*.txt	The normalized volume change of the disposal room from *.num

run*.log	The log file from the SANTOS run
*_pgas.dat	The result file of the gas pressure change in the disposal room
poro*.dat	The result file of the porosity change in the disposal room
SANTOS_data_for_BRAGFLO_*.xls	The excel file containing the porosity history data transferred to BRAGFLO analysis team
*.run	The batch files for running SANTOS
XYZ_*.grd	The three dimensional data for plotting the porosity surfaces
*.mcd	The Mathcad file to provide the calculation sheets
*.doc	The MS Word files for the report

5 ANALYSES RESULTS

In performance assessment calculations, room closure initially proceeds as if the room were open. The free air space is eliminated early by creep closure without resistance from the waste package. Eventually the salt contacts the waste package stacks and deforms the waste package according to the relevant response model. At the same time, the conceptual models for corrosion and gas generation allow internal pressure to build within the room. Thus, the room closure owing to salt creep is modified by the structural response of the waste and by gas generation. These competing conditions (creep closure, waste package rigidity, gas generation) yield porosity histories for each waste package configuration that are compiled into a porosity surface for incorporation into performance assessment calculations as described in Section 2.2.

Closure calculations for a room containing the standard waste inventory (i.e., the baseline waste packages underpinning the CCA) were completed as part of the assessment of the effects of raising the repository to Clay Seam G (Park and Holland, 2003). An additional five hypothetical waste inventory configurations were considered to evaluate maximal possible variations in room closure. To recap, the cases being considered include:

1. All standard waste (55-gallon drums)
2. All 6-inch POPs
3. All 12-inch POPs
4. A combination of 1/3 supercompacted waste and 2/3 standard waste
5. A combination of 2/3 supercompacted waste and 1/3 standard waste
6. All supercompacted waste

As explained in Section 5.2, thirteen cases of gas generation were investigated for each inventory type. All analyses were run for a simulation time of 10,000 years. Representative examples of input files for the 12-inch POP and the all-AMWTP SANTOS runs are included in Appendix I. The other input files are identical except for the title line and the waste data. The gas generation parameter, f, is set in the user-supplied subroutine FPRES. Stone (1997a) used the user-supplied subroutine INITST to provide an initial stress state to SANTOS. In this analysis, the INITST subroutine is used unchanged from Stone (1997a). A sample INITST and FPRES subroutine for all AMWTP with f=0.1 is also given in Appendix J. In the SANTOS runs, gas pressure bleed-off by flow through the surrounding lithology is not permitted.

Disposal Room Creep Closure

The computational results are best illustrated by figures. The following discussion displays all six cases to facilitate comparison of results. As noted in the analysis report (Park and Hansen, 2004) that examined the structural rigidity of the pipe overpack, the results of the 6-inch and 12-inch pipe overpacks are essentially identical. The figures of both overpacks have been retained here for completeness.

Figures 22 to 27 illustrate room closure as a function of time—without gas generation. Figure 22 replicates the room closure calculations that comprise the CCA baseline with the room full of standard waste packages. In the first few years the roof rock will contact

the waste stack. Observations in Panel 1 confirm this rate of room closure (see Hansen, 2003). Approximately one meter of salt was trimmed to re-establish the vertical dimension of four meters after the rooms had stood open for about twelve years. After the creeping salt contacts the waste stack, the standard waste offers backstress to the salt in accord with the volumetric plasticity model incorporated in SANTOS.

Figures 23 and 24 illustrate room closure for the cases in which the rooms are filled entirely with 6-inch and 12-inch POPs, respectively. The closure of the open space in the rooms is identical in all simulations until the country rock impacts the waste stack. Thereupon, the POPs offer considerably more resistance to closure than offered by standard waste packages.

The simulations that include AMWTP supercompacted waste forms also included MgO on top of the waste. Vertical dimensions of the waste stack are slightly greater (0.5m) to account for the MgO, which is simulated structurally as standard waste. The inconsistency of inclusion or exclusion of the MgO was discussed previously. In terms of mechanical response and global features of these analyses, the inclusion or exclusion of MgO makes little difference to the major phenomena. The rigidity of the AMWTP supercompacted waste, however, has a strong influence on room closure.

Figures 25, 26 and 27 illustrate the room closure response for simulations including 1/3 AMWTP, 2/3 AMWTP, and a room filled with AMWTP supercompacted waste packages. The modeling assumptions implemented to define grid elements for the waste were recounted in Section 3.3. The assumptions were consistent with those applied to the original calculations of the porosity surface in that the free air space was removed by effectively pushing the waste together. For the AMWTP, the pucks are modeled as a rigid material and the free air space, the annular space, and the vertical open space in the containers are simulated as compliant material surrounding the pucks. All the dimensions of these elements account for the actual amounts of compliant material and rigid pucks. Room closure is eventually dominated by the cribbing effect of the pucks, even when the room is only 1/3 third full of the AMWTP wastes.

This phenomenon is illustrated most clearly in this sequence of figures, because no gas is produced inside the room. Gas production would counterbalance the inward creep of the rooms, as will be discussed subsequently. The cribbing effect will be discussed in more detail in Section 6.

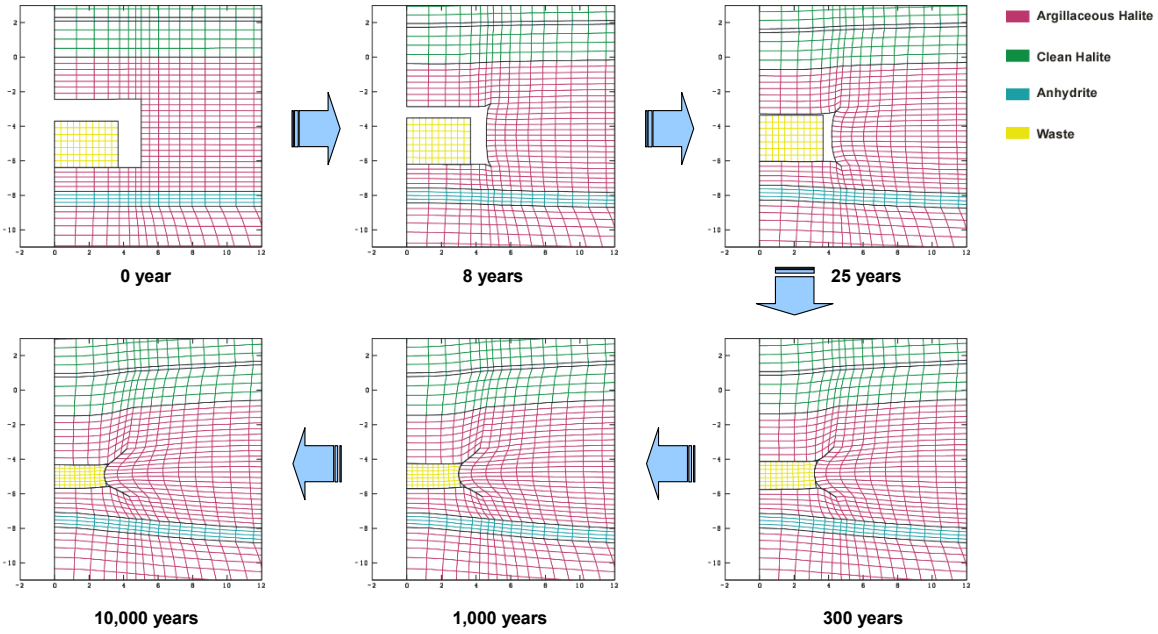

Figure 22: Close-up views of the deformed disposal room containing the standard waste for *f*=0.0

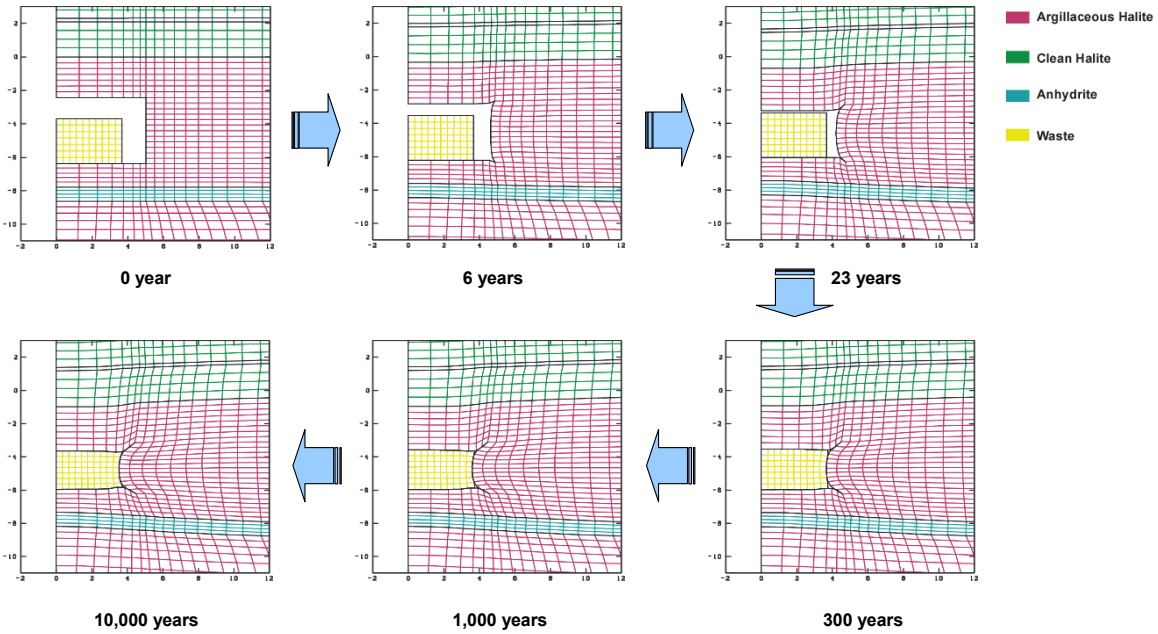

Figure 23: Close-up views of the deformed disposal room containing the 6-inch POP waste for *f*=0.0

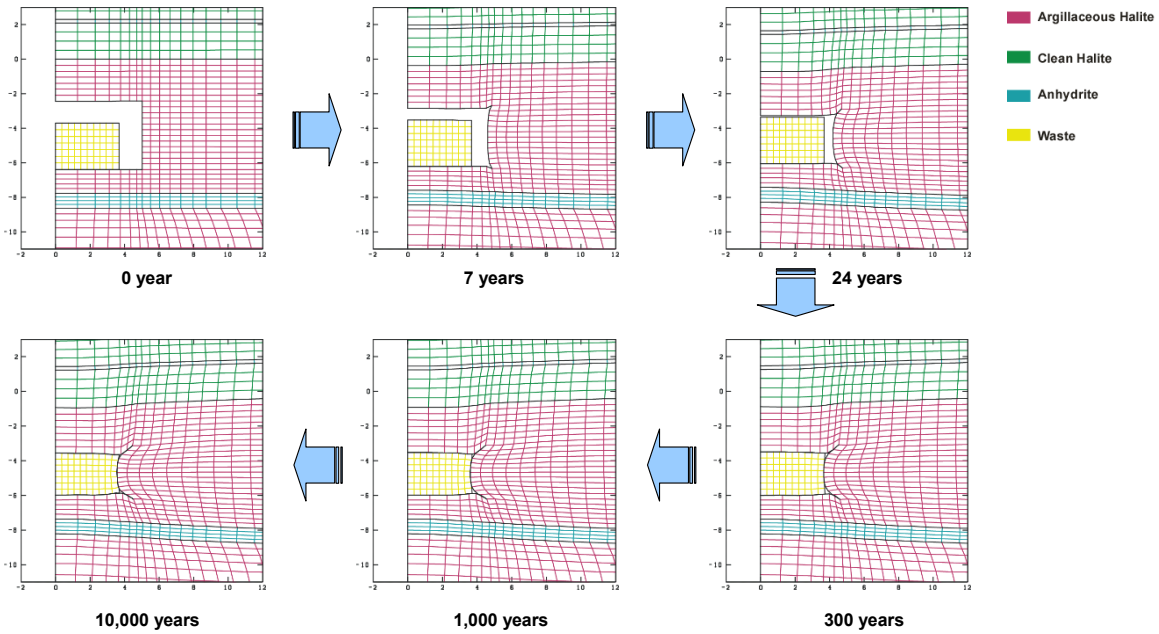

Figure 24: Close-up views of the deformed disposal room containing the 12-inch POP waste for *f*=0.0

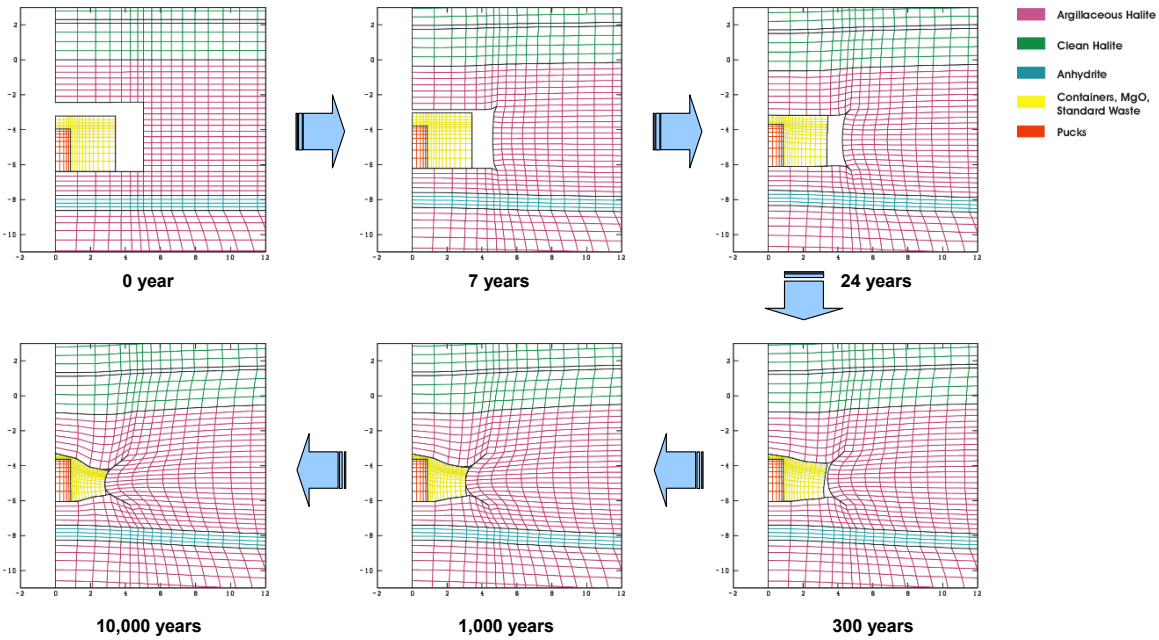

Figure 25: Close-up views of the deformed disposal room containing the 1/3 AMWTP + 2/3 Standard waste for *f*=0.0

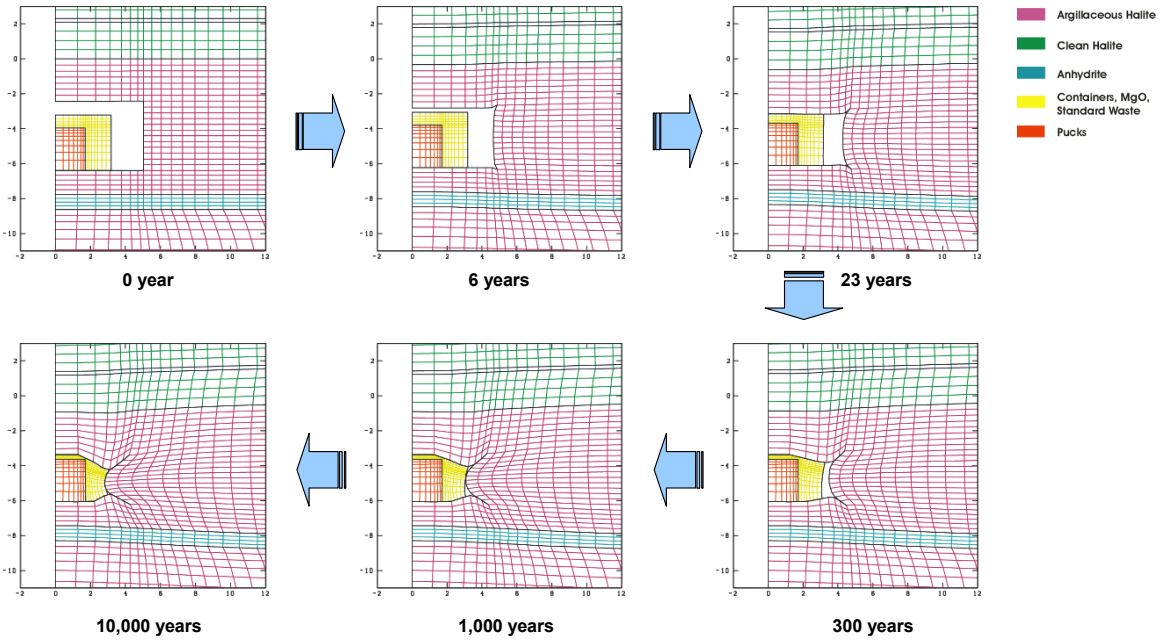

Figure 26: Close-up views of the deformed disposal room containing the 2/3 AMWTP + 1/3 Standard waste for f=0.0

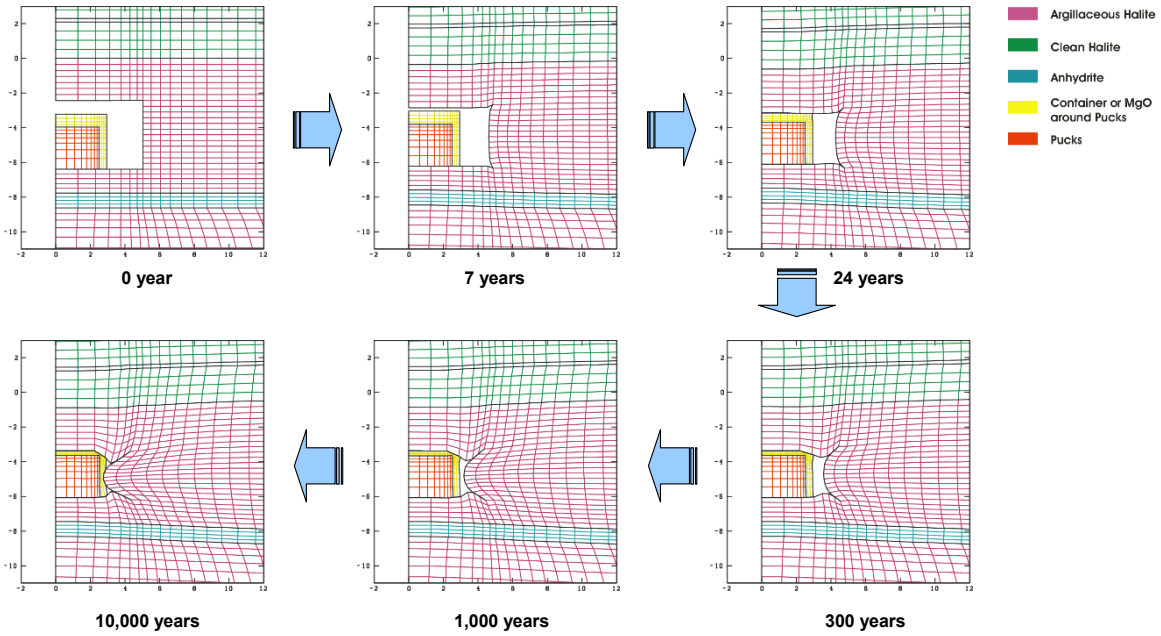

Figure 27: Close-up views of the deformed disposal room containing the All AMWTP waste for f=0.0

Pressure Histories

Figures 28 through 33 plot gas pressure history for the six case studies of hypothetical waste inventories. The resulting pressure histories calculated by SANTOS are meant to envelop the pressure histories calculated by BRAGFLO (WIPP PA, 2003a). Thirteen gas generation scenarios for SANTOS are determined by multiplying a base gas generation potential and rate by a factor, *f*, as follows: *f*=0.0 (no gas generation), 0.025, 0.05, 0.1, 0.2, 0.4, 0.5, 0.6, 0.8, 1.0, 1.2, 1.6, and 2.0 (twice the base rate). Thus, SANTOS runs consider cases from no gas generation ($f = 0$) to cases in which the total amount of gas and rate at which it is produced is twice the base gas generation potential and rate ($f = 2$).

The base gas generation potential used in the CCA and CRA is set at 1050 moles of gas/drum from corrosion and 550 moles of gas/drum from microbial degradation. The base gas production rate is set at 1 mole of gas per drum per year for corrosion and 1 mole of gas per drum per year for microbial degradation. Since the rate and the potential vary by the same *f* - factor, gas production rates vary between 0 and 4 moles/drum/year for 550 years, when corrosion and microbial degradation occur simultaneously. From 550 to 1,050 years gas is produced only from corrosion at half the full rate (from 0 to 2 moles/drum/year). No additional gas is produced after 1,050 years.

The pressure build up in the disposal room is a result of gas generation and available room porosity. Figures 28 through 33 show the disposal room pressure histories for the various values of gas generation parameter, *f*, for each waste inventory in the room. The amount of gas generated from the POP waste package is identical to that of standard waste, as described in Section 2.2. However, as shown Figures 29 and 30, the pressure histories of POP for lower *f* reflect much lower pressure than that experienced in rooms filled with standard waste. Greater void space is retained in the rooms filled with the POP waste because of the rigidity of the POP, which cribs the room open relative to the standard waste. Therefore, for the same amount of gas production, the POP rooms would have lower gas pressure.

In the case of AMWTP wastes, the amount of gas production varies in proportion to the amount of celluloses, plastics and rubber (CPR). Gas generation from iron-based metal corrosion is similar for all waste types. The amount of gas generated by corrosion is brine-limited, so the amount of gas produced in this manner is the same whether the waste is packaged as AMWTP, standard waste, POP or any other packaging. The differences in gas generation noted in the pressure profiles are a reflection of the microbial gas generation. As noted in Section 2.2, the total gas production is a function of CPR available for microbial consumption. A room full of supercompacted AMWTP increases the ratio of CPR from the original compliance basis by a factor of 12/7, because each seven pack of standard waste is replaced on the same footprint by 12 supercompacted pucks.

The deformed shapes and volumes of the disposal rooms also differ somewhat because of the structural resistance of the various ratios of AMWTP disposed in the room. The pressure histories are influenced by a competing interaction between the room closure and the amount of gas. In a general sense, the pressure histories of these various runs are strikingly similar. The gas pressures for more than f=1.0 at 10,000 years cluster around 18.0 MPa for all cases.

The results displayed from the SANTOS calculations exhibit pressures higher than lithostatic stress (approximately 15 MPa). This is a modeling artifact that occurs because SANTOS does not have a fracture mechanism to bleed off high gas pressure. BRAGFLO, on the other hand, allows hydrofracture to proceed when internal gas pressure approaches lithostatic. However, because the transient pressures in BRAGFLO may exceed lithostatic, the pressures from SANTOS are necessary to provide a full range of porosity values.

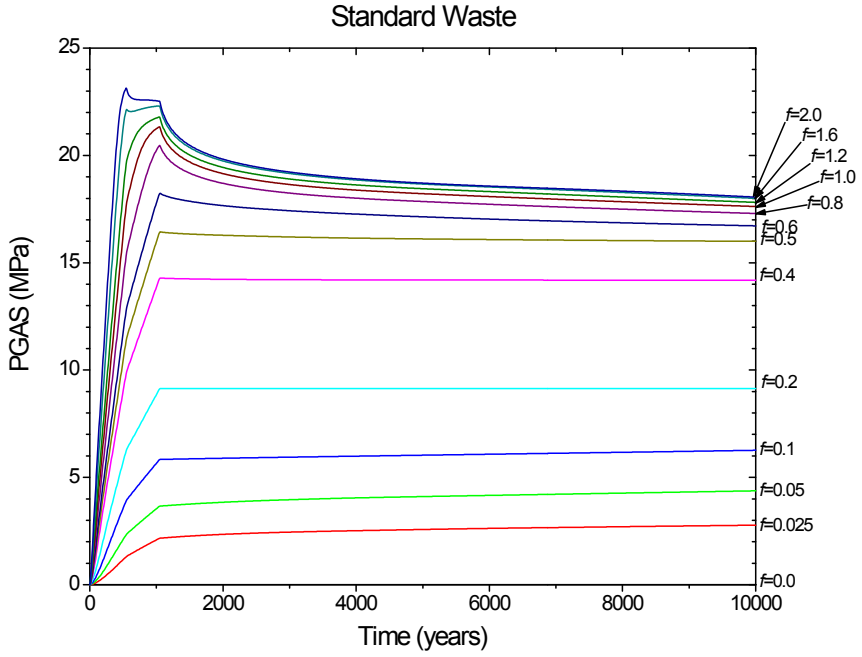

Figure 28: Pressure histories for a disposal room containing the standard waste

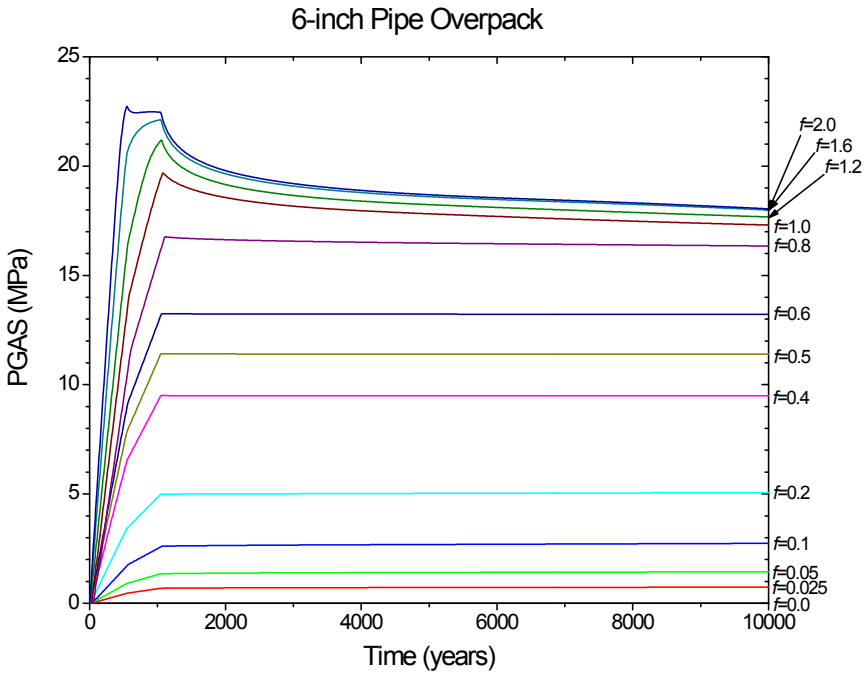

Figure 29: Pressure histories for a disposal room containing the 6-inch POP waste

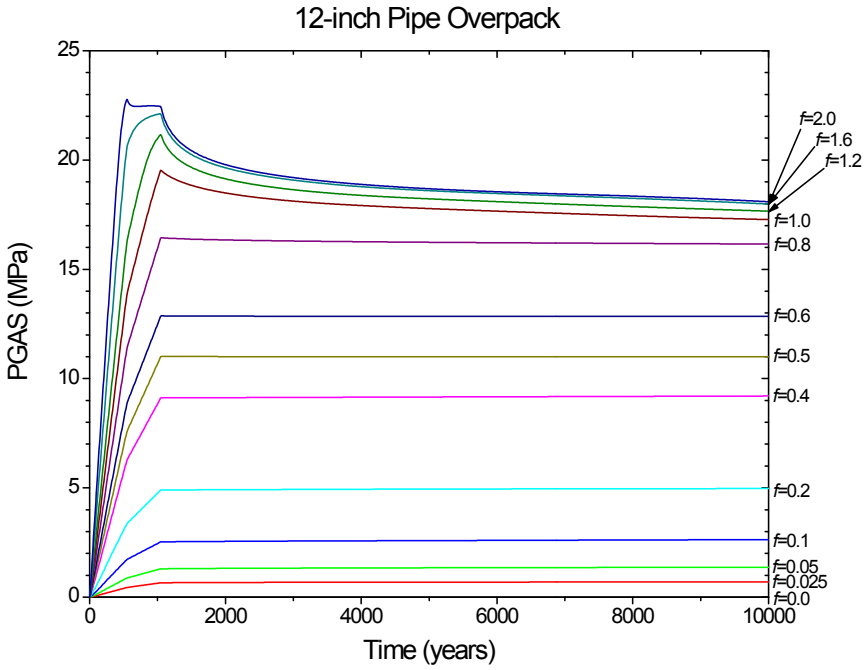

Figure 30: Pressure histories for a disposal room containing the 12-inch POP waste

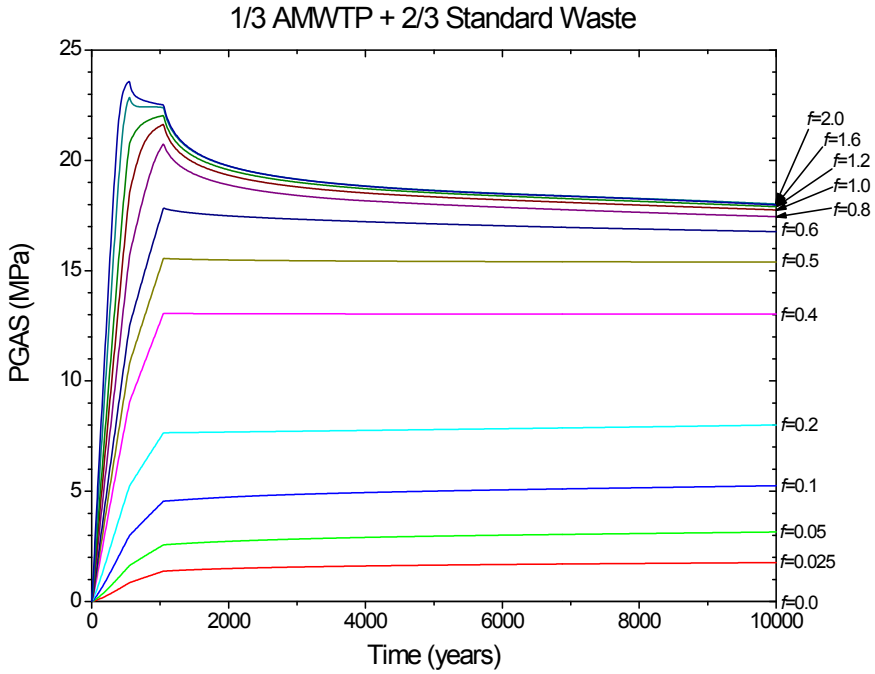

Figure 31: Pressure histories for disposal room a containing the 1/3 AMWTP + 2/3 Standard waste

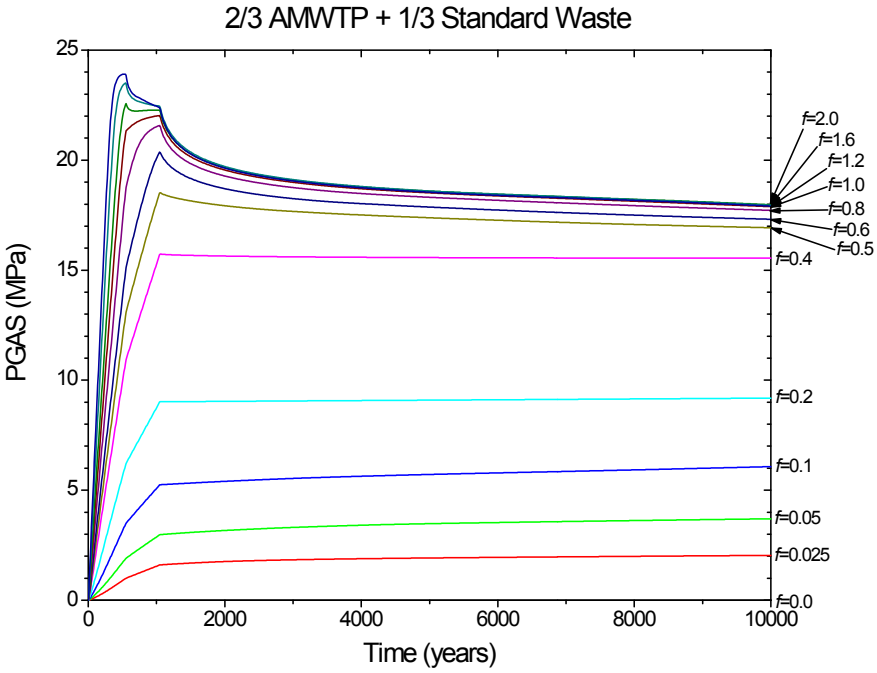

Figure 32: Pressure histories for disposal room a containing the 2/3 AMWTP + 1/3 Standard waste

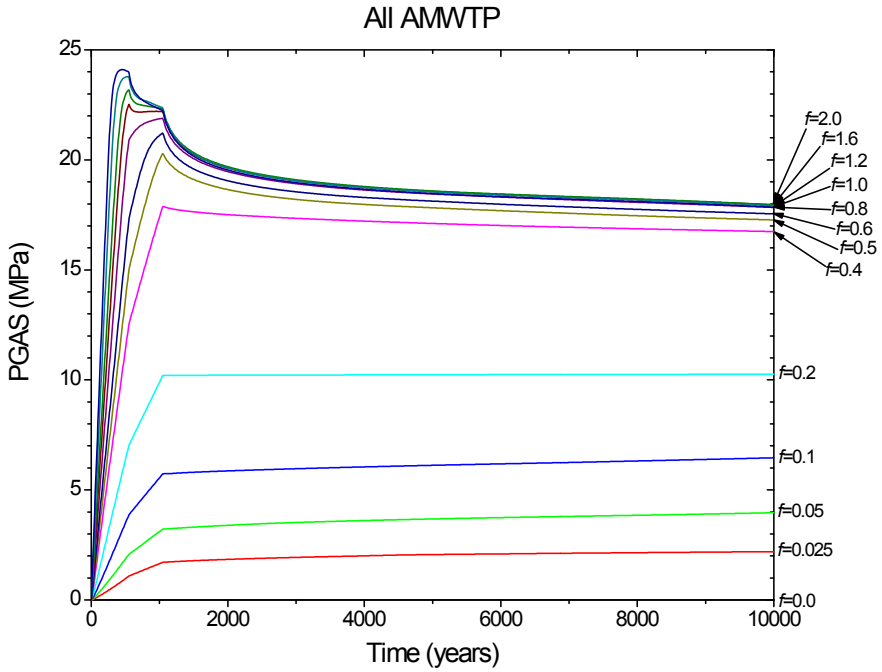

Figure 33: Pressure histories for a disposal room containing the AMWTP waste

Porosity Histories

The SANTOS calculations provide porosity surface input for BRAGFLO simulations (Helton et al., 1998). The porosity surface is essentially a lookup table that gives the value of room porosity in the BRAGFLO grid for a given pressure and time. The SANTOS calculations are run only for a discrete set of representative gas generation scenarios to provide a wide range of porosity results. In contrast, gas generation simulated by BRAGFLO occurs at rates determined by sampled parameters and temporally and spatially varying brine saturation levels. These rates are completely independent of the rates used in the SANTOS calculations. Pressures calculated in BRAGFLO simulations are used to determine waste room porosity by way of interpolating porosity values from the porosity lookup table. This procedure is described below.

Each of the thirteen SANTOS calculations results in a distinct pressure and porosity history (as shown in the following Figures 28 through 39). The porosity calculated by SANTOS is the "true" porosity, meaning it is the porosity that one would expect to measure if one could access a representative piece of the waste room at some time in the future. Because SANTOS simulates room closure, the total volume of the waste rooms changes with time and pressure. In contrast, BRAGFLO employs a non-deformable mesh and thus the total volume of the waste rooms remains constant for the entire 10,000-year simulation. The porosity values used by BRAGFLO for the waste rooms are modified from the "true" porosity values calculated by SANTOS to preserve total pore volume. The BRAGFLO porosity is related to the SANTOS porosity by the following relationship:

$$\phi_B = \frac{\phi_S V_S}{V_B} \tag{3}$$

where ϕ is porosity, V is room volume, and the subscripts indicate values for BRAGFLO (B) and SANTOS (S). V_S changes as rooms creep close; V_B remains constant (and greater than V_s) and thus ϕ_B is always somewhat less than ϕ_S.

The pressure and modified BRAGFLO "porosity" histories for the thirteen closure scenarios form the porosity lookup table used by BRAGFLO. Porosity is interpolated by identifying the two *f*-values for which the SANTOS pressure brackets the pressure in BRAGFLO at the particular simulation time being considered. During a BRAGFLO simulation, it is possible that the pair of *f*-values used for the porosity interpolation may change as the simulation proceeds. If BRAGFLO pressures ever exceed the range defined by the SANTOS scenarios, the calculation of porosity defaults to the $f = 2$ scenario.

Figures 34 through 39 show the disposal room porosity histories for the thirteen cases of gas generation considered for each waste inventory. For the case involving standard waste, as shown Figure 34, there are large differences in the histories for each gas generation factor. These results replicate the porosity surface calculations in the CCA,

and were replicated most recently by Park and Holland (2003). The situation for a room filled with POP waste packages, as shown in Figures 35 and 36, is substantially different at low gas production rates because the small amount of gas produced fills a relatively open room (held open by the POPs). For the AMWTP cases as shown in Figures 37 through 39, the porosity trends have similar patterns, although there are slight differences owing to the ratio of AMWTP disposed. The distribution of porosity histories at low *f* is broader in the cases involved with AMWTP waste than in the cases of the POP's because room closure still proceeds over the 10,000 years due to the compressible elements surrounding the relatively small volume of the supercompacted pucks.

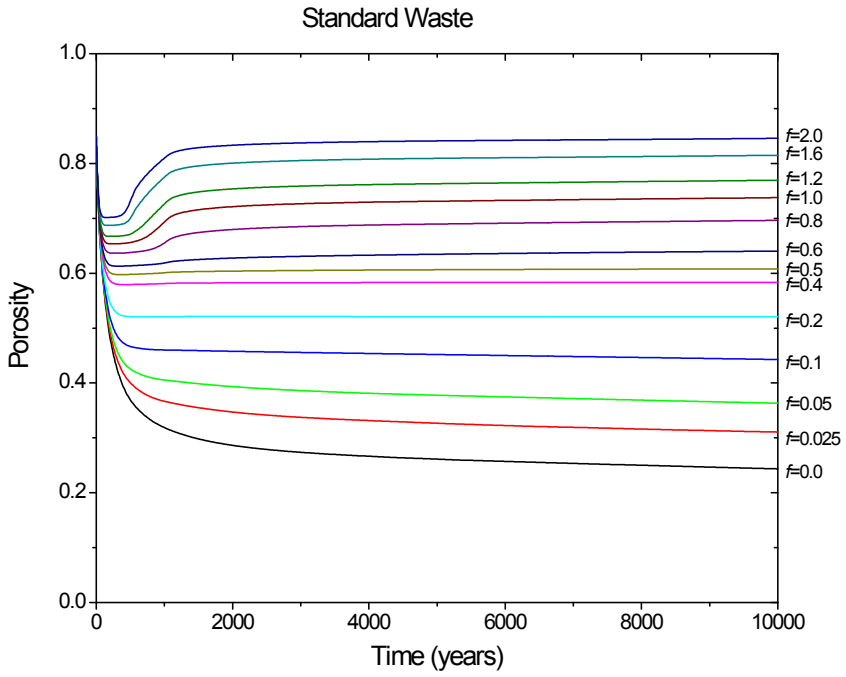

Figure 34: Porosity histories for a disposal room containing the standard waste

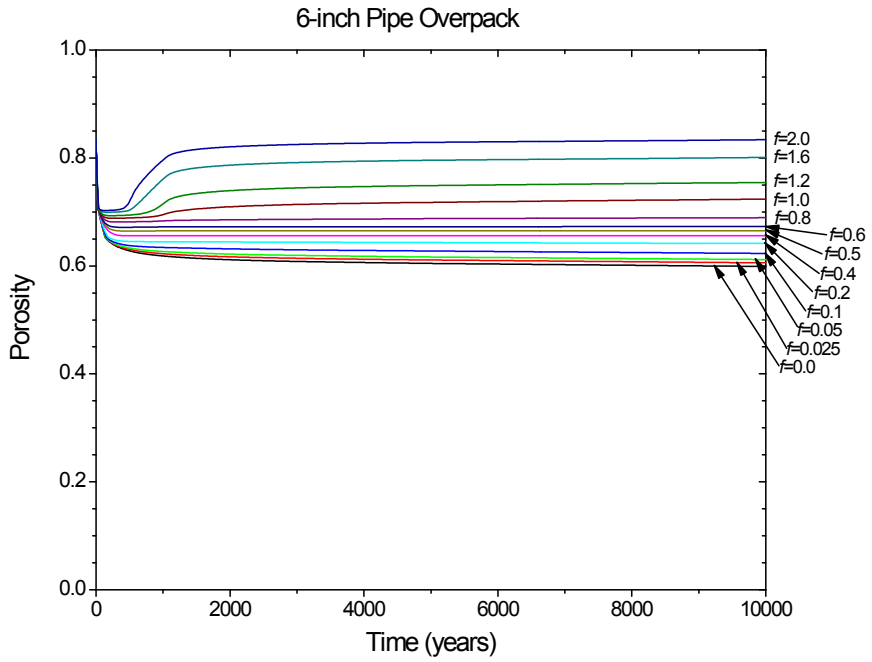

Figure 35: Porosity histories for a disposal room containing the 6-inch POP waste

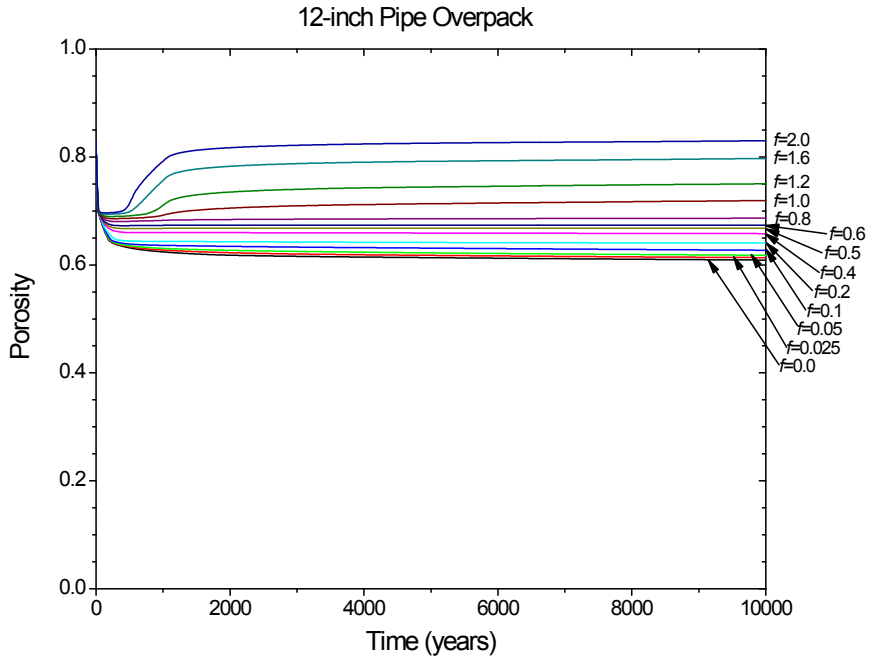

Figure 36: Porosity histories for a disposal room containing the 12-inch POP waste

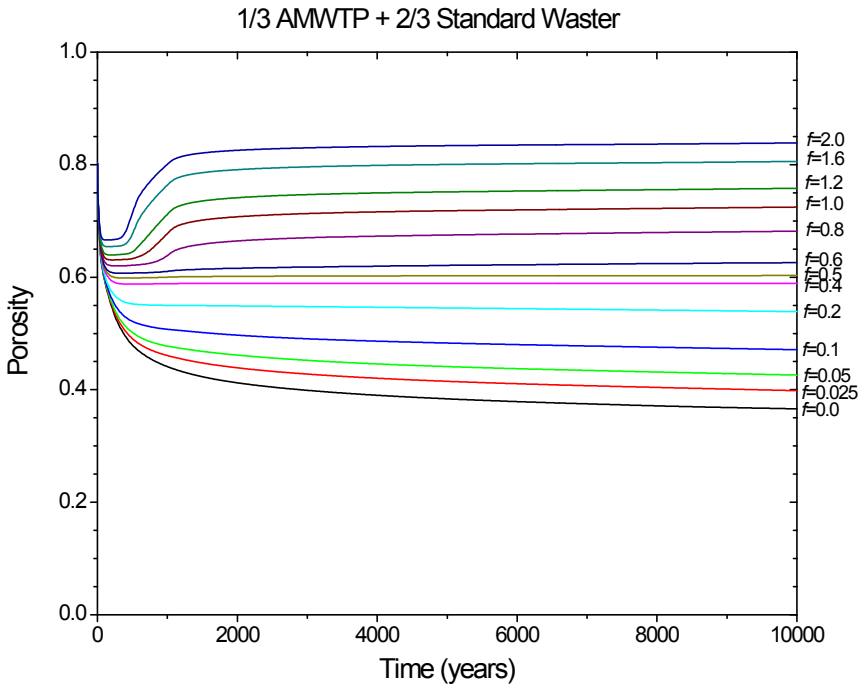

Figure 37: Porosity histories for a disposal room containing 1/3 AMWTP+2/3 standard waste

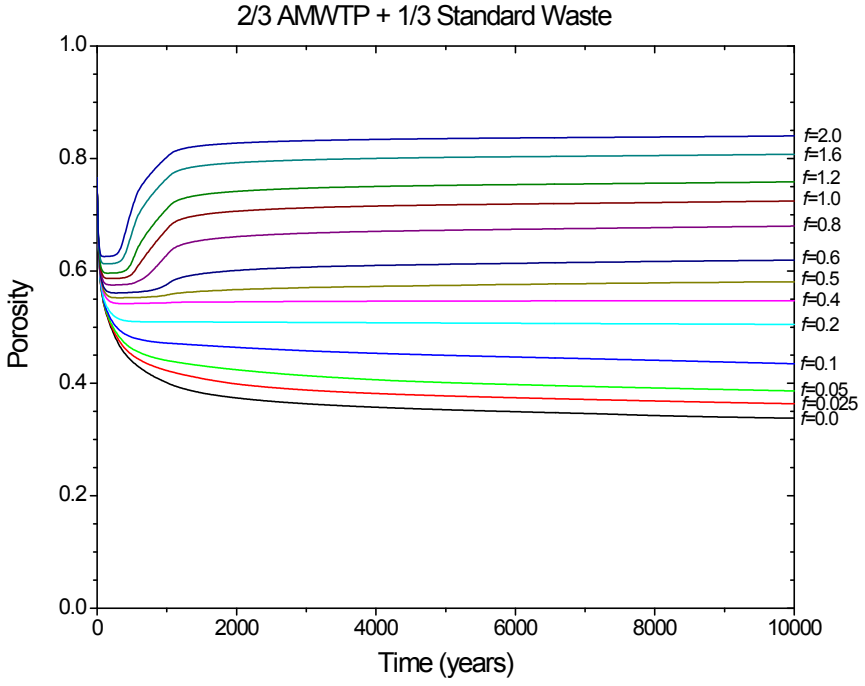

Figure 38: Porosity histories for a disposal room containing 2/3 AMWTP+1/3 Standard waste

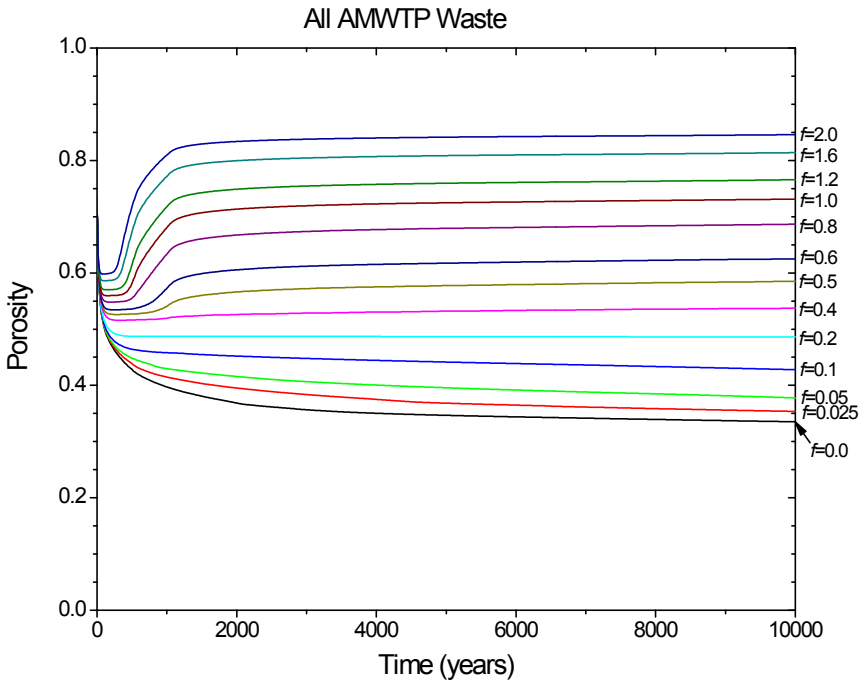

Figure 39: Porosity histories for a disposal room containing all AMWTP waste

Porosity History Comparisons

The next sequence of figures (Figures 40 through 43) compares the porosity surfaces for the six cases over the 10,000 year simulation period for selected gas generation factors of 0.0, 0.4, 1.0, and 2.0. The histories for all thirteen *f* values are provided in Appendix K. The initial porosities are actually very similar because the solid material comprises little of the available space in a room, regardless of packaging. Initial porosity used for these plots are as follows: standard wastes (0.849), 6-inch POPs (0.835), 12-inch POPs (0.831), 1/3 AMWTP (0.802), 2/3 AMWTP (0.766), and all AMWTP (0.739). The all AMWTP case includes MgO in the calculation of initial porosity. However, the standard waste and POP calculations do not include MgO; if MgO is included the initial porosity would be about 5% lower.

In the case of no gas generation, the standard waste as modeled in the CCA has the smallest porosity, 0.243, and 12-inch POP has the largest porosity, 0.612, at 10,000 years. It should be reiterated here that these calculations do not include any structural effects of corrosion and degradation. The structural effects of rampant corrosion and microbial degradation would be significant as would MgO hydration, salt precipitation, and volume increase associated with corrosion by-products.

To estimate the effects of the porosity surfaces with various inventories on the WIPP PA, it is informative to examine extreme cases, such as the upper and lower bounds. Appendix K includes plots for all values of *f*. When *f* is less than 0.1 the standard waste rooms have the lowest porosity. If *f* is larger than 0.1, the lower bound is the porosity surface associated with the all-AMWTP case. Over the first 1000 years, or so, the highest porosity results from the case simulating rooms filled with POPs. The porosity surfaces tend to merge over time as *f* increases from 0.4 to 1.0. For *f* values greater than 1.0 there is little difference between the porosities for any of the inventories after 1,000 years.

Porosity is defined as the ratio of the void volume to the room volume at specific time. The void volume is calculated by subtracting the volume of the waste solid in the room from the room volume. The solid volume remains constant for the entire analysis period. Therefore, the change in porosity comes from change in room volume. The room volume is a function of salt creep, waste form resistance and gas generation. The creep closure is impeded by the rigidity of the waste and gas production decreases the rate of the room closure. If pressures are sufficiently high, internal gas pressure can increase room volume. If the gas generation factor, *f*, is larger than a certain value (0.4 approximately), the room is beginning to be inflated at a certain time. If *f* is larger than 1.0, the room is inflated for all six types of waste.

The key factors to determine the porosity of the room are the waste solid volume and the gas production rate because the initial room volume is constant. In other words, a larger solid volume yields a smaller porosity and a larger gas production rate creates a larger porosity. For example, the all-AMWTP case has the greatest solid volume, 935.9 m^3, and the standard case has the smallest solid volume, 551.2 m^3. In contrast, the all-AMWTP case has the greatest gas production rate and the standard case has the smallest rate, as discussed in Section 2.2. In the case of f=2.0, the inflated volumes of the room at 10,000 years are 3,576.8 m^3 for the standard, 6,164.5 m^3 for the all AMWTP respectively. Finally, the porosities of the room at 10,000 years are 0.846 $\left(=\frac{3576.8-551.2}{3576.8}\right)$ for the standard, 0.848 $\left(=\frac{6164.5-935.9}{6164.5}\right)$ for the all AMWTP. These values are dramatically similar. Likewise, when *f* is more than 1.0, the room porosities at 10,000 years are similar to each other for all waste inventories.

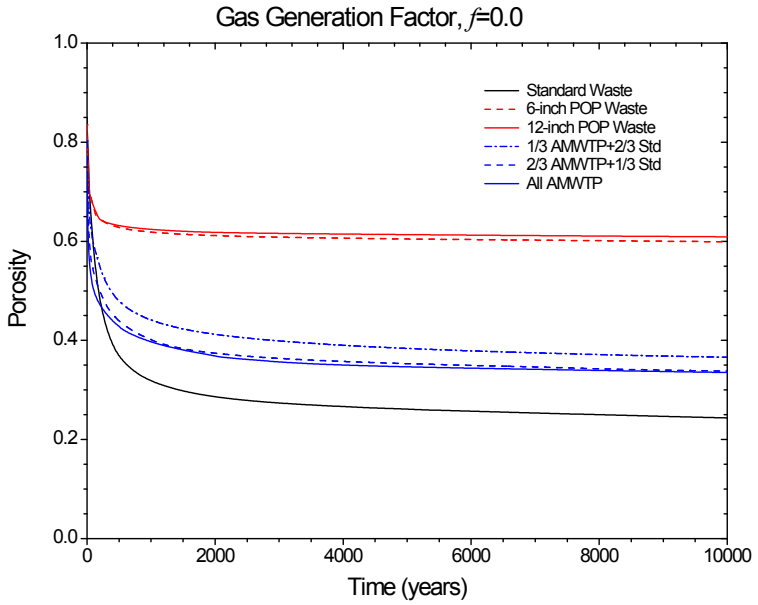

Figure 40: Comparison between porosity histories for the disposal room containing various waste inventories, f=0.0

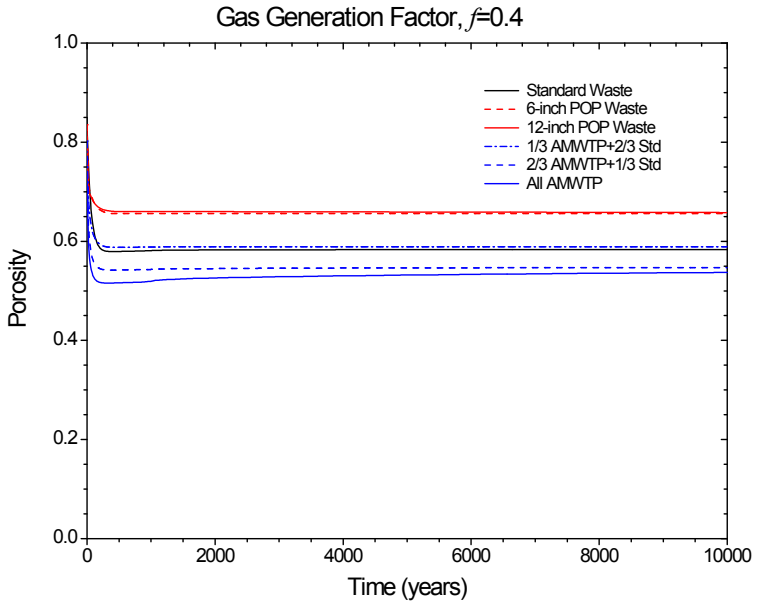

Figure 41: Comparison between porosity histories for the disposal room containing various waste inventories, f=0.4

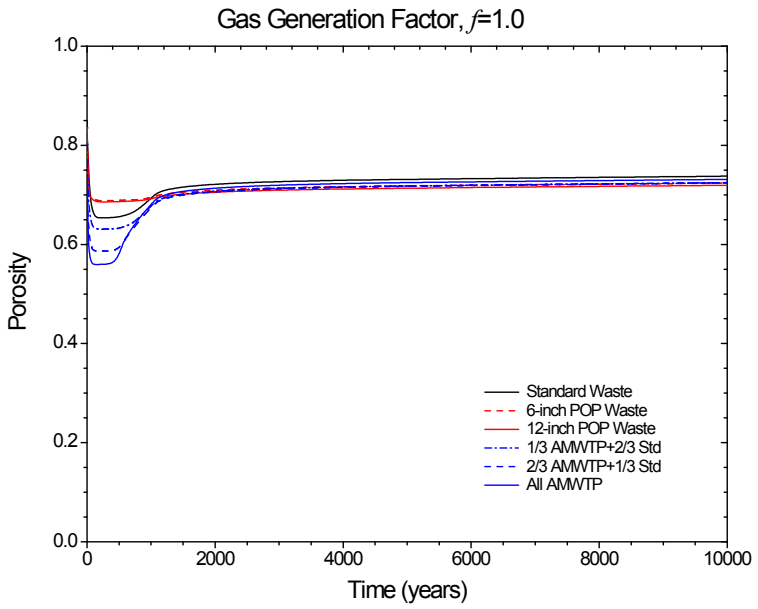

Figure 42: Comparison between porosity histories for the disposal room containing various waste inventories, *f*=1.0

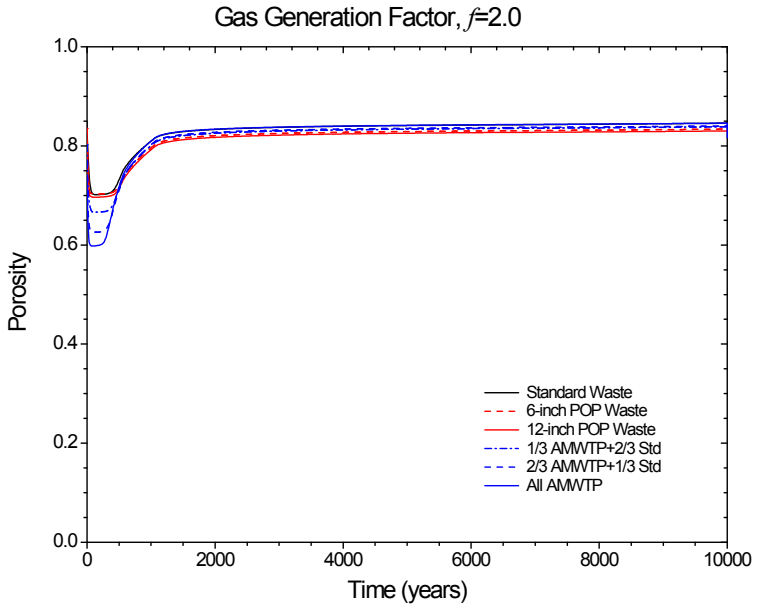

Figure 43: Comparison between porosity histories for the disposal room containing various waste inventories, f=2.0

Porosity Surface

The porosity histories described in Section 5.3 are converted into the surface in the three-dimensional space as shown in Figures 44 through 49 for each waste inventory respectively. The porosity surface data will be provided for BRAGFLO analyses.

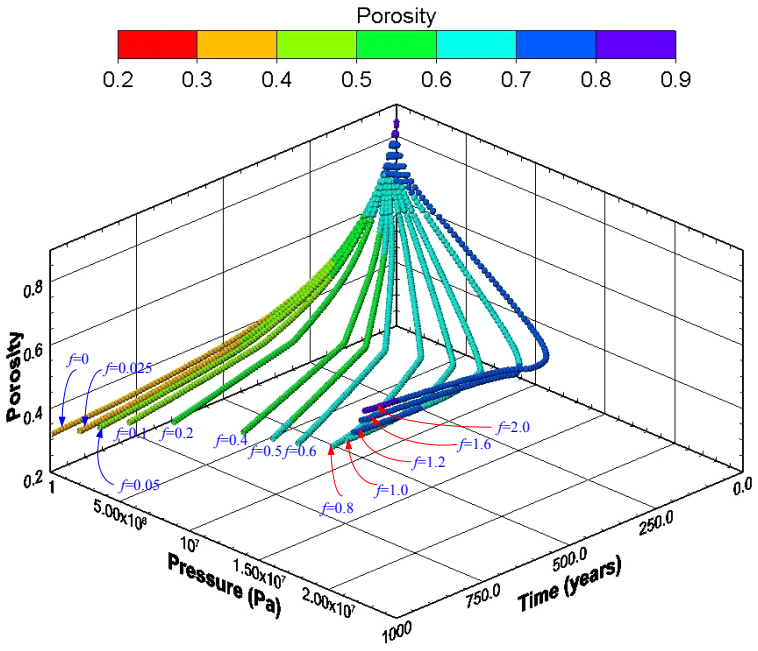

Figure 44: Porosity surface for the room containing the standard waste

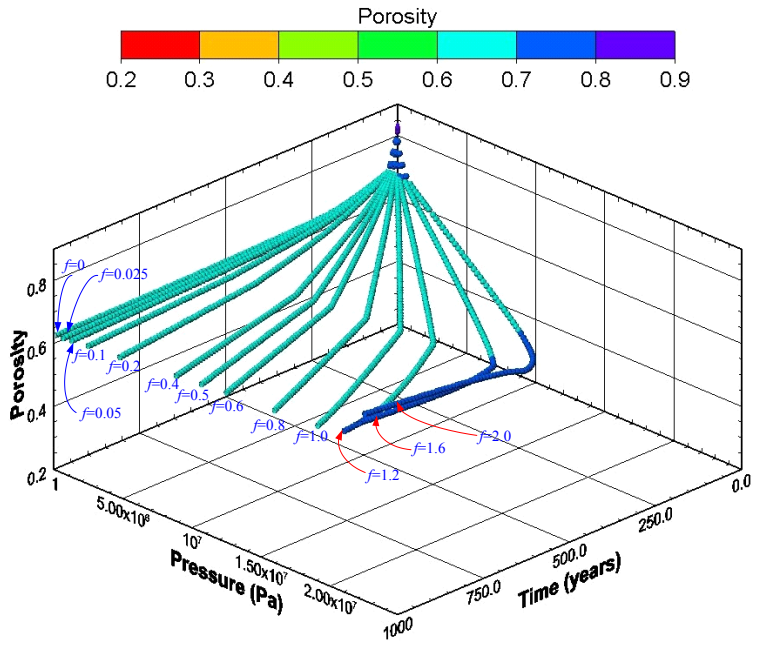

Figure 45: Porosity surface for the room containing the 12-inch POP waste

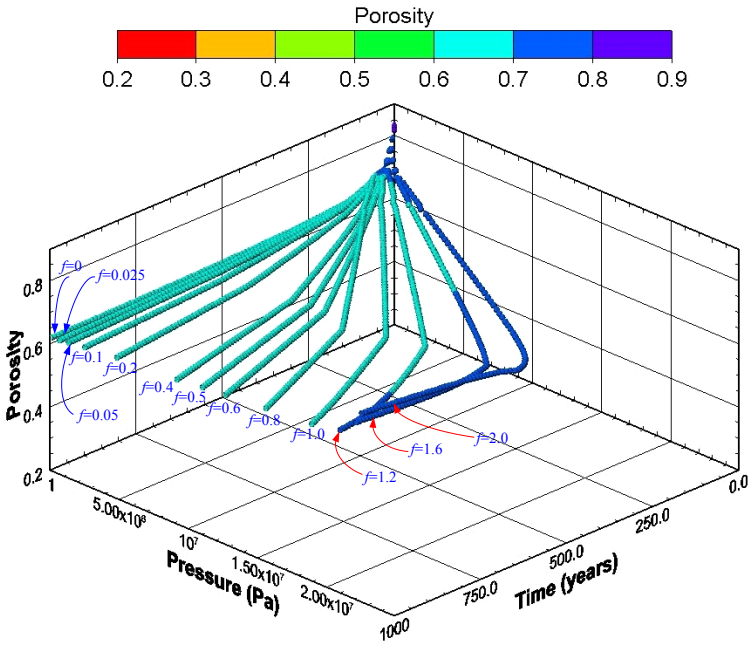

Figure 46: Porosity surface for the room containing the 6-inch POP waste

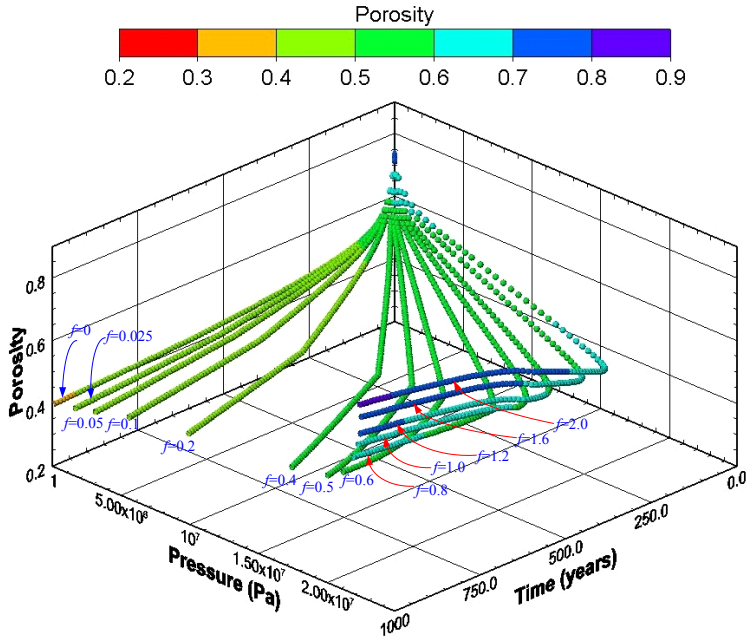

Figure 47: Porosity surface for the room containing the AMWTP waste

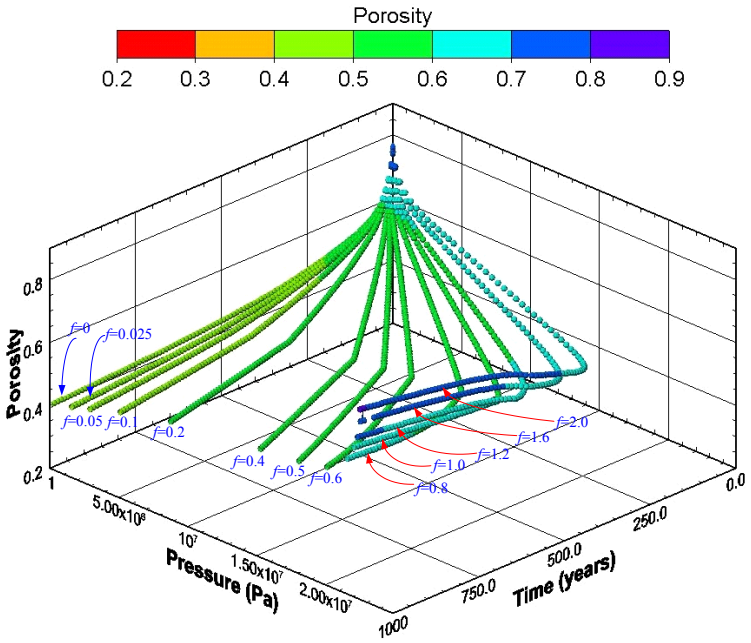

Figure 48: Porosity surface for the room containing 2/3 AMWTP + 1/3 standard waste

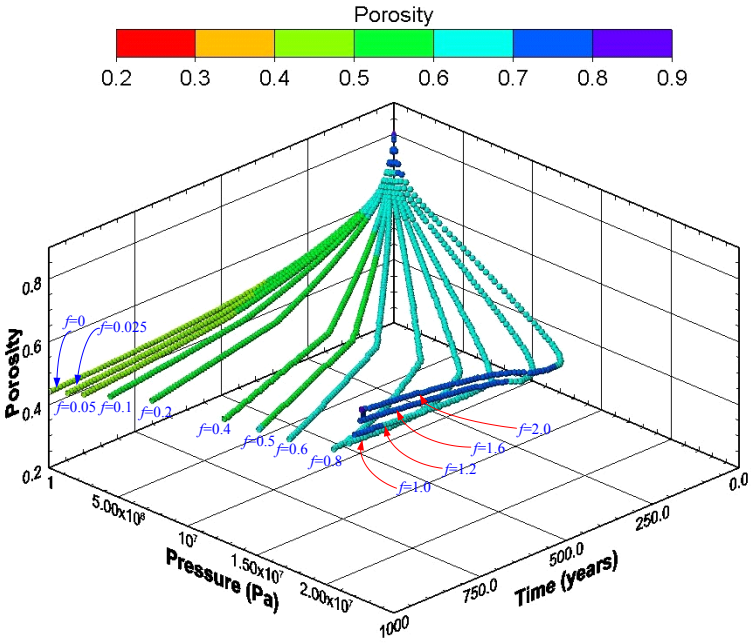

Figure 49: Porosity surface for the room containing 1/3 AMWTP + 2/3 standard waste

6 DISCUSSION AND CONCLUDING REMARKS

The primary purpose of these analyses is to assess the structural/mechanical impact to room closure and porosity development resulting from waste packages that differ from those assumed in the baseline configuration supporting the original compliance calculations. The primary waste packaging examined includes the pipe overpacks and the supercompacted waste. The POPs have already been placed in significant quantities in Panel 1, whereas plans have been made to ship AMWTP supercompacted waste. In support of the re-certification, an evaluation of possible structural effects of these waste packages is required.

Both waste package configurations--POPs and AMWTP--are structurally more rigid than a typical 55-gallon waste drum. The structural response of the underground couples creep closure, gas generation and the response of the waste. The models used for creep closure and gas generation are identical to those previously implemented for the porosity surface used in the CCA. The supercompacted wastes generate more gas than the standard waste model and the more rigid waste packages tend to hold the room open and to preserve porosity. The combination of these effects gives rise to porosity surfaces that differ from the baseline supporting the CCA.

The particular case when there is no gas generation is of no consequence to performance assessment scenarios that address a drilling intrusion. For the cases of gas generation at an f less than 0.1 rooms filled with standard waste have the lowest porosity. When f is larger than 0.1, the lower bound of the porosity surface is associated with the all-AMWTP case. Over the first 1000 years, or so, the highest porosity surface results from the case simulating rooms filled with POPs. The porosity surfaces tend to merge over time as f increases from 0.4 to 1.0. For f values greater than 1.0 there is little difference between the porosities for any of the inventories from 1,000 to 10,000 years.

These analyses demonstrate possible extreme effects regarding room closure. Fundamentally, the assumptions involve filling rooms entirely with robust waste packages such as the POPs or AMWTP supercompacted waste. Resistance to room closure is increased by these waste packages in comparison to the standard waste packages assumed in the original compliance calculations. It must be noted in viewing these results that the calculations underlying them assume that the structural integrity of the waste stacks is preserved. If the waste stack corrodes at the base then they may become more deformable, while other reactions, which are not accounted for in PA occur (such as MgO hydration and salt precipitation) may provide more resistance to closure and loss of porosity due to chemical action. In any of these cases the evolution of room closure would be different than modeled here.

The phenomenon of stress uptake by rigid pillars is well known in the mining industry. In particular, in salt mines, the deformation of pillars is a function of the stress that is applied to them. If all the pillars are the same size and shape, they will each creep at the same rate. If the strata over the pillars is extremely stiff or if the mined area is not wide, then the individual pillar stresses are responsive to the deformation rate imposed on the pillar by movement of the stiff overlying rock or massive abutment pillars adjacent the

smaller pillars. Hence, pillar stresses and behavior can be influenced and changed from what might have existed naturally when the pillar was first created, and the stresses and deformation may be much less than indicated by the size of the pillar. This influence can occur if a stiff crib is placed in a room. In this case the crib will absorb or redistribute vertical stress from the salt pillars onto itself. The rate of vertical stress increase in the crib is proportional to the elastic deformation of the crib (Hooke's law), while the deformation of the softer salt pillar is limited by the deformation of the crib. It appears as if the pillar sheds its vertical stress because any elastic rebound is completely overshadowed by the previous and contemporary creep shortening. Eventually a new stress equilibrium is reached where the salt pillar adjacent the crib no longer shortens by creep because the crib now carries the vertical stress that was in excess and causing the salt to creep. The rigid material in the present case comprises particular inventories of waste, which act to crib the rooms open. Simultaneous with load uptake in the waste stack, stress in the pillars between rooms tends to decrease, and vertical room closure is restricted due to the decrease in the stress differences that give rise to creep deformation. Thus, the lateral deformation of the rooms also decreases appreciably when rigid materials are placed within them.

The structural models evaluated in this report simulate rooms filled with robust waste forms, such as the pipe overpacks and the AMWTP supercompacted pucks. If a room were filled with structurally competent materials, the resulting porosity surface would exhibit characteristics that differ from the single porosity surface derived for the original compliance determination. The differences in porosity surfaces are greatest in the absence of gas generation.

With gas generation, the porosity surfaces undergo a transitory period lasting some thousand years. This is the period over which gas generation counterbalances the stresses driving salt creep. Over that period the porosity surfaces developed for the rooms filled with supercompacted AMWTP waste packages are lower than the surface used in the CCA. On the other hand, rooms filled with POPs produce higher porosity surfaces. With significant gas generation, i.e., when human intrusion scenarios are most important, the porosity surfaces tend to converge to a single porosity value over the regulatory period, regardless of the simulated inventory. Rooms filled with POPs and the AMWTP supercompacted waste packages are propped open by the stiffer waste stacks. The cribbing effect results from the assumption that the rooms are filled with these robust waste packages and provide the structural equivalent of rigid columns, three tiers tall.

The porosity surface calculations presented in this report have evaluated the structural response of rooms filled completely with different forms of waste packages. In the absence of gas generation by metal corrosion and microbial consumption of the waste, the standard waste packages (as represented in the CCA) consolidate more than other, more rigid packages. In the absence of gas generation there is no scenario in which regulatory release limits might be exceeded. If waste packages remain intact, or relatively intact, they would be difficult to penetrate with a conventional drill and waste would not spall or cave into the wellbore. Therefore, gas generation scenarios coupled with human intrusion pose the only possible threat to regulatory compliance.

Degradation and other changes to the waste packages, such as the structural effects of MgO hydration, salt precipitation, and corrosion by product, are not taken into account in any of the porosity surface structural calculations, either here or in the original compliance application. Obviously, massive changes to the waste would affect room closure and porosity surface development and massive changes to the waste are necessary to create gas pressure. In addition, any salt material spalling from the back would tend to agglomerate owing to the well-established mechanism of pressure solution and re-deposition, and would tend to create a solid mass in the waste rooms (Hansen, 2003). Clearly these structural models provide only a superficial view of the underground evolution over the life of the repository.

7 REFERENCES

Butcher, B.M. 1997. *A Summary of the Sources of Input Parameter Values for the WIPP Final Porosity Surface Calculations*. SAND97-0796. Albuquerque, NM: Sandia National Laboratories.

Butcher, B.M., T.W. Thompson, R.G. VanBuskirk, and N.C. Patti. 1991. *Mechanical Compaction of Waste Isolation Pilot Plant Simulated Waste*. SAND90-1206. Albuquerque, NM: Sandia National Laboratories.

Chavez, M.J. 2003. "Software Requirements, NP 19-1, Revision 10." Carlsbad, NM: Sandia National Laboratories (Copy on file in the Sandia WIPP Records Center as ERMS# 529692).

Gilkey, A.P., and J.H. Glick. 1988. *BLOT – A Mesh and Curve Plot Program for the Output of a Finite Element Analysis*. SAND88-1432. Albuquerque, NM: Sandia National Laboratories.

Griswold, L.W. 2002. "Specification for Prepackaged MgO Backfill, Revision 4." Carlsbad, NM: U.S. Department of Energy, WIPP, Westinghouse TRU Solutions.

Hansen, C.W., L.H. Brush, M.B. Gross, F.D. Hansen, B. Y. Park, J.S. Stein, T.W. Thompson, and D. Kessel. 2003a. "Effects of Supercompacted Waste and Heterogeneous Waste Emplacement on Repository Performance, Revision 1." Carlsbad, NM: Sandia National Laboratories (Copy on file in the Sandia WIPP Records Center as ERMS# 532475).

Hansen, C.W., L.H. Brush, F.D. Hansen, and J.S. Stein. 2003b. "Analysis Plan for Evaluating Assumptions of Waste Homogeneity in WIPP Performance Assessment (AP-107), Revision 1." Carlsbad, NM: Sandia National Laboratories (Copy on file in the Sandia WIPP Records Center as ERMS# 531067).

Hansen, F.D. 2003. *The Disturbed Rock Zone at the Waste Isolation Pilot Plant*. SAND2005-423642363407. Albuquerque, NM: Sandia National Laboratories.

Helton, J.C., J.E. Bean, J.W. Berglund, F.J. Davis, K. Economy, J.W. Garner, J.D. Johnson, R.J. MacKinnon, J. Miller, D.G. O'Brien, J.L. Ramsey, J.D. Schreiber, A. Shinta, L.N. Smith, D.M. Stoelzel, C. Stockman, and P. Vaughn. 1998. *Uncertainty and Sensitivity Analysis Results Obtained in the 1996 Performance Assessment for the Waste Isolation Pilot Plant*. SAND98-0365. Albuquerque, NM: Sandia National Laboratories.

Leigh, C.D. 2003. "Estimate of Waste Material Percentages in Pipe Overpacks in Support of AP-107, Revision 0." Carlsbad, NM: Sandia National Laboratories (Copy on file in the Sandia WIPP Records Center as ERMS# 533194).

Ludwigsen, J.S., D.J. Ammerman, and H.D. Radloff. 1998. *Analysis in Support of Storage of Residues in the Pipe Overpack Container.* SAND98-1003. Albuquerque, NM: Sandia National Laboratories.

Munson, D.E., A.F. Fossum, and P.E. Senseny. 1989. *Advances in Resolution of Discrepancies between Predicted and Measured In Situ Room Closures*. SAND88-2948. Albuquerque, NM: Sandia National Laboratories.

Park, B.Y., and F.D. Hansen. 2004. *Simulations of the Pipe Overpack to Compute Constitutive Model Parameters for Use in WIPP Room Closure Calculations*. SAND2005-423642361390. Albuquerque, NM: Sandia National Laboratories.

Park, B.Y., and J.F. Holland. 2003. *Analysis Report for Structural Evaluation of WIPP Disposal Room Raised to Clay Seam G*. SAND2005-423642363409. Albuquerque, NM: Sandia National Laboratories,.

Sandia WIPP Project. 1992. *Preliminary Performance Assessment for the Waste Isolation Pilot Plant, December 1992, Volume 3: Model Parameters*. SAND92-0700/3. Albuquerque, NM: Sandia National Laboratories.

Sandia National Laboratories. 2002. "User Manual for nSIGHTS, Version 1.0." Carlsbad, NM: Sandia National Laboratories (Copy on file in the Sandia WIPP Records Center as ERMS# 522061).

Sjaardema, G.D. 1989. *NUMBERS: A Collection of Utilities for Pre- and Post-processing Two- and Three-Dimensional EXODUS Finite Element Models*. SAND88-0737. Albuquerque, NM: Sandia National Laboratories.

Smith, A.C., and P.S. Blanton. 2001. *Effect of Glue Layers on Response of Cellulose Fiberboard at Low Temperature*. WSRC-TR-2001-00083. Aiken, SC: Westinghouse Savannah River Company.

Stone, C.M. 1997a. *Final Disposal Room Structural Response Calculations.* SAND97-0795. Albuquerque, NM: Sandia National Laboratories.

Stone, C.M. 1997b. *SANTOS--A Two-Dimensional Finite Element Program for the Quasistatic, Large Deformation, Inelastic Response of Solids*. SAND90-0543. Albuquerque, NM: Sandia National Laboratories.

U.S. DOE (U.S. Department of Energy). 1996. *Title 40 CFR Part 191 Compliance Certification for the Waste Isolation Pilot Plant.* DOE/CAO-1996-2184. Vols. I-XXI. Carlsbad, NM: Carlsbad Area Office, U.S. Department of Energy.

WIPP PA (Performance Assessment). 2003a. "Design Document for BRAGFLO Version 5.00." Carlsbad, NM: Sandia National Laboratories.(Copy on file in the Sandia WIPP Records Center as ERMS# 525700).

WIPP PA (Performance Assessment). 2003b. "Verification and Validation Plan/Validation Document for SANTOS 2.1.7." Carlsbad, NM: Sandia National Laboratories (Copy on file in the Sandia WIPP Records Center as ERMS# 530091).

WTS (Washington TRU Solutions, LLC.). 2003. "TRUPACT-II Authorized Methods for Payload Control (TRAMPACT), Revision 19c." Carlsbad, NM Westinghouse TRU Solutions.

APPENDIX A: CALCULATION SHEET TO COMPUTE THE VOLUME OF EACH COMPONENT IN THE WASTE DRUM

A-1 12 inch-POP

Note: Dimensions taken from Park and Hansen, 2004.

Drum Shell:

Upper and Lower Shell:

$t_D := 0.055\,in$ $t_D = 0.0014m$ "Shell Thickness"

$r_I := .27305\,m$ "Inside diameter of drum"

$r_D := r_I + t_D$ $r_D = 0.27445m$ "outside diameter of drum

$V_{UD} := \pi \cdot r_D^2 \cdot t_D$ $V_{UD} = 0.00033m^3$ "upper shell volume"

$V_{ULD} := 2 \cdot V_{UD}$ $V_{ULD} = 0.00066m^3$ "Upper and Lower shell volume'

Side Shell:

$h_{SD} := .79502\,m$ "height of side shell"

$V_{OD} := \pi \cdot r_D^2 \cdot h_{SD}$ $V_{OD} = 0.18812m^3$ $r_D = 0.27445m$

$V_{ID} := \pi \cdot r_I^2 \cdot h_{SD}$ $V_{ID} = 0.18621m^3$ $r_I = 0.27305m$

$V_{SD} := V_{OD} - V_{ID}$ $V_{SD} = 0.00191m^3$

Volume of Drum Shell:

$V_D := V_{ULD} + V_{SD}$ $V_D = 0.00257m^3$

Impact Limiter:

Upper IL:

$t_{UI} := .79502\,m - .72898\,m$ $t_{UI} = 2.6\,in$

$V_{UI} := \pi \cdot r_I^2 \cdot t_{UI}$ $V_{UI} = 0.01547m^3$ $r_I = 0.27305m$

Lower IL:

$t_{LI} := 0.04\,m$

$V_{LI} := \pi \cdot r_I^2 \cdot t_{LI}$ $V_{LI} = 0.00937m^3$

Side IL:

Lower Side:

$h_{LSI} := .64516\,m - .05334\,m$ $h_{LSI} = 23.3\,in$

$V_{OLSI} := \pi \cdot r_I^2 \cdot h_{LSI}$ $V_{OLSI} = 0.13862\,m^3$

$r_{ILSI} := .16256\,m$

$V_{ILSI} := \pi \cdot r_{ILSI}^2 \cdot h_{LSI}$ $V_{ILSI} = 0.04913\,m^3$

$V_{LSI} := V_{OLSI} - V_{ILSI}$ $V_{LSI} = 0.08949\,m^3$

Middle Side:

$h_{MSI} := .68326\,m - .64516\,m$ $h_{MSI} = 1.5\,in$

$V_{OMSI} := \pi \cdot r_I^2 \cdot h_{MSI}$ $V_{OMSI} = 0.00892\,m^3$ $r_I = 0.27305\,m$

$r_{IMSI} := .20701\,m$

$V_{IMSI} := \pi \cdot r_{IMSI}^2 \cdot h_{MSI}$ $V_{IMSI} = 0.00513\,m^3$

$V_{MSI} := V_{OMSI} - V_{IMSI}$ $V_{MSI} = 0.00379\,m^3$

Upper Side:

$h_{USI} := .72898\,m - .68326\,m$ $h_{USI} = 1.8\,in$

$V_{OUSI} := \pi \cdot r_I^2 \cdot h_{USI}$ $V_{OUSI} = 0.01071\,m^3$ $r_I = 0.27305\,m$

$r_{IUSI} := r_{IMSI}$ $r_{IMSI} = 0.20701\,m$

$V_{IUSI} := \pi \cdot r_{IUSI}^2 \cdot h_{USI}$ $V_{IUSI} = 0.00616\,m^3$

$V_{USI} := V_{OUSI} - V_{IUSI}$ $V_{USI} = 0.00455\,m^3$

Side IL Volume:

$V_{SI} := V_{LSI} + V_{MSI} + V_{USI}$ $V_{SI} = 0.09784\,m^3$

Impact Limiter Volume:

$V_I := V_{UI} + V_{LI} + V_{SI}$

$V_I = 0.12267\text{m}^3$

Pipe:

Bottom Pipe:

$t_P := 0.25\cdot\text{in}$ $t_P = 0.00635\text{m}$

$r_{OP} := .16256\text{m}$

$V_{BP} := \pi\cdot r_{OP}^2\cdot t_P$ $V_{BP} = 0.00053\text{m}^3$

Side Pipe:

Lower:

$h_{LSP} := .64516\text{m} - .05969\text{m}$ $h_{LSP} = 23.05\text{in}$

$r_{IP} := .1569974\text{m}$

$V_{OLSP} := \pi\cdot r_{OP}^2\cdot h_{LSP}$ $V_{OLSP} = 0.04861\text{m}^3$

$V_{ILSP} := \pi\cdot r_{IP}^2\cdot h_{LSP}$ $V_{ILSP} = 0.04534\text{m}^3$

$V_{LSP} := V_{OLSP} - V_{ILSP}$ $V_{LSP} = 0.00327\text{m}^3$

Middle:

$h_{MSP} := .68326\text{m} - .64516\text{m}$ $h_{MSP} = 1.5\text{in}$

$r_{OOP} := .1665224\text{m}$

$r_{OMSP} := \frac{(r_{OOP} + r_{OP})}{2}$ $r_{OMSP} = 0.16454\text{m}$

$V_{OMSP} := \pi\cdot r_{OMSP}^2\cdot h_{MSP}$ $V_{OMSP} = 0.00324\text{m}^3$

$V_{IMSP} := \pi\cdot r_{IP}^2\cdot h_{MSP}$ $V_{IMSP} = 0.00295\text{m}^3$

$V_{MSP} := V_{OMSP} - V_{IMSP}$ $V_{MSP} = 0.00029\text{m}^3$

Upper:

$h_{USP} := .70612\,m - .68326\,m$ $\quad h_{USP} = 0.9\,in$ $\quad r_{IMSI} = 0.20701\,m$

$V_{OUSP} := \pi \cdot r_{IMSI}^{2} \cdot h_{USP}$ $\quad V_{OUSP} = 0.00308\,m^3$

$V_{IUSP} := \pi \cdot r_{IP}^{2} \cdot h_{USP}$ $\quad V_{IUSP} = 0.00177\,m^3$

$V_{USP} := V_{OUSP} - V_{IUSP}$ $\quad V_{USP} = 0.00131\,m^3$

Side Pipe Volume:

$V_{SP} := V_{LSP} + V_{MSP} + V_{USP}$ $\quad V_{SP} = 0.00487\,m^3$

Lid:

$t_{LP} := .72898\,m - .70612\,m$ $\quad t_{LP} = 0.9\,in$

$V_{LP} := \pi \cdot r_{IMSI}^{2} \cdot t_{LP}$ $\quad V_{LP} = 0.00308\,m^3$

Pipe Volume:

$V_P := V_{BP} + V_{SP} + V_{LP}$ $\quad V_P = 0.00847\,m^3$

Waste:

$h_W := .70612\,m - .05969\,m$ $\quad h_W = 25.45\,in$

$V_W := \pi \cdot r_{IP}^{2} \cdot h_W$ $\quad V_W = 0.05006\,m^3$

Plywood:

$t_{PW} := .05334\,m - .04\,m$ $\quad t_{PW} = 0.01334\,m$

$V_{PW} := \pi \cdot r_I^{2} \cdot t_{PW}$ $\quad V_{PW} = 0.00312\,m^3$

Space:

$$V_{SP} := \pi \cdot r_{IMSI}^{2} \cdot h_{MSP} - \pi \cdot r_{OMSP}^{2} \cdot h_{MSP} \qquad V_{SP} = 0.00189\,m^3$$

Total Volume:

$$V_T := V_D + V_I + V_P + V_W + V_{PW} + V_{SP} \qquad V_T = 0.18879\,m^3$$

Checking:

$$V_{TR} := \pi \cdot r_D^{2} \cdot \left(.79502\,m + 2 \cdot t_D\right) \qquad V_{TR} = 0.18879\,m^3$$

$$Diff := V_T - V_{TR} \qquad Diff = 0\,m^3$$

Volume of Impact Limiter: $V_I = 0.12267\,m^3$

Volume of Pipe: $V_P = 0.00847\,m^3$

Volume of Plywood: $V_{PW} = 0.00312\,m^3$

Volume of Waste: $V_W = 0.05006\,m^3$

Volume of Drum Shell: $V_D = 0.00257\,m^3$

A-2 6-inch POP

Note: Dimensions taken from Park and Hansen, 2004.

Drum Shell:

Upper and Lower Shell:

$t_D := 0.055\,in$ $t_D = 0.0014m$

$r_I := .27305\,m$

$r_D := r_I + t_D$ $r_D = 0.27445m$

$V_{UD} := \pi \cdot r_D^2 \cdot t_D$ $V_{UD} = 0.00033m^3$

$V_{ULD} := 2 \cdot V_{UD}$ $V_{ULD} = 0.00066m^3$

Side Shell:

$h_{SD} := .79502\,m$

$V_{OD} := \pi \cdot r_D^2 \cdot h_{SD}$ $V_{OD} = 0.18812m^3$ $r_D = 0.27445m$

$V_{ID} := \pi \cdot r_I^2 \cdot h_{SD}$ $V_{ID} = 0.18621m^3$ $r_I = 0.27305m$

$V_{SD} := V_{OD} - V_{ID}$ $V_{SD} = 0.00191m^3$

$V_D := V_{ULD} + V_{SD}$ $V_D = 0.00257m^3$

Impact Limiter:

Upper IL:

$t_{UI} := .79502\,m - .73660\,m$ $t_{UI} = 2.3\,in$

$V_{UI} := \pi \cdot r_I^2 \cdot t_{UI}$ $V_{UI} = 0.01368m^3$ $r_I = 0.27305m$

Lower IL:

$t_{LI} := 0.04\,m$

$V_{LI} := \pi \cdot r_I^2 \cdot t_{LI}$ $V_{LI} = 0.00937m^3$

Side IL:

Lower:

$h_{LSI} := .64516\,m - .05334\,m$ $h_{LSI} = 23.3\,in$

$V_{OLSI} := \pi \cdot r_I^2 \cdot h_{LSI}$ $V_{OLSI} = 0.13862\,m^3$

$r_{ILSI} := .08509\,m$

$V_{ILSI} := \pi \cdot r_{ILSI}^2 \cdot h_{LSI}$ $V_{ILSI} = 0.01346\,m^3$

$V_{LSI} := V_{OLSI} - V_{ILSI}$ $V_{LSI} = 0.12516\,m^3$

Middle:

$h_{MSI} := .69088\,m - .64516\,m$ $h_{MSI} = 1.8\,in$

$V_{OMSI} := \pi \cdot r_I^2 \cdot h_{MSI}$ $V_{OMSI} = 0.01071\,m^3$ $r_I = 0.27305\,m$

$r_{IMSI} := .13970\,m$

$V_{IMSI} := \pi \cdot r_{IMSI}^2 \cdot h_{MSI}$ $V_{IMSI} = 0.0028\,m^3$

$V_{MSI} := V_{OMSI} - V_{IMSI}$ $V_{MSI} = 0.00791\,m^3$

Upper:

$h_{USI} := .73660\,m - .69088\,m$ $h_{USI} = 1.8\,in$

$V_{OUSI} := \pi \cdot r_I^2 \cdot h_{USI}$ $V_{OUSI} = 0.01071\,m^3$ $r_I = 0.27305\,m$

$r_{IUSI} := r_{IMSI}$ $r_{IMSI} = 0.1397\,m$

$V_{IUSI} := \pi \cdot r_{IUSI}^2 \cdot h_{USI}$ $V_{IUSI} = 0.0028\,m^3$

$V_{USI} := V_{OUSI} - V_{IUSI}$ $V_{USI} = 0.00791\,m^3$

$V_{SI} := V_{LSI} + V_{MSI} + V_{USI}$ $V_{SI} = 0.14097\,m^3$

$V_I := V_{UI} + V_{LI} + V_{SI}$ $V_I = 0.16402\,m^3$

Pipe:

Bottom Pipe:

$t_P := 0.25 \cdot in$ $t_P = 0.00635 m$

$r_{OP} := .08509 m$

$V_{BP} := \pi \cdot r_{OP}^2 \cdot t_P$ $V_{BP} = 0.00014 m^3$

Side Pipe:

Lower:

$h_{LSP} := .64516 m - .05969 m$ $h_{LSP} = 23.05 in$

$r_{IP} := .07887 m$

$V_{OLSP} := \pi \cdot r_{OP}^2 \cdot h_{LSP}$ $V_{OLSP} = 0.01332 m^3$

$V_{ILSP} := \pi \cdot r_{IP}^2 \cdot h_{LSP}$ $V_{ILSP} = 0.01144 m^3$

$V_{LSP} := V_{OLSP} - V_{ILSP}$ $V_{LSP} = 0.00188 m^3$

Middle:

$h_{MSP} := .69088 m - .64516 m$ $h_{MSP} = 1.8 in$

$r_{OOP} := .08905 m$

$r_{OMSP} := \frac{(r_{OOP} + r_{OP})}{2}$ $r_{OMSP} = 0.08707 m$

$V_{OMSP} := \pi \cdot r_{OMSP}^2 \cdot h_{MSP}$ $V_{OMSP} = 0.00109 m^3$

$V_{IMSP} := \pi \cdot r_{IP}^2 \cdot h_{MSP}$ $V_{IMSP} = 0.00089 m^3$

$V_{MSP} := V_{OMSP} - V_{IMSP}$ $V_{MSP} = 0.0002 m^3$

Space:

$$V_{SP} := \pi \cdot r_{IMSI}^{2} \cdot h_{MSP} - \pi \cdot r_{OMSP}^{2} \cdot h_{MSP} \qquad V_{SP} = 0.00171\,m^3$$

Total Volume:

$$V_T := V_D + V_I + V_P + V_W + V_{PW} + V_{SP} \qquad V_T = 0.18879\,m^3$$

$$V_{TR} := \pi \cdot r_D^{2} \cdot \left(.79502\,m + 2 \cdot t_D\right) \qquad V_{TR} = 0.18879\,m^3$$

$$Diff := V_T - V_{TR} \qquad Diff = 0\,m^3$$

Volume of Impact Limiter: $V_I = 0.16402\,m^3$

Volume of Pipe: $V_P = 0.00457\,m^3$

Volume of Plywood: $V_{PW} = 0.00312\,m^3$

Volume of Waste: $V_W = 0.01278\,m^3$

Volume of Drum Shell: $V_D = 0.00257\,m^3$

A-3 AMWTP Debris Waste

Note: Dimensions taken from Figure 4.

Radius of Puck:	$r_P := 12.5 \cdot in$	$r_P = 0.3175m$
Space of Side:	$S_S := 3.0 \cdot in$	$S_S = 0.0762m$
Radius of Container (Inside):	$r_{DI} := r_P + S_S$	$r_{DI} = 0.3937m$
Thick of Container Shell:	$t_D := 0.055 \cdot in$	$t_D = 0.0014m$
Radius of Container (Outside):	$r_{DO} := r_{DI} + t_D$	$r_{DO} = 0.3951m$
		$2 \cdot r_{DO} = 0.79019m$
Height of Container:	$H_D := 35 \cdot in + \frac{t_D}{2}$	$H_D = 0.8897m$
Bottom of Upper Lid	$L_{BU} := H_D - t_D$	$L_{BU} = 0.8883m$
Height of Upper Space:	$H_{US} := 1.5 \cdot in - t_D$	$H_{US} = 0.0367m$
Top of Lower Lid:	$L_{TL} := H_D - t_D - H_{US}$	$L_{TL} = 0.8516m$
Bottom of Lower Lid:	$L_{BL} := L_{TL} - t_D$	$L_{BL} = 0.8502m$
Height of Lower Space:	$H_{LS} := 1.75 \cdot in - \frac{t_D}{2}$	$H_{LS} = 0.04375m$
Top of Puck:	$P_T := L_{BL} - H_{LS}$	$P_T = 0.80645m$
Bottom of Puck	$P_B := t_D$	$P_B = 0.0014m$
Height of Puck:	$H_P := P_T - P_B$	$H_P = 0.80505m$

Volume Calculation of Each Puck Elements:

Container Shell:

Upper and Lower Shell:

$V_{UD} := \pi \cdot r_{DO}^{2} \cdot t_D$ $V_{UD} = 0.00069 m^3$

$V_{ULD} := 2 \cdot V_{UD}$ $V_{ULD} = 0.00137 m^3$

Side Shell:

Height of Side: $h_{SD} := H_D - \frac{t_D}{2} - t_D$ $h_{SD} = 0.8876 m$

$V_{SD} := \pi \cdot \left(r_{DO}^{2} - r_{DI}^{2} \right) \cdot h_{SD}$ $V_{SD} = 0.00307 m^3$

Middle Lid:

$V_{MD} := \pi \cdot r_{DI}^{2} \cdot t_D$ $V_{MD} = 0.00068 m^3$

Volume of Container Shell: $V_D := V_{ULD} + V_{SD} + V_{MD}$ $V_D = 0.00512 m^3$

Waste:

$V_W := \pi \cdot r_P^{2} \cdot H_P$ $V_W = 0.25495 m^3$

Space:

Upper Space:

$V_{US} := \pi \cdot r_{DI}^{2} \cdot H_{US}$ $V_{US} = 0.01787 m^3$

Lower Space:

$$V_{LS} := \pi \cdot r_{DI}^{2} \cdot H_{LS} \qquad V_{LS} = 0.0213 m^3$$

Side Space:

$$V_{SS} := \pi \cdot \left(r_{DI}^{2} - r_{P}^{2} \right) \cdot H_P \qquad V_{SS} = 0.13706 m^3$$

Volume of Space:

$$V_S := V_{US} + V_{LS} + V_{SS} \qquad V_S = 0.17624 m^3$$

Total Volume:

$$V_T := V_D + V_W + V_S \qquad V_T = 0.43632 m^3$$

Checking:

$$V_{TC} := \pi \cdot r_{DO}^{2} \cdot H_D \qquad V_{TC} = 0.43632 m^3$$

Volume of Container Shell $V_D = 0.00512 m^3$

Volume of Pucks: $V_W = 0.25495 m^3$

Volume of Incompressible Material: $V_I := V_D + V_W \qquad V_I = 0.26008 m^3$

Volume of Space: $V_S = 0.17624 m^3$

APPENDIX B: CALCULATION SHEET FOR THE INITIAL POROSITY OF THE UNDEFORMED DISPOSAL ROOM

Note: POP dimensions taken from Park and Hansen, 2004; Room dimensions taken from Park and Holland, 2003.

B-1 12-inch POP

Hight of Disposal Room: $H_R := 3.96\,m$

Wide of Disposal Room: $W_R := 10.06\,m$

Length of Disposal Room: $L_R := 91.44\,m$

Initial Room Volume: $V_{R.i} := H_R \cdot W_R \cdot L_R$ $V_{R.i} = 3642.8\,m^3$

Number of Drums in a Disposal Room: $N_{D.R} := 6804$

Number of Drums in a Pack: $N_{D.P} := 7$

Number of Packs in a Disposal Room: $N_{P.R} := \frac{N_{D.R}}{N_{D.P}}$ $N_{P.R} = 972$

Volume of 55-gal Steel Drums filled with Waste (SAND92-0700/3 p.3-10): $V_D := 0.2539\,m^3$

Volume of the All Drums filled with Waste in a Room: $V_{D.W} := V_D \cdot N_{D.R}$ $V_{D.W} = 1727.5\,m^3$

Initial Density of the All of Drums filled with Waste: $\rho_0 := 655.94\,\frac{kgf}{m^3}$

Solid Waste Density: $\rho_s := 1840.46\,\frac{kgf}{m^3}$

Initial Porosity of the All of Drums with Waste: $\phi_0 := 1 - \frac{\rho_0}{\rho_s}$ $\phi_0 = 0.644$

Initial Void Volume of the All of Drums with Waste:

$V_{v.D.W} := V_{D.W} \cdot \phi_0$ $V_{v.D.W} = 1111.8\,m^3$

Initial Solid Waste Volume: $V_s := V_{D.W} - V_{v.D.W}$ $V_s = 615.694\,m^3$

Initial Porosity of the Undeformed Disposal Room:

$\phi_{R.i} := \frac{V_{R.i} - V_s}{V_{R.i}}$ $\phi_{R.i} = 0.83098$

B-2 6-inch POP

Hight of Disposal Room: $H_R := 3.96\,m$

Wide of Disposal Room: $W_R := 10.06\,m$

Length of Disposal Room: $L_R := 91.44\,m$

Initial Room Volume: $V_{R.i} := H_R \cdot W_R \cdot L_R$ $V_{R.i} = 3642.8 m^3$

Number of Drums in a Disposal Room: $N_{D.R} := 6804$

Number of Drums in a Pack: $N_{D.P} := 7$

Number of Packs in a Disposal Room: $N_{P.R} := \frac{N_{D.R}}{N_{D.P}}$ $N_{P.R} = 972$

Volume of 55-gal Steel Drums filled with Waste (SAND92-0700/3 p.3-10): $V_D := 0.2539\,m^3$

Volume of the All Drums filled with Waste in a Room: $V_{D.W} := V_D \cdot N_{D.R}$ $V_{D.W} = 1727.5 m^3$

Initial Density of the All of Drums filled with Waste: $\rho_0 := 489.02 \frac{kgf}{m^3}$

Solid Waste Density: $\rho_s := 1404.82 \frac{kgf}{m^3}$

Initial Porosity of the All of Drums with Waste: $\phi_0 := 1 - \frac{\rho_0}{\rho_s}$ $\phi_0 = 0.652$

Initial Void Volume of the All of Drums with Waste:

$V_{v.D.W} := V_{D.W} \cdot \phi_0$ $V_{v.D.W} = 1126.2 m^3$

Initial Solid Waste Volume: $V_s := V_{D.W} - V_{v.D.W}$ $V_s = 601.358 m^3$

Initial Porosity of the Undeformed Disposal Room:

$\phi_{R.i} := \frac{V_{R.i} - V_s}{V_{R.i}}$ $\phi_{R.i} = 0.8349$

B-3 All AMWTP waste

Hight of Disposal Room: $H_R := 3.96\,m$

Wide of Disposal Room: $W_R := 10.06\,m$

Length of Disposal Room: $L_R := 91.44\,m$

Initial Room Volume: $V_{R.i} := H_R \cdot W_R \cdot L_R$ $V_{R.i} = 3642.8\,m^3$

Number of Packs in a Disposal Room: $N_{P.D} := 972$

Number of Containers in a Pack: $N_{D.P} := 3$

Number of Containers in a Disposal Room: $N_{D.R} := N_{P.D} \cdot N_{D.P}$ $N_{D.R} = 2916$

Thick of Container Shell: $t_D := 0.055\,in$ $t_D = 0.0014m$

Diameter of 100-gal Container: $D_D := 31 \cdot in + 2t_D$ $D_D = 0.79m$

Height of 100-gal Container: $H_D := 35 \cdot in + \frac{t_D}{2}$ $H_D = 0.89m$

Volume of 100-gal Steel Containers filled with Waste: $V_D := \frac{\pi \cdot D_D^{\,2}}{4} \cdot H_D$ $V_D = 0.436m^3$

Volume of the All Containers filled with Waste in a Room: $V_{D.W} := V_D \cdot N_{D.R}$ $V_{D.W} = 1272.3m^3$

Diameter of Supercompacted Waste(Puck): $D_P := 25 \cdot in$ $D_P = 0.635m$

Space between inner lid and outer lid: $S_L := 1.5 \cdot in$ $S_L = 0.038m$

Space between puck and inner lid: $S_P := 5 \cdot \% \cdot H_D$ $S_P = 0.044m$

Height of Puck: $H_P := H_D - S_L - S_P - \frac{3}{2}t_D$ $H_P = 0.805m$

Height of 3 Layer Puck: $H_{P.3} := H_P \cdot 3$ $H_{P.3} = 2.415m$

Volume of Puck: $V_P := \frac{\pi \cdot D_P^{\,2}}{4} \cdot H_P$ $V_P = 0.255m^3$

Total Volume of Puck $V_{P.T} := V_P \cdot N_{D.R}$ $V_{P.T} = 743.414m^3$

Volume of Container Shell (from Drawing): $V_{CS} := 0.00512\,m^3$

Total Volume of Container Shell: $V_{CS.T} := V_{CS} \cdot N_{D.R}$ $V_{CS.T} = 14.93\,m^3$

Number of Layer in a Stack: $N_L := 3$

Number of Stacks in a Disposal Room: $N_S := \frac{N_{P.D}}{N_L}$ $N_S = 324$

Volume of supersacks of MgO on a Top of Stack: $V_M := 1 \cdot m^3$

Total Volume of MgO sacks: $V_{M.T} := V_M \cdot N_S$ $V_{M.T} = 324\,m^3$

Total Volume of Containers plus MgO sacks: $V_{D.M} := V_{D.W} + V_{M.T}$ $V_{D.M} = 1596.295\,m^3$

Porosity of MgO Sacks: $\phi_M := 41 \cdot \%$

Volume of Solid of MgO Sacks: $V_{S.M} := V_{M.T} \cdot (1 - \phi_M)$ $V_{S.M} = 191.16\,m^3$

Total Volume of Incompressible Solid: $V_{T.I} := V_{P.T} + V_{CS.T} + V_{S.M}$ $V_{T.I} = 949.503\,m^3$

Initial Room Porosity: $\phi_{R.i} := 1 - \frac{V_{T.I}}{V_{R.i}}$ $\phi_{R.i} = 0.739$

Ratio of the solid volume of MgO to the total volume of a room:

$$R_{MgO} := \frac{V_{S.M}}{V_{R.i}} \qquad R_{MgO} = 5.248\%$$

B-4 1/3 AMWTP waste and 2/3 Standard waste

Hight of Disposal Room: $H_R := 3.96\,m$

Wide of Disposal Room: $W_R := 10.06\,m$

Length of Disposal Room: $L_R := 91.44\,m$

Initial Room Volume: $V_{R.i} := H_R \cdot W_R \cdot L_R$ $V_{R.i} = 3642.8\,m^3$

Portion of Satandard Waste: $P_S := \frac{2}{3}$

Portion of AMWTP Waste: $P_A := 1 - P_S$ $P_A = 0.33$

Volume of All AMWTP(Container+MgO Sack) in a Room: $V_{D.W.A} := 1596.3\,m^3$

Volume of All Standard Waste Drum in a Room: $V_{D.W.S} := 1727.5\,m^3$

Volume of 1/3 AMWTP Type Waste: $V_{D.W} := P_A \cdot V_{D.W.A} + P_S \cdot V_{D.W.S}$ $V_{D.W} = 1683.77\,m^3$

Initial Density of All AMWTP (Container+MgO Sack): $\rho_{0.A} := 1399.21 \frac{kgf}{m^3}$

Solid Waste Density of AMWTP: $\rho_{s.A} := 2352.26 \frac{kgf}{m^3}$

Initial Density of All Std. Drum: $\rho_{0.S} := 559.5 \frac{kgf}{m^3}$

Solid Waste Density of Std. Waste: $\rho_{s.S} := 1757 \frac{kgf}{m^3}$

Initial Density of 1/3 AMWTP Type: $\rho_{0.TP} := P_A \cdot \rho_{0.A} + P_S \cdot \rho_{0.S}$ $\rho_{0.TP} = 839.4 \frac{kgf}{m^3}$

Solid Waste Density of 1/3 AMWTP Type: $\rho_{s.TP} := P_A \cdot \rho_{s.A} + P_S \cdot \rho_{s.S}$ $\rho_{s.TP} = 1955.42 \frac{kgf}{m^3}$

Initial Porosity of 1/3 AMWTP Type: $\phi_0 := 1 - \frac{\rho_{0.TP}}{\rho_{s.TP}}$ $\phi_0 = 0.57$

Initial Void Volume of 1/3 AMWTP Type: $V_{v.D.W} := V_{D.W} \cdot \phi_0$ $V_{v.D.W} = 960.98 m^3$

Initial Solid Waste Volume $V_s := V_{D.W} - V_{v.D.W}$ $V_s = 722.79 m^3$

Initial Porosity of the Undeformed Disposal Room:

$$\phi_{R.i} := \frac{V_{R.i} - V_s}{V_{R.i}} \qquad \phi_{R.i} = 0.802$$

B-5 2/3 AMWTP waste and 1/3 Standard waste

Hight of Disposal Room: $H_R := 3.96\,m$

Wide of Disposal Room: $W_R := 10.06\,m$

Length of Disposal Room: $L_R := 91.44\,m$

Initial Room Volume: $V_{R.i} := H_R \cdot W_R \cdot L_R$ $V_{R.i} = 3642.8\,m^3$

Portion of Satandard Waste: $P_S := \frac{1}{3}$

Portion of AMWTP Waste: $P_A := 1 - P_S$ $P_A = 0.67$

Volume of All AMWTP(Containers+MgO Sacks) in a Room: $V_{D.W.A} := 1596.3\,m^3$

Volume of All Standard Waste Drum in a Room: $V_{D.W.S} := 1727.5\,m^3$

Volume of 2/3 AMWTP Type Waste: $V_{D.W} := P_A \cdot V_{D.W.A} + P_S \cdot V_{D.W.S}$ $V_{D.W} = 1640.03\,m^3$

Initial Density of All AMWTP (Drum+MgO Sack): $\rho_{0.A} := 1399.21 \cdot \frac{kgf}{m^3}$

Solid Waste Density of AMWTP: $\rho_{s.A} := 2352.26 \frac{kgf}{m^3}$

Initial Density of All Std. Drum: $\rho_{0.S} := 559.5 \frac{kgf}{m^3}$

Solid Waste Density of Std. Waste: $\rho_{s.S} := 1757 \cdot \frac{kgf}{m^3}$

Initial Density of 2/3 AMWTP Type: $\rho_{0.TP} := P_A \cdot \rho_{0.A} + P_S \cdot \rho_{0.S}$ $\rho_{0.TP} = 1119.31 \frac{kgf}{m^3}$

Solid Waste Density of 2/3 AMWTP Type: $\rho_{s.TP} := P_A \cdot \rho_{s.A} + P_S \cdot \rho_{s.S}$ $\rho_{s.TP} = 2153.84 \frac{kgf}{m^3}$

Initial Porosity of 2/3 AMWTP Type: $\phi_0 := 1 - \frac{\rho_{0.TP}}{\rho_{s.TP}}$ $\phi_0 = 0.48$

Initial Void Volume of 2/3 AMWTP Type: $V_{v.D.W} := V_{D.W} \cdot \phi_0$ $V_{v.D.W} = 787.74 m^3$

Initial Solid Waste Volume $V_s := V_{D.W} - V_{v.D.W}$ $V_s = 852.29 m^3$

Initial Porosity of the Undeformed Disposal Room:

$$\phi_{R.i} := \frac{V_{R.i} - V_s}{V_{R.i}} \qquad \phi_{R.i} = 0.766$$

APPENDIX C: GAS GENERATION POTENTIAL AND RATE

C-1 Standard Waste and POP Waste

Number of Drums in a Disposal Room: $N_{D.R} := 6804 \cdot drum$

Number of Drums in a Pack: $N_{D.P} := 7 \cdot drum$

Number of Packs in a Disposal Room: $N_{P.R} := \frac{N_{D.R}}{N_{D.P}}$ $N_{P.R} = 972$

Number of Pucks in a Drum $N_{P.D} := 1$

Total Number of Pucks in a Disposal Room: $N_{T.P} := N_{D.R} \cdot N_{P.D}$ $N_{T.P} = 6.804 \times 10^{3}\ drum$

Estimated Gas Production Rate from Anoxic Corrosion: $GPR_A := 1 \cdot \frac{mol}{drum \cdot yr}$ $drum \equiv 55 \cdot gal$

Estimated Gas Production Rate from Microbial Activity: $GPR_M := 1 \cdot \frac{mol}{drum \cdot yr}$

Anoxic Corrosion Period: $t_A := 1050 \cdot yr$

Microbial Activity Period: $t_M := 550 \cdot yr$

Total Gas Potential from 0 yr to 550 yr: $PVALUE_1 := (GPR_A + GPR_M) \cdot t_M \cdot N_{T.P}$

$PVALUE_1 = 7.484 \times 10^{6}\ mol$

Gas Production Rate from 0 yr to 550 yr $RATE_1 := \frac{PVALUE_1}{t_M}$

$RATE_1 = 4.312 \times 10^{-4} \frac{mol}{s}$

Total Gas Potential from 550 yr to 1050 yr: $PVALUE_2 := (GPR_A)(t_A - t_M) N_{T.P}$

$PVALUE_2 = 3.402 \times 10^{6}\ mol$

Gas Production Rate from 550 yr to 1050 yr $RATE_2 := \frac{PVALUE_2}{(t_A - t_M)}$

$RATE_2 = 2.156 \times 10^{-4} \frac{mol}{s}$

Total Gas Potential from 0 yr to 1050 yr: $PVALUE := PVALUE_1 + PVALUE_2$

$PVALUE = 1.0886 \times 10^{7}\ mol$

C-2 1/3 AMWTP and 2/3 Standard Waste

Number of Packs in a Disposal Room: $N_{P.R} := 972$

$cont \equiv 100 \cdot gal$

$drum \equiv 55 \cdot gal$

Portion of Satandard Waste: $P_S := \frac{2}{3}$

Portion of AMWTP Waste: $P_A := 1 - P_S$ $P_A = 0.333$

Number of Standard Waste Packs in a Disposal Room: $N_{S.P} := N_{P.R} \cdot P_S$ $N_{S.P} = 648$

Number of AMWTP Waste Packs in a Disposal Room: $N_{A.P} := N_{P.R} \cdot P_A$ $N_{A.P} = 324$

Number of Standard Drums in a Pack: $N_{SD.P} := 7 \cdot drum$

Number of Standard Drums in a Disposal Room: $N_{S.R} := N_{SD.P} \cdot N_{S.P}$ $N_{S.R} = 4536drum$

Number of 100-gal Containers in a Pack: $N_{D.P} := 3 \cdot cont$

Number of 100-gal Containers in a Disposal Room: $N_{D.R} := N_{A.P} \cdot N_{D.P}$ $N_{D.R} = 972cont$

Number of Pucks(Compressed Drum) in a Container: $N_{P.D} := 4 \cdot \frac{drum}{cont}$

Total Number of Pucks in a Disposal Room: $N_{T.P} := N_{D.R} \cdot N_{P.D}$ $N_{T.P} = 3888drum$

Total Number of Pucks and Std. Drum in a Disposal Room: $N_{T.P.S} := N_{S.R} + N_{T.P}$

$N_{T.P.S} = 8424drum$

Estimated Gas Production Rate from Anoxic Corrosion: $GPR_A := 1 \cdot \frac{mol}{drum \cdot yr}$

Estimated Gas Production Rate from Microbial Activity: $GPR_M := 1 \cdot \frac{mol}{drum \cdot yr}$

Anoxic Corrosion Period:

$$t_A := 1050 \cdot yr$$

Microbial Activity Period:

$$t_M := 550 \cdot yr$$

Total Gas Potential from 0 yr to 550 yr:

$$PVALUE_1 := \left(GPR_A + GPR_M\right) t_M \cdot N_{T.P.S}$$

$$PVALUE_1 = 9.266 \times 10^{6}\ mol$$

Gas Production Rate from 0 yr to 550 yr

$$RATE_1 := \frac{PVALUE_1}{t_M}$$

$$RATE_1 = 5.339 \times 10^{-4}\ \frac{mol}{s}$$

Total Gas Potential from 550 yr to 1050 yr:

$$PVALUE_2 := \left(GPR_A\right)\left(t_A - t_M\right) N_{T.P.S}$$

$$PVALUE_2 = 4.212 \times 10^{6}\ mol$$

Gas Production Rate from 550 yr to 1050 yr

$$RATE_2 := \frac{PVALUE_2}{\left(t_A - t_M\right)}$$

$$RATE_2 = 2.669 \times 10^{-4}\ \frac{mol}{s}$$

Total Gas Potential from 0 yr to 1050 yr:

$$PVALUE := PVALUE_1 + PVALUE_2$$

$$PVALUE = 1.3478 \times 10^{7}\ mol$$

C-3 2/3 AMWTP and 1/3 Standard Waste

Number of Packs in a Disposal Room: $N_{P.R} := 972$

$cont \equiv 100 \cdot gal$

$drum \equiv 55 \cdot gal$

Portion of Satandard Waste: $P_S := \frac{1}{3}$

Portion of AMWTP Waste: $P_A := 1 - P_S$ $P_A = 0.667$

Number of Standard Waste Packs in a Disposal Room: $N_{S.P} := N_{P.R} \cdot P_S$ $N_{S.P} = 324$

Number of AMWTP Waste Packs in a Disposal Room: $N_{A.P} := N_{P.R} \cdot P_A$ $N_{A.P} = 648$

Number of Standard Drums in a Pack: $N_{SD.P} := 7 \cdot drum$

Number of Standard Drums in a Disposal Room: $N_{S.R} := N_{SD.P} \cdot N_{S.P}$ $N_{S.R} = 2268 drum$

Number of 100-gal Containers in a Pack: $N_{D.P} := 3 \cdot cont$

Number of 100-gal Containers in a Disposal Room: $N_{D.R} := N_{A.P} \cdot N_{D.P}$ $N_{D.R} = 1944 cont$

Number of Pucks(Compressed Drum) in a Container: $N_{P.D} := 4 \cdot \frac{drum}{cont}$

Total Number of Pucks in a Disposal Room: $N_{T.P} := N_{D.R} \cdot N_{P.D}$ $N_{T.P} = 7776 drum$

Total Number of Pucks and Std. Drum in a Disposal Room: $N_{T.P.S} := N_{S.R} + N_{T.P}$

$N_{T.P.S} = 10044 drum$

Estimated Gas Production Rate from Anoxic Corrosion: $GPR_A := 1 \cdot \frac{mol}{drum \cdot yr}$

Estimated Gas Production Rate from Microbial Activity: $GPR_M := 1 \cdot \frac{mol}{drum \cdot yr}$

Anoxic Corrosion Period:

$$t_A := 1050 \cdot yr$$

Microbial Activity Period:

$$t_M := 550 \cdot yr$$

Total Gas Potential from 0 yr to 550 yr:

$$PVALUE_1 := \left(GPR_A + GPR_M\right) t_M \cdot N_{T.P.S}$$

$$PVALUE_1 = 1.105 \times 10^{7}\ mol$$

Gas Production Rate from 0 yr to 550 yr

$$RATE_1 := \frac{PVALUE_1}{t_M}$$

$$RATE_1 = 6.366 \times 10^{-4}\ \frac{mol}{s}$$

Total Gas Potential from 550 yr to 1050 yr:

$$PVALUE_2 := \left(GPR_A\right)\left(t_A - t_M\right) N_{T.P.S}$$

$$PVALUE_2 = 5.022 \times 10^{6}\ mol$$

Gas Production Rate from 550 yr to 1050 yr

$$RATE_2 := \frac{PVALUE_2}{\left(t_A - t_M\right)}$$

$$RATE_2 = 3.183 \times 10^{-4}\ \frac{mol}{s}$$

Total Gas Potential from 0 yr to 1050 yr:

$$PVALUE := PVALUE_1 + PVALUE_2$$

$$PVALUE = 1.607 \times 10^{7}\ mol$$

C-4 All AMWTP Waste

Number of Packs in a Disposal Room: $N_{P.R} := 972$

$cont \equiv 100 \cdot gal$

Number of 100-gal Container in a Pack: $N_{D.P} := 3 \cdot cont$

$drum \equiv 55 \cdot gal$

Number of 100-gal Container in a Disposal Room: $N_{D.R} := N_{P.R} \cdot N_{D.P}$ $N_{D.R} = 2916 cont$

Number of Pucks(Compressed Drum) in a Container: $N_{P.D} := 4 \cdot \frac{drum}{cont}$

Total Number of Pucks in a Disposal Room: $N_{T.P} := N_{D.R} \cdot N_{P.D}$ $N_{T.P} = 11664 drum$

Estimated Gas Production Rate from Anoxic Corrosion: $GPR_A := 1 \cdot \frac{mol}{drum \cdot yr}$

Estimated Gas Production Rate from Microbial Activity: $GPR_M := 1 \cdot \frac{mol}{drum \cdot yr}$

Anoxic Corrosion Period: $t_A := 1050 \cdot yr$

Microbial Activity Period: $t_M := 550 \cdot yr$

Total Gas Potential from 0 yr to 550 yr: $PVALUE_1 := (GPR_A + GPR_M) t_M \cdot N_{T.P}$

$PVALUE_1 = 1.283 \times 10^7 mol$

Gas Production Rate from 0 yr to 550 yr $RATE_1 := \frac{PVALUE_1}{t_M}$

$RATE_1 = 7.392 \times 10^{-4} \frac{mol}{s}$

Total Gas Potential from 550 yr to 1050 yr: $PVALUE_2 := (GPR_A)(t_A - t_M) N_{T.P}$

$PVALUE_2 = 5.832 \times 10^6 mol$

Gas Production Rate from 550 yr to 1050 yr $RATE_2 := \frac{PVALUE_2}{(t_A - t_M)}$

$RATE_2 = 3.696 \times 10^{-4} \frac{mol}{s}$

Total Gas Potential from 0 yr to 1050 yr: $PVALUE := PVALUE_1 + PVALUE_2$

$PVALUE = 1.8662 \times 10^7 mol$

APPENDIX D: HEIGHT OF THE AMWTP MODEL IN THE DISPOSAL ROOM

Number of Packs in a Disposal Room: $N_{P.D} := 972$

Number of Drums in a Pack: $N_{D.P} := 3$

Number of Drums in a Disposal Room: $N_{D.R} := N_{P.D} \cdot N_{D.P}$ $N_{D.R} = 2916$

Number of Layer in a Stack: $N_L := 3$

Number of Stacks in a Disposal Room: $N_S := \frac{N_{P.D}}{N_L}$ $N_S = 324$

Volume of supersacks of MgO on a Top of Stack: $V_M := 1 \cdot m^3$

Total Volume of MgO Sacks: $V_{M.T} := V_M \cdot N_S$ $V_{M.T} = 324 m^3$

Modified uncompressed width of the stored waste: $W_0 := 7.35 \cdot m$ (SAND97-0795, p.18)

Modified length of the disposal room available for storing waste: $L_0 := 87.85 \cdot m$ (SAND97-0795, p.18)

Norminal area of the disposal room available for storing waste: $A_0 := W_0 \cdot L_0$ $A_0 = 645.697 m^2$

Uncompressed height of MgO sacks: $H_M := \frac{V_{M.T}}{A_0}$ $H_M = 0.502m$

Height of Pucks in a Container: $H_P := 31.75 \cdot in$

Total Height of Pucks in Three Layers Containers: $H_{P.3} := 3 \cdot H_P$ $H_{P.3} = 2.419m$

Elevation of the Bottom of Waste in the Model: $E_B := -6.39 \cdot m$

Elevation of the Top of Pucks in the Model: $E_{TP} := E_B + H_{P.3}$ $E_{TP} = -3.971m$

Height of Container: $H_C := 35 \cdot in$ $H_C = 0.889m$

Total Height of Three Layers Containers: $H_{C.3} := 3 \cdot H_C$ $H_{C.3} = 2.667m$

Total Height of Containers with MgO Sacks: $H_{TCM} := H_{C.3} + H_M$ $H_{TCM} = 3.169m$

Elevation of the Top of Waste in the Model: $E_{TW} := E_B + H_{TCM}$ $E_{TW} = -3.221m$

APPENDIX E: MODIFIED WIDTH AND LENGTH OF THE WASTE

E-1 All AMWTP Waste Case

Norminal uncompressed width of the stored 100-gallon container in the disposal room: $W_0 := 6.243 \cdot m$ (Figure 12)

Number of Containers in a Layer: $N_{P.R} := 972$

Number of Containers Line due to Rearrangement: $N_L := 9$ (Figure 12)

Number of Containers in a Line: $N_{P.L} := \frac{N_{P.R}}{N_L}$ $N_{P.L} = 108$

Diameter of Containers: $D_C := 31 \cdot in$ $D_C = 0.787m$

Nominal length of the disposal room available for storing waste: $L_0 := N_{P.L} \cdot D_C$ $L_0 = 85.039m$

Height of the three stacked waste containers with MgO sacks: $H_0 := 3.169 \cdot m$ (Appendix D)

Guess $D := 1 \cdot m$

Given

$(W_0 - 2 \cdot D)(L_0 - 2 \cdot D) H_0 = 1596 m^3$ (Appendix B-3)

$D := Find(D)$

Amount of space that must be eliminated between the containers: $D = 0.15m$

$W := W_0 - 2D$

Modified width of the waste: $W = 5.943m$

Half modified width of the waste for mesh: $H := \frac{W}{2}$ $H = 2.972m$

$L := L_0 - 2 \cdot D$

Modified length of the disposal room available for storing waste: $L = 84.739m$

E-2 2/3 AMWTP + 1/3 Standard Waste Case

Norminal uncompressed width of the stored 100-gallon container in the disposal room: $W_0 := 4.197\cdot m$ (Figure 16)

Number of Containers in a Layer: $N_{P.R} := 972\cdot\left(\frac{2}{3}\right)$

Number of Containers Line due to Rearrange: $N_L := 6$ (Figure 16)

Number of Containers in a Line: $N_{P.L} := \frac{N_{P.R}}{N_L}$ $N_{P.L} = 108$

Diameter of Containers: $D_C := 31\cdot in$ $D_C = 0.787m$

Nominal length of the disposal room available for storing waste: $L_0 := N_{P.L}\cdot D_C$ $L_0 = 85.039m$

Height of the three stacked waste containers with MgO sacks: $H_0 := 3.169\cdot m$ (Appendix D)

Guess $D := 1\cdot m$

Given

$$(W_0 - 2\cdot D)(L_0 - 2\cdot D)H_0 = 1064\cdot m^3 \quad \left(= 1596\cdot m^3\cdot\frac{2}{3}\right)$$

$D := Find(D)$

$D = 0.119m$

Amount of space that must be eliminated between the containers:

$W_c := W_0 - 2D$

Modified width of the container part: $W_c = 3.959m$

Modified width of the standard part: $W_s := 7.35\cdot m\cdot\frac{1}{3}$ $W_s = 2.45m$

Modified width of the waste: $W := W_c + W_s$ $W = 6.409m$

Half modified width of the waste: $H := \frac{W}{2}$ $H = 3.205m$

$L := L_0 - 2\cdot D$

Modified length of the disposal room available for storing waste: $L = 84.801m$

E-3 1/3 AMWTP and 2/3 Standard Waste Case

Norminal uncompressed width of the stored 100-gallon container in the disposal room: $W_0 := 2.151 \cdot m$ (Figure 19)

Number of Containers in a Layer: $N_{P.R} := 972 \cdot \left(\frac{1}{3}\right)$

Number of Containers Line due to Rearrange: $N_L := 3$ (Figure 19)

Number of Containers in a Line: $N_{P.L} := \frac{N_{P.R}}{N_L}$ $N_{P.L} = 108$

Diameter of Containers: $D_C := 31 \cdot in$ $D_C = 0.787m$

Nominal length of the disposal room available for storing waste: $L_0 := N_{P.L} \cdot D_C$ $L_0 = 85.039m$

Height of the three stacked waste containers with MgO sacks: $H_0 := 3.169 \cdot m$ (Appendix D)

Guess $D := 1 \cdot m$

Given

$$(W_0 - 2 \cdot D)(L_0 - 2 \cdot D) H_0 = 532 \cdot m^3 \qquad (= \ 1596 \cdot m^3 \cdot \frac{1}{3} = 532 m^3)$$

$D := Find(D)$

$D = 0.086m$

Amount of space that must be eliminated between the containers:

$W_c := W_0 - 2D$

Modified width of the container part: $W_c = 1.978m$

Modified width of the standard part: $W_s := 7.35 \cdot m \cdot \frac{2}{3}$ $W_s = 4.9m$

Modified width of the waste: $W := W_c + W_s$ $W = 6.878m$

Half modified width of the waste: $H := \frac{W}{2}$ $H = 3.439m$

$L := L_0 - 2 \cdot D$

Modified length of the disposal room available for storing waste: $L = 84.866m$

APPENDIX F: POROSITY CALCULATION FOR THE PUCK PART

Note: Room dimensions taken from Park and Holland, 2003.

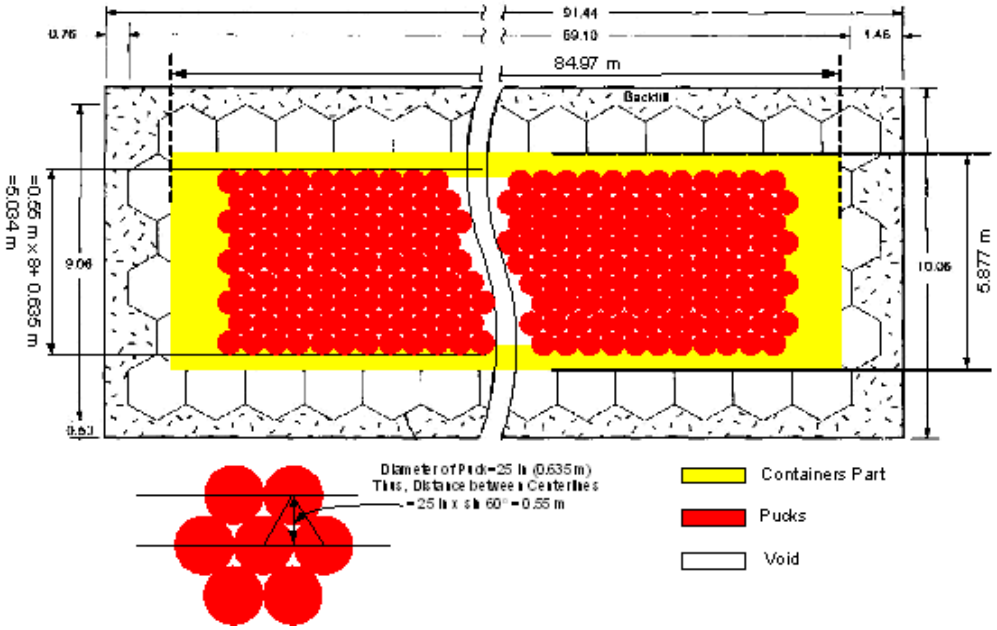

Diameter of Puck: $D_P := 25 \cdot in$

Width of Pucks in the mesh: $W_P := 5.034 \cdot m$

Length of Pucks in the mesh: $L_P := 108 \cdot D_P + \frac{1}{2} \cdot D_P$ $L_P = 68.897 m$

Height of Pucks in the mesh: $H_P := 2.419 \cdot m$

Volume of Pucks in the mesh: $V_{PM} := W_P \cdot L_P \cdot H_P$ $V_{PM} = 838.982 m^3$





Area of Triangle: $A_T := \frac{1}{2} D_P \cdot D_P \cdot \sin(60 \cdot deg)$ $A_T = 0.175 m^2$

Area of Half Circle:

$$A_{HC} := \frac{1}{2}\cdot\pi\cdot\left(\frac{D_P}{2}\right)^2 \qquad A_{HC} = 0.158\text{m}^2$$

Area of space between 3 pucks: $A_{3S} := A_T - A_{HC}$ $A_{3S} = 0.016\text{m}^2$

Total area of space between 3 pucks: $A_{T3S} := A_{3S}\cdot 107\cdot 8\cdot 2$ $A_{T3S} = 27.829\text{m}^2$

Area of Rectangle at both side: $A_R := D_P\cdot\frac{1}{2}\cdot D_P$ $A_R = 0.202\text{m}^2$

Area of space between 2 puck at both side: $A_{2S} := A_R - A_{HC}$ $A_{2S} = 0.043\text{m}^2$

Total area of space between 2pucks: $A_{T2S} := 107\cdot A_{2S}\cdot 2$ $A_{T2S} = 9.259\text{m}^2$

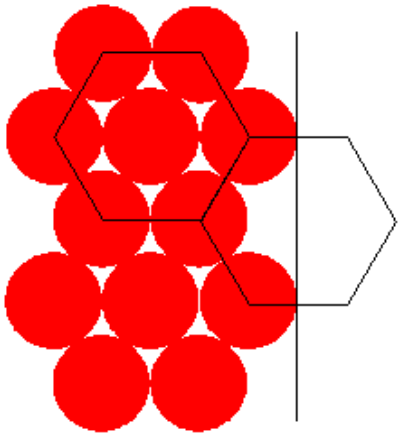

Area of Hexagon: $A_H := 6\cdot A_T$ $A_H = 1.048\text{m}^2$

Area of space at both end: $A_{SE} := \frac{1}{2}A_H - 2A_{HC}$ $A_{SE} = 0.207\text{m}^2$

Total area of space at both end: $A_{TSE} := 9\cdot A_{SE}$ $A_{TSE} = 1.864\text{m}^2$

Total area of space: $A_{TS} := A_{T3S} + A_{T2S} + A_{TSE}$ $A_{TS} = 38.952\text{m}^2$

Area of Pucks: $A_P := L_P \cdot W_P - A_{TS}$ $A_P = 307.878 m^2$

Total void volume in puck mesh: $V_{TS} := A_{TS} \cdot H_P$ $V_{TS} = 94.226 m^3$

Volume of Pucks: $V_P := A_P \cdot H_P$ $V_P = 744.756 m^3$

Porosity of the puck mesh in FEM model: $\phi_P := \frac{A_{TS}}{L_P \cdot W_P}$ $\phi_P = 0.112$

$\phi_P := \frac{(V_{PM} - V_P)}{V_{PM}}$ $\phi_P = 0.112$

APPENDIX G: SAMPLE FASTQ FILE (2/3 AMWTP+1/3STANDARD CASE)

```
TITLE
DISPOSAL ROOM CONTAINING 2/3AMWTP-MULTIMATERIAL STRATIGRAPHY-B.Y.PARK
POINT    1     0.00    -54.19
POINT    2    20.27    -54.19
POINT    3     0.00     -8.63
POINT    4    20.27     -8.63
POINT    5     0.00     -8.63
POINT    6    20.27     -8.63
POINT    7     0.00     -7.77
POINT    8    20.27     -7.77
POINT    9     0.00     -6.39
POINT   10     5.03     -6.39
$ around Pucks
POINT   11     0.00     -6.39
POINT   12     3.205    -6.39
POINT   13     0.00     -3.221
POINT   14     3.205    -3.221
$ Pucks
POINT   62     1.693    -6.39
POINT   63     0.00     -3.971
POINT   64     1.693    -3.971
POINT   65     3.205    -3.971
POINT   66     1.693    -3.221
$
POINT   15     5.03     -2.43
POINT   16     0.00     -2.43
POINT   17     0.00      0.00
POINT   18    20.27      0.00
POINT   19     0.00      4.27
POINT   20    20.27      4.27
POINT   21     0.00     52.87
POINT   22    20.27     52.87
POINT   23    20.27     -2.43
POINT   24    20.27     -6.39
POINT   25     5.03      0.00
POINT   26     5.03     -7.77
POINT   27     5.03      4.27
POINT   28     5.03     -8.63
POINT   29     0.0       2.10
POINT   30     5.03      2.10
POINT   31    20.27      2.10
POINT   32     0.0       2.31
POINT   33     5.03      2.31
POINT   34    20.27      2.31
LINE     1     STR    1    2    0    22   1.0
LINE     2     STR    1    5    0    20   0.85
LINE     3     STR    2    6    0    20   0.85
$LINE    4     STR    5    6    0    15
LINE     5     STR   28    6    0    15   1.1
LINE     6     STR    5    7    0     4
LINE     7     STR    6    8    0     4
LINE     8     STR    7    9    0     5
LINE     9     STR   26    8    0    15   1.1
LINE    10     STR   24    8    0     5
LINE    11     STR   10   24    0    15   1.1
LINE    12     STR    9   10    0     7   0.8
$ around Pucks
LINE    13     STR   62   12    0     8   1.15
LINE    14     STR   12   65    0     8   0.8
LINE    15     STR   13   66    0     7   0.8
LINE    16     STR   63   13    0     5   1.2
```

```
LINE    67     STR   64   65    0     8   1.15
LINE    68     STR   65   14    0     5   1.2
LINE    69     STR   66   14    0     8   1.15
LINE    70     STR   64   66    0     5   1.2
$ Pucks
LINE    63     STR   11   62    0     7   0.8
LINE    64     STR   62   64    0     8   0.8
LINE    65     STR   63   64    0     7   0.8
LINE    66     STR   11   63    0     8   0.8
$
LINE    17     STR   10   15    0    12
LINE    18     STR   24   23    0    12
LINE    19     STR    8   18    0    12
LINE    20     STR   16   17    0     7
LINE    21     STR   16   15    0     7   0.8
LINE    22     STR   15   23    0    15   1.1
LINE    23     STR   18   23    0     7
LINE    24     STR   25   18    0    15   1.1
LINE    25     STR   17   19    0     8
LINE    26     STR   18   20    0     8
LINE    27     STR   27   20    0    15   1.1
$LINE    28     STR   25   20    0     8
LINE    29     STR   19   21    0    20   1.15
LINE    30     STR   20   22    0    20   1.15
LINE    31     STR   21   22    0    22   1.0
LINE    32     STR   17   25    0     7   0.8
LINE    33     STR   19   27    0     7   0.8
LINE    34     STR    7   26    0     7   0.8
LINE    35     STR    5   28    0     7   0.8
LINE    36     STR   17   29    0     4
LINE    37     STR   18   31    0     4
LINE    38     STR   29   30    0     7   0.8
LINE    39     STR   30   31    0    15   1.1
LINE    40     STR   29   32    0     1
LINE    41     STR   31   34    0     1
LINE    42     STR   32   33    0     7   0.8
LINE    43     STR   33   34    0    15   1.1
LINE    44     STR   32   19    0     4
LINE    45     STR   34   20    0     4
SIDE   100    11  12
SIDE   101    21  22
SIDE   102    32  24
SIDE   103    33  27
SIDE   104    35   5
SIDE   105    34   9
SIDE   106    38  39
SIDE   107    42  43
$ NODEBC CARDS
NODEBC   2    1
NODEBC   1    2    6    8   66   16   20   36   40   44   29
NODEBC   1    3    7   10   18   23   37   41   45   30
$ SIDEBC CARDS
SIDEBC  10   31   $ Top of the Model
SIDEBC  20    1   $ Bottom of the Model
SIDEBC 100   12   $ Room Floor
SIDEBC 200   17   $ Room Wall
SIDEBC 300   21   $ Room Roof
SIDEBC 400   13  63   $ Waste Bottom
SIDEBC 500   14  68   $ Waste Side
SIDEBC 600   15  69   $ Waste Top
SIDEBC 700   12   17   21  $ Room Boundary
$ REGION CARDS
REGION   1    1   -1   -3  104   -2
```

```
REGION   2    2  104   -7  105   -6
REGION   3    1  105  -10  100   -8
REGION   4    1  -11  -18  -22  -17
REGION   5    1  101  -23  102  -20
REGION   6    3  102  -37  106  -36
REGION   7    1  103  -30  -31  -29
$ around Pucks
REGION  11    4  -13  -14  -67  -64
REGION  12    4  -67  -68  -69  -70
REGION  13    4  -65  -70  -15  -16
$ Pucks
REGION  14    5  -63  -64  -65  -66
$
REGION   9    2  106  -41  107  -40
REGION  10    3  107  -45  103  -44
SCHEME   P
EXIT
```

APPENDIX H: SAMPLE AWK SCRIPT TO CALCULATE THE POROSITY CHANGE IN THE ROOM WITH TIME (ALL AMWTP CASE)

```
#
# This awk script computes the porosity change in the room an outputs
# it as a function of time (Based upon SANTOS output, All AMWTP)
#
BEGIN {
  dens_ws = 2352.26
  dens_w  = 1399.21
  vol_room = 3642.8
  vol_waste = 1596.3
  mass_ws = dens_w*vol_waste
  dens_room = mass_ws/vol_room
  ratio = dens_room/dens_ws
}
{
  if ( $1 ~/[0-9]/ ) {
    vol_ratio = 19.92/$2
    poro = 1. - ratio*vol_ratio
    print $1,poro
  }
}
```

APPENDIX I: SAMPLE SANTOS INPUT FILE

I-1: 12-inch POP

```
TITLE
Porosity Surface Calculation for the Disposal Room with 12" POP Waste: f=0.4
PLANE STRAIN
INITIAL STRESS = USER
GRAVITY = 1 = 0. = -9.79 = 0.
PLOT ELEMENT, STRESS, STRAIN, VONMISES, PRESSURE
PLOT NODAL, DISPLACEMENT, RESIDUAL
PLOT STATE, EQCS, EV
RESIDUAL TOLERANCE = 0.5
MAXIMUM ITERATIONS = 1000
MAXIMUM TOLERANCE = 100.
INTERMEDIATE PRINT = 100
ELASTIC SOLUTION
PREDICTOR SCALE FACTOR = 3
AUTO STEP .015 2.592E6 NOREDUCE 1.E-5
TIME STEP SCALE = 0.5
HOURGLASS STIFFENING = .005
STEP CONTROL
500 3.1536e7
2000 3.1536e9
36000 3.1536e11
END
OUTPUT TIME
1 3.1536e7
1 3.1536e9
200 3.1536e11
END
PLOT TIME
10 3.1536e7
100 3.1536e9
120 3.1536e11
END
MATERIAL, 1, M-D CREEP MODEL, 2300. $ ARGILLACEOUS HALITE
TWO MU = 24.8E9
BULK MODULUS = 20.66E9
A1 = 1.407E23
Q1/R = 41.94
N1 = 5.5
B1 = 8.998E6
A2 = 1.314E13
Q2/R = 16.776
N2 = 5.0
B2 = 4.289E-2
SIG0 = 20.57E6
QLC = 5335.
M = 3.0
K0 = 2.47E6
C = 2.759
ALPHA = -14.96
BETA = -7.738
DELTLC = .58
RN3 = 2.
AMULT = .95
END
MATERIAL, 2, SOIL N FOAMS, 2300. $ ANHYDRITE
TWO MU = 5.563E10
BULK MODULUS = 8.3444E10
A0 = 2.338e6
```

```
A1 = 2.338
A2 = 0.
PRESSURE CUTOFF = 0.0
FUNCTION ID = 0
END
MATERIAL, 3, M-D CREEP MODEL, 2300. $ PURE HALITE
TWO MU = 24.8E9
BULK MODULUS = 20.66E9
A1 = 8.386E22
Q1/R = 41.94
N1 = 5.5
B1 = 6.086E6
A2 = 9.672E12
Q2/R = 16.776
N2 = 5.0
B2 = 3.034E-2
SIG0 = 20.57E6
QLC = 5335.
M = 3.0
K0 = 6.275E5
C = 2.759
ALPHA = -17.37
BETA = -7.738
DELTLC = .58
RN3 = 2.
AMULT = .95
END
MATERIAL, 4, SOIL N FOAMS, 655.94  $ Waste
TWO MU = 1.442E9
BULK MODULUS = 1.561E9
A0 = 8.473E6
A1 = 0.
A2 = 0.
PRESSURE CUTOFF = 0.
FUNCTION ID = 2
END
NO DISPLACEMENT X = 1
NO DISPLACEMENT Y = 2
PRESSURE, 10, 1, 13.57E6
CONTACT SURFACE, 100, 400, 0., 1.E-3, 1.E40
CONTACT SURFACE, 200, 500, 0., 1.E-3, 1.E4
CONTACT SURFACE, 300, 600, 0., 1.E-3, 1.E4
CONTACT SURFACE, 300, 200, 0., 1.E-3, 1.E4
CONTACT SURFACE, 100, 200, 0., 1.E-3, 1.E4
ADAPTIVE PRESSURE, 700, 1.e-6, -6.4
FUNCTION,1 $ FUNCTION TO DEFINE PRESCRIBED PRESSURE
0., 1.
3.1536e11, 1.
END
FUNCTION,2
0.000E+00    0.000E+00
4.767E-03    1.000E+06
8.475E-03    1.600E+06
9.534E-03    1.800E+06
1.059E-02    1.900E+06
1.218E-02    2.000E+06
3.125E-02    3.000E+06
5.085E-02    4.000E+06
7.044E-02    5.000E+06
1.091E-01    7.000E+06
1.637E-01    1.000E+07
2.172E-01    1.300E+07
END
```

```
FUNCTION = 3
0. 0.5
3.1536E11 1.
END
EXIT
```

I-2: All AMWTP

```
TITLE
Porosity Surface Calculation for the Disposal Room with AMWTP Waste: f=0.4
PLANE STRAIN
INITIAL STRESS = USER
GRAVITY = 1 = 0. = -9.79 = 0.
PLOT ELEMENT, STRESS, STRAIN, VONMISES, PRESSURE
PLOT NODAL, DISPLACEMENT, RESIDUAL
PLOT STATE, EQCS, EV
RESIDUAL TOLERANCE = 0.5
MAXIMUM ITERATIONS = 1000
MAXIMUM TOLERANCE = 100.
INTERMEDIATE PRINT = 100
ELASTIC SOLUTION
PREDICTOR SCALE FACTOR = 3
AUTO STEP .015 2.592E6 NOREDUCE 1.E-5
TIME STEP SCALE = 0.5
HOURGLASS STIFFENING = .005
STEP CONTROL
500 3.1536e7
2000 3.1536e9
36000 3.1536e11
END
OUTPUT TIME
1 3.1536e7
1 3.1536e9
200 3.1536e11
END
PLOT TIME
10 3.1536e7
100 3.1536e9
120 3.1536e11
END
MATERIAL, 1, M-D CREEP MODEL, 2300. $ ARGILLACEOUS HALITE
TWO MU = 24.8E9
BULK MODULUS = 20.66E9
A1 = 1.407E23
Q1/R = 41.94
N1 = 5.5
B1 = 8.998E6
A2 = 1.314E13
Q2/R = 16.776
N2 = 5.0
B2 = 4.289E-2
SIG0 = 20.57E6
QLC = 5335.
M = 3.0
K0 = 2.47E6
C = 2.759
ALPHA = -14.96
BETA = -7.738
DELTLC = .58
RN3 = 2.
AMULT = .95
END
```

```
MATERIAL, 2, SOIL N FOAMS, 2300. $ ANHYDRITE
TWO MU = 5.563E10
BULK MODULUS = 8.3444E10
A0 = 2.338e6
A1 = 2.338
A2 = 0.
PRESSURE CUTOFF = 0.0
FUNCTION ID = 0
END
MATERIAL, 3, M-D CREEP MODEL, 2300. $ PURE HALITE
TWO MU = 24.8E9
BULK MODULUS = 20.66E9
A1 = 8.386E22
Q1/R = 41.94
N1 = 5.5
B1 = 6.086E6
A2 = 9.672E12
Q2/R = 16.776
N2 = 5.0
B2 = 3.034E-2
SIG0 = 20.57E6
QLC = 5335.
M = 3.0
K0 = 6.275E5
C = 2.759
ALPHA = -17.37
BETA = -7.738
DELTLC = .58
RN3 = 2.
AMULT = .95
END
MATERIAL, 4, SOIL N FOAMS, 559.5  $ around Pucks
TWO MU = 6.66E8
BULK MODULUS = 2.223E8
A0 = 1.0e6
A1 = 3.
A2 = 0.
PRESSURE CUTOFF = 0.
FUNCTION ID = 2
END
MATERIAL, 5, SOIL N FOAMS, 1399.21 $ Pucks
TWO MU = 5.563E10
BULK MODULUS = 8.3444E10
A0 = 2.338e6
A1 = 2.338
A2 = 0.
PRESSURE CUTOFF = 0.0
FUNCTION ID = 0
END
NO DISPLACEMENT X = 1
NO DISPLACEMENT Y = 2
PRESSURE, 10, 1, 13.57E6
$ Card 39: Coarser mesh should be designated as the master surface.
$             master,slave,   mu,   dis, tenrel
CONTACT SURFACE, 100, 400, 0., 1.E-3, 1.E40 $ btwn room floor and waste bottom
CONTACT SURFACE, 500, 200, 0., 1.E-3, 1.E4  $ btwn waste side and room wall
CONTACT SURFACE, 300, 600, 0., 1.E-3, 1.E4  $ btwn room roof and waste top
CONTACT SURFACE, 200, 300, 0., 1.E-3, 1.E4  $ btwn room wall and room roof
CONTACT SURFACE, 200, 100, 0., 1.E-3, 1.E4  $ btwn room wall and room floor
ADAPTIVE PRESSURE, 700, 1.e-6, -6.4
FUNCTION,1 $ FUNCTION TO DEFINE PRESCRIBED PRESSURE
0., 1.
3.1536e11, 1.
```

```
END
FUNCTION,2
0.0000, 0.0000
0.5101, 1.5300E6
0.6314, 2.0307E6
0.7189, 2.5321E6
0.7855, 3.0312E6
0.8382, 3.5301E6
0.8808, 4.0258E6
0.9422, 4.9333E6
1.1400, 12.000E6
END
FUNCTION = 3
0. 0.5
3.1536E11 1.
END
EXIT
```

APPENDIX J: SAMPLE USER SUBROUTINES (ALL AMWTP WITH *f*=0.1)

J-1 Initial Stress State

```
      SUBROUTINE INITST( SIG,COORD,LINK,DATMAT,KONMAT,SCREL )
C
C *********************************************************************
C
C   DESCRIPTION:
C     THIS ROUTINE PROVIDES AN INITIAL STRESS STATE TO SANTOS
C
C   FORMAL PARAMETERS:
C     SIG      REAL        ELEMENT STRESS ARRAY WHICH MUST BE RETURNED
C                          WITH THE REQUIRED STRESS VALUES
C     COORD    REAL        GLOBAL NODAL COORDINATE ARRAY
C     LINK     INTEGER     CONNECTIVITY ARRAY
C     DATMAT   REAL        MATERIAL PROPERTIES ARRAY
C     KONMAT   INTEGER     MATERIAL PROPERTIES INTEGER ARRAY
C
C   CALLED BY: INIT
C
C *********************************************************************
C
      INCLUDE 'precision.blk'
      INCLUDE 'params.blk'
      INCLUDE 'psize.blk'
      INCLUDE 'contrl.blk'
      INCLUDE 'bsize.blk'
      INCLUDE 'timer.blk'
C
      DIMENSION LINK(NELNS,NUMEL),KONMAT(10,NEMBLK),COORD(NNOD,NSPC),
     *          SIG(NSYMM,NUMEL),DATMAT(MCONS,*),SCREL(NEBLK,*)
C
      DO 1000 I = 1,NEMBLK
         MATID = KONMAT(1,I)
         MKIND = KONMAT(2,I)
         ISTRT = KONMAT(3,I)
         IEND = KONMAT(4,I)
            DO 500 J = ISTRT,IEND
               II = LINK( 1,J )
               JJ = LINK( 2,J )
               KK = LINK( 3,J )
               LL = LINK( 4,J )
               ZAVG = 0.25 * ( COORD(II,2) + COORD(JJ,2) + COORD(KK,2) +
     *              COORD(LL,2) )
               STRESS = - 2300. * 9.79 * ( 655. - ZAVG )
               IF( MATID .EQ. 4 )THEN
                  STRESS = 0.
               END IF
               SIG(1,J) = STRESS
               SIG(2,J) = STRESS
               SIG(3,J) = STRESS
               SIG(4,J) = 0.0

  500       CONTINUE
 1000 CONTINUE
      RETURN
      END
```

J-2 Adaptive Pressure Boundary Condition

```
      SUBROUTINE FPRES( VOLUME,TIME,PGAS )
C ....
C .... THE PRESSURE IS COMPUTED ON THE BASIS OF THE IDEAL GAS LAW,
C .... PV = NRT. THE TOTAL NUMBER OF MOLES OF GAS, N (EN), PRESENT
C .... AT ANY TIME IS DETERMINED ON THE BASIS OF A CONSTANT RATE OF GAS
C .... GENERATION. R IS THE UNIVERSAL GAS CONSTANT AND THETA IS THE ROOM
C .... TEMPERATURE, 300 K. V IS THE CURRENT VOLUME OF THE ROOM. THE VOLUME
C .... MUST BE CORRECTED BY MULTIPLYING BY 2 OR 4 TO ACCOUNT FOR THE USE OF
C .... HALF OR QUARTER-SYMMETRY MODELS. THE VOLUME MUST ALSO BE MULTIPLIED
C .... BY A FACTOR TO ACCOUNT FOR 3D LENGTH.
C ....
C
      INCLUDE 'precision.blk'
C
      R = 8.3144
      THETA = 300.
C
      IF( TIME .LT. 1.7325E10 )THEN
         PVALUE = 0.0
         RATE = 7.392E-4
         TSTAR = 0.0
      ELSE IF( TIME .LT. 3.3075E10 )THEN
         PVALUE = 1.283E7
         RATE = 3.696E-4
         TSTAR = 1.7325E10
      ELSE
         PVALUE = 1.8662E7
         RATE = 0.0
         TSTAR = 0.0
      END IF
C
C .... CORRECT VOLUME AT THIS TIME TO GET VOLUME OF VOIDS
C
      EN = PVALUE + RATE * ( TIME - TSTAR )
      SCALE = 0.1
      SYMFAC = 2.
      XLENG = 91.44
C
C .... THIS MODIFICATION REMOVES THE BACKFILL FROM VSOLID
C
C VSOLID FOR WASTE AND DRUMS ONLY 949.5
      VSOLID = 949.5
      VOLUME = SYMFAC * VOLUME * XLENG - VSOLID
      IF( VOLUME .LE. 0.0 )VOLUME = 1.
C
      PGAS = SCALE * EN * R * THETA / VOLUME
C
      RETURN
      END
```

APPENDIX K: COMPARISON BETWEEN POROSITY HISTORIES FOR THE DISPOSAL ROOM CONTAINING VARIOUS WASTE INVENTORIES

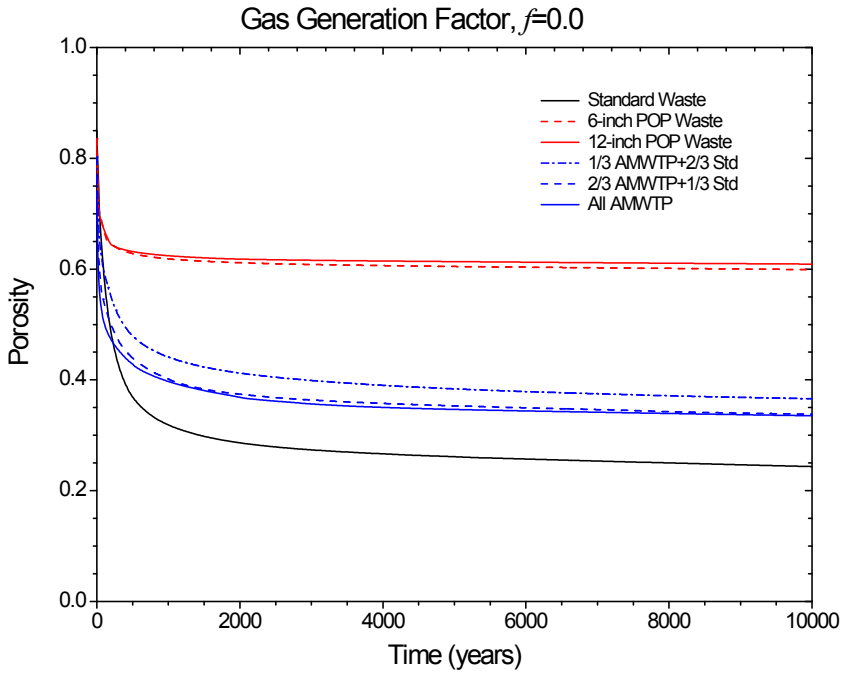

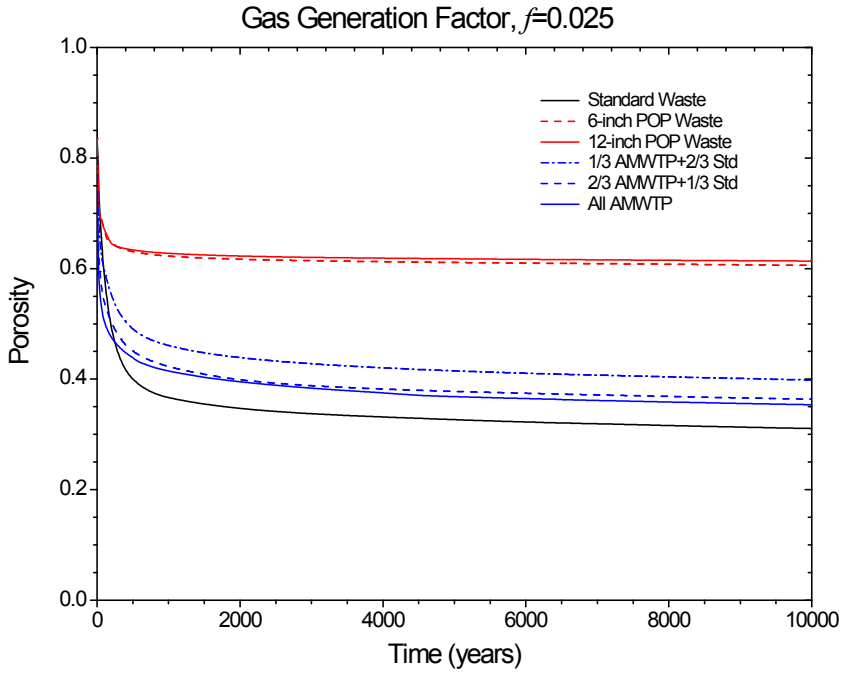

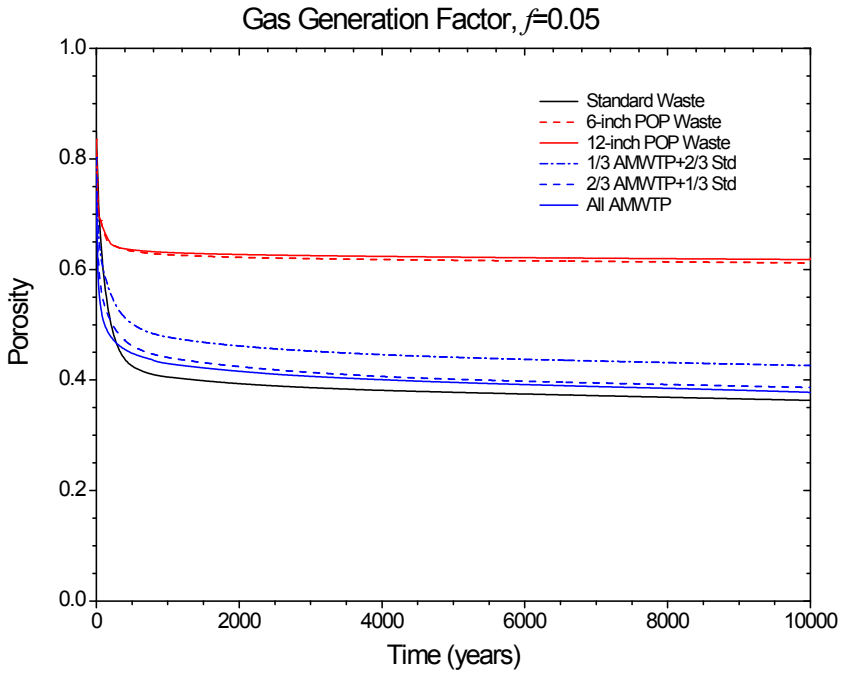
Gas Generation Factor, f=0.05
Porosity
Time (years)
Standard Waste
6-inch POP Waste
12-inch POP Waste
1/3 AMWTP+2/3 Std
2/3 AMWTP+1/3 Std
All AMWTP
1.0
0.8
0.6
0.4
0.2
0.0
0
2000
4000
6000
8000
10000

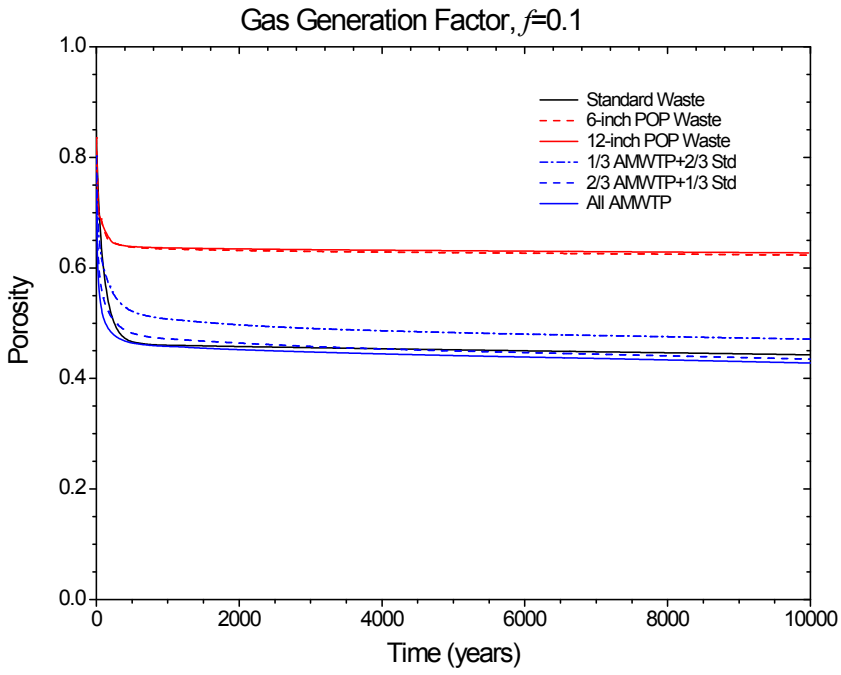
Gas Generation Factor, f=0.1
Porosity
Time (years)
Standard Waste
6-inch POP Waste
12-inch POP Waste
1/3 AMWTP+2/3 Std
2/3 AMWTP+1/3 Std
All AMWTP
1.0
0.8
0.6
0.4
0.2
0.0
0
2000
4000
6000
8000
10000

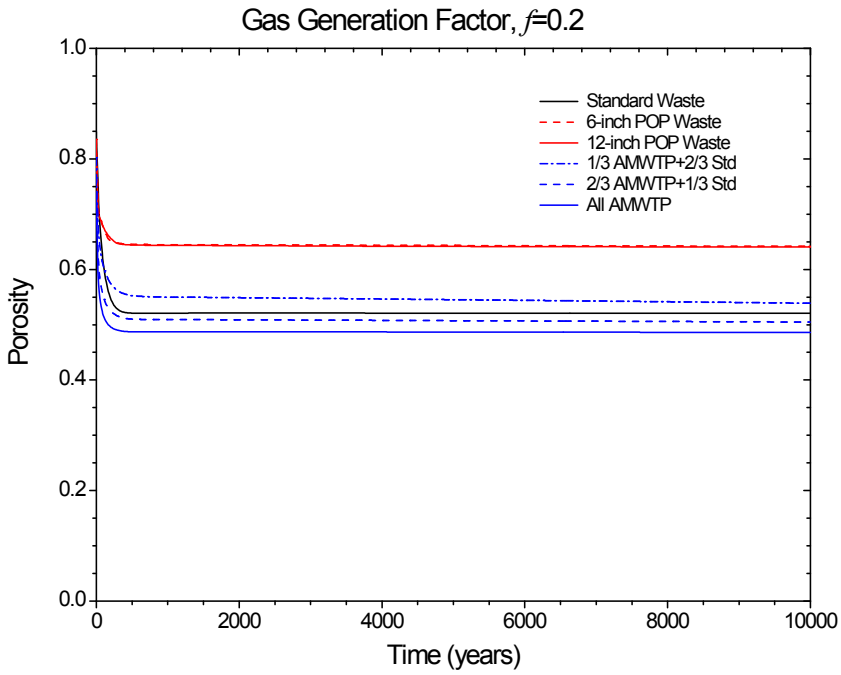
Gas Generation Factor, f=0.2
Porosity
Time (years)
Standard Waste
6-inch POP Waste
12-inch POP Waste
1/3 AMWTP+2/3 Std
2/3 AMWTP+1/3 Std
All AMWTP
1.0
0.8
0.6
0.4
0.2
0.0
0
2000
4000
6000
8000
10000

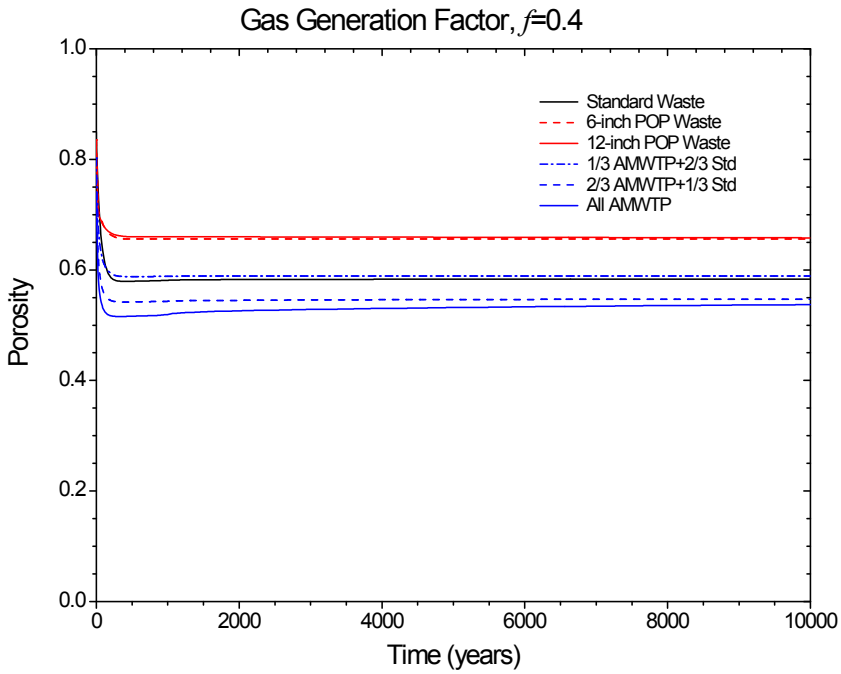
Gas Generation Factor, f=0.4
Porosity
Time (years)
Standard Waste
6-inch POP Waste
12-inch POP Waste
1/3 AMWTP+2/3 Std
2/3 AMWTP+1/3 Std
All AMWTP
1.0
0.8
0.6
0.4
0.2
0.0
0
2000
4000
6000
8000
10000

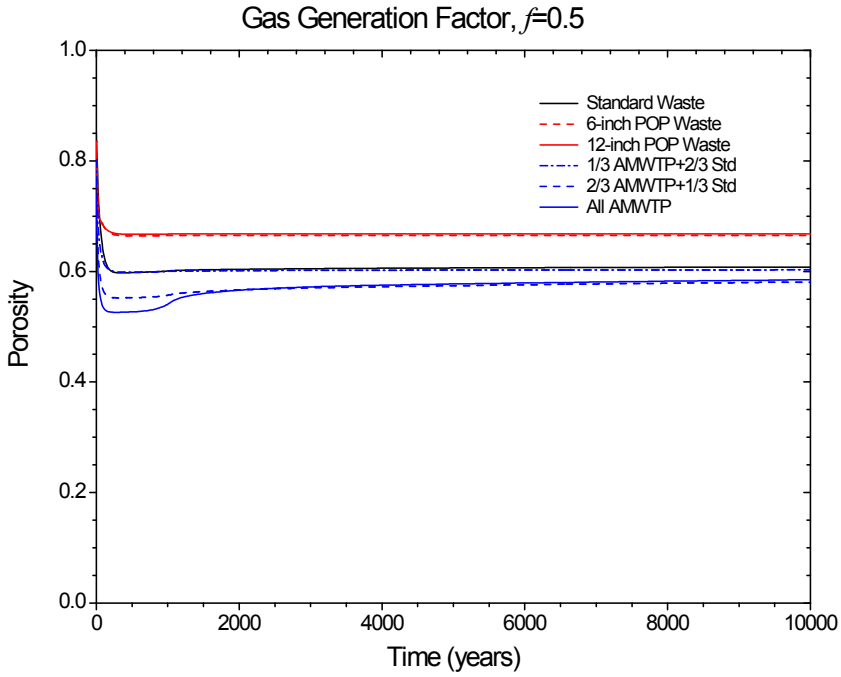
Gas Generation Factor, f=0.5
Porosity
Time (years)
Standard Waste
6-inch POP Waste
12-inch POP Waste
1/3 AMWTP+2/3 Std
2/3 AMWTP+1/3 Std
All AMWTP
0.0
0.2
0.4
0.6
0.8
1.0
0
2000
4000
6000
8000
10000

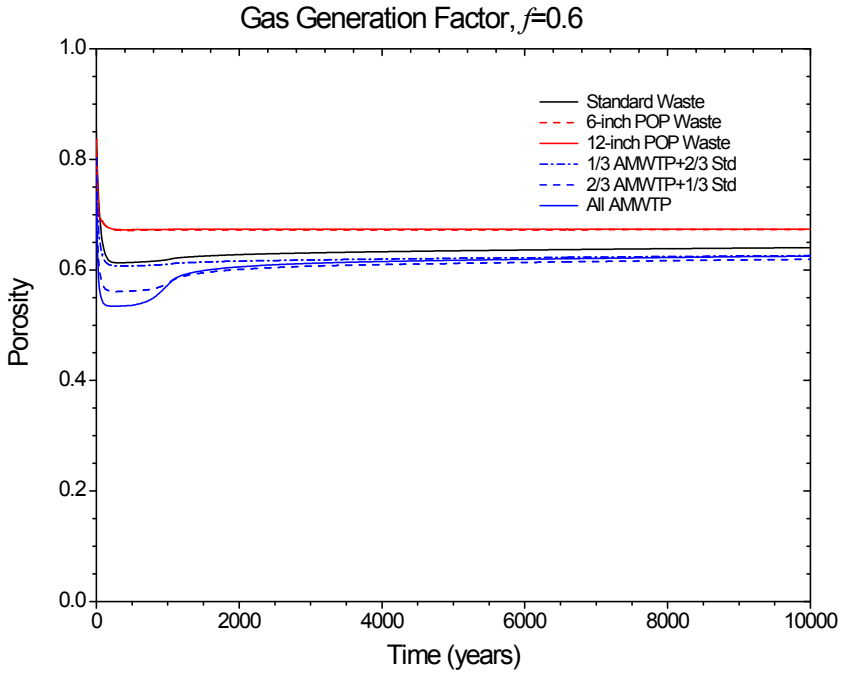
Gas Generation Factor, f=0.6
Porosity
Time (years)
Standard Waste
6-inch POP Waste
12-inch POP Waste
1/3 AMWTP+2/3 Std
2/3 AMWTP+1/3 Std
All AMWTP
0.0
0.2
0.4
0.6
0.8
1.0
0
2000
4000
6000
8000
10000

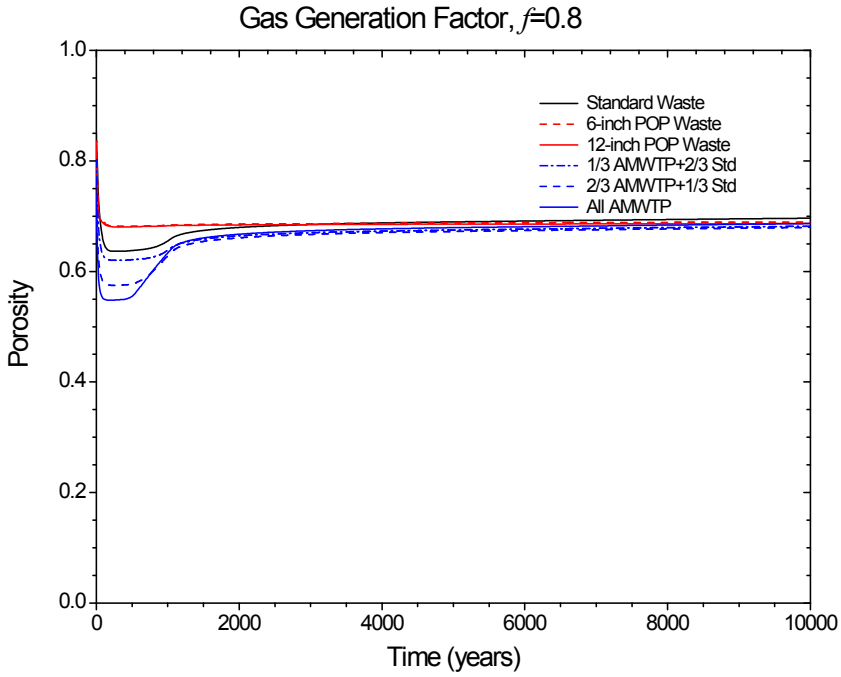
Gas Generation Factor, f=0.8
Porosity
Time (years)
Standard Waste
6-inch POP Waste
12-inch POP Waste
1/3 AMWTP+2/3 Std
2/3 AMWTP+1/3 Std
All AMWTP
0.0
0.2
0.4
0.6
0.8
1.0
0
2000
4000
6000
8000
10000

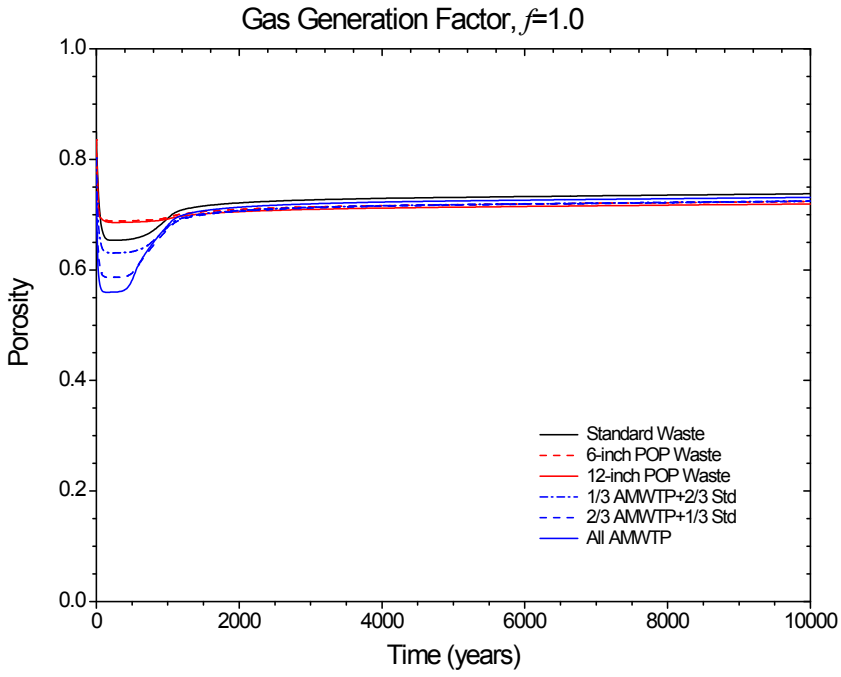
Gas Generation Factor, f=1.0
Porosity
Time (years)
Standard Waste
6-inch POP Waste
12-inch POP Waste
1/3 AMWTP+2/3 Std
2/3 AMWTP+1/3 Std
All AMWTP
0.0
0.2
0.4
0.6
0.8
1.0
0
2000
4000
6000
8000
10000

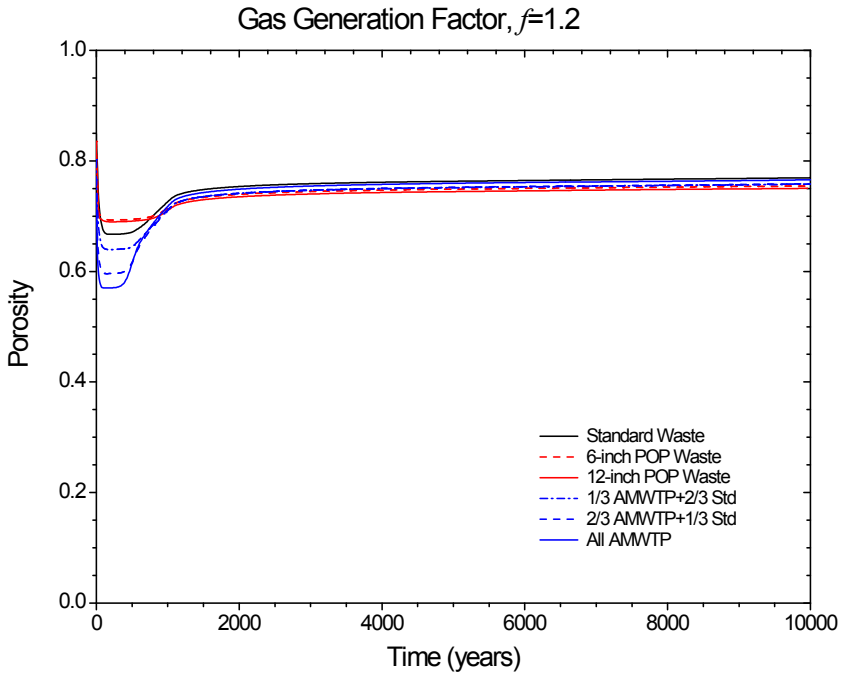
Gas Generation Factor, f=1.2
Porosity
Time (years)
1.0
0.8
0.6
0.4
0.2
0.0
0
2000
4000
6000
8000
10000
Standard Waste
6-inch POP Waste
12-inch POP Waste
1/3 AMWTP+2/3 Std
2/3 AMWTP+1/3 Std
All AMWTP

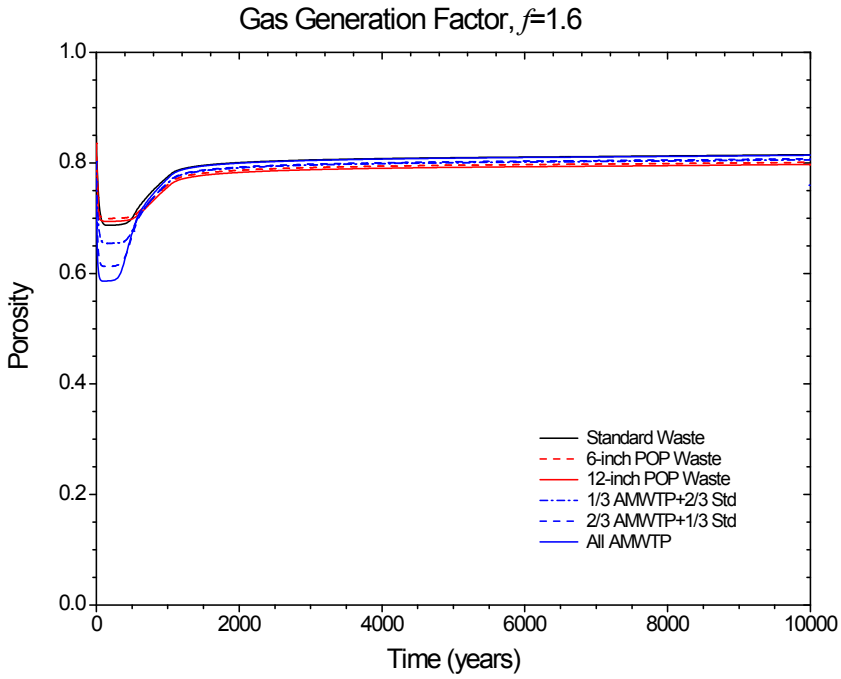
Gas Generation Factor, f=1.6
Porosity
Time (years)
1.0
0.8
0.6
0.4
0.2
0.0
0
2000
4000
6000
8000
10000
Standard Waste
6-inch POP Waste
12-inch POP Waste
1/3 AMWTP+2/3 Std
2/3 AMWTP+1/3 Std
All AMWTP

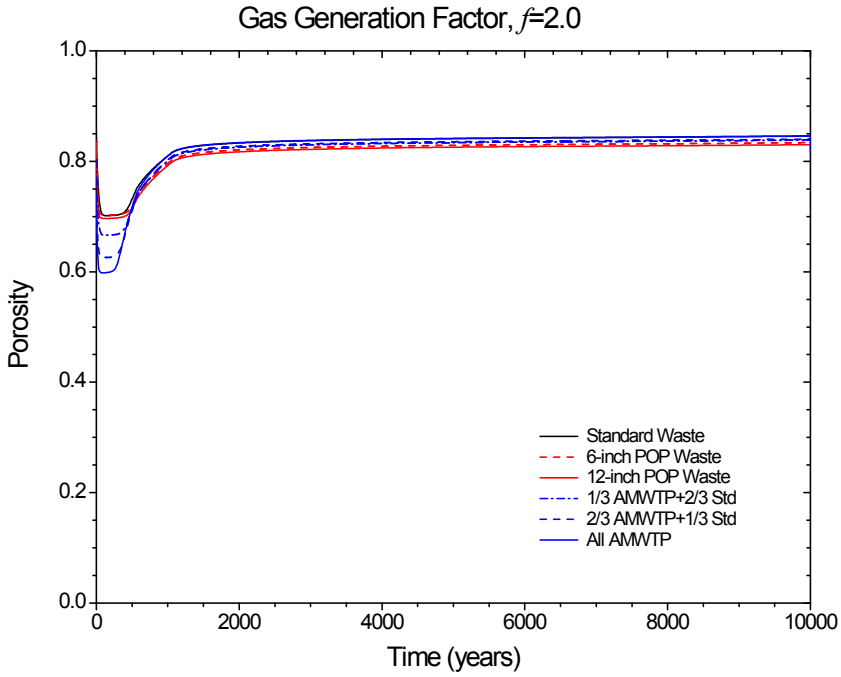
Gas Generation Factor, f=2.0
Porosity
Time (years)
1.0
0.8
0.6
0.4
0.2
0.0
0
2000
4000
6000
8000
10000
Standard Waste
6-inch POP Waste
12-inch POP Waste
1/3 AMWTP+2/3 Std
2/3 AMWTP+1/3 Std
All AMWTP

APPENDIX L: CALCULATION OF POROSITY SURFACES USED IN THE AMW PA

This information is included here for completeness and reproducibility. The porosity surfaces reported in the main body of this report represent an improvement upon earlier analyses conducted in support of the evaluation of the effects of supercompacted waste on repository performance (Hansen et al. 2003b). These improved porosity surfaces were not completed in time for inclusion in the PA reported in Hansen et al. (2003a). This appendix documents the calculation of the earlier porosity surfaces that were used in the AMW PA (2003a).

L-1 Overview

The calculation of the porosity surfaces used in Hansen et al. (2003a) and described in this appendix followed the same methodology outlined in Section 2.0 of this report. The same six configurations of waste were considered:

1. All standard waste (55-gallon drums)
2. All 6-inch POPs
3. All 12-inch POPs
4. A mix of 1/3 supercompacted waste and 2/3 standard waste
5. A mix of 2/3 supercompacted waste and 1/3 standard waste
6. All supercompacted waste

The gas generation potentials and rates, and the constitutive models for the waste were the same as described in Section 2.0 of this report. The porosity surfaces computed for configurations 1 (all standard waste), 2 (all 6-inch POPs) and 3 (all 12-inch POPs), as used in Hansen et al. (2003a) are described in Section 5.0 of this report.

However, Hansen et al. (2003a) report porosity surfaces for configuration 5 (2/3 AMWTP) and configuration 6 (all AMWTP) that differ from the results for these configurations presented in Section 5.0 of this report, because these earlier porosity surfaces were computed using a different mesh representation for the AMWTP waste. Figure L-1 illustrates these meshes in which AMWTP and standard waste were separated into columns; in the later calculations described in this report, the standard waste was placed as a shell around the AMWTP waste to better represent closure of the interstitial space between waste packages (see Figure 10). For completeness this appendix includes the earlier results for configuration 4 (1/3 AMWTP) although this porosity surface was not discussed in Hansen et al. (2003a). In addition, the total volume of the container shells (14.9 m^3) was not considered in the earlier AMWTP waste calculations described in this appendix, but was considered in the later calculations described in Section 5.0. Thus, the initial porosities of the disposal room containing AMWTP waste were slightly different as listed in Table L-1.

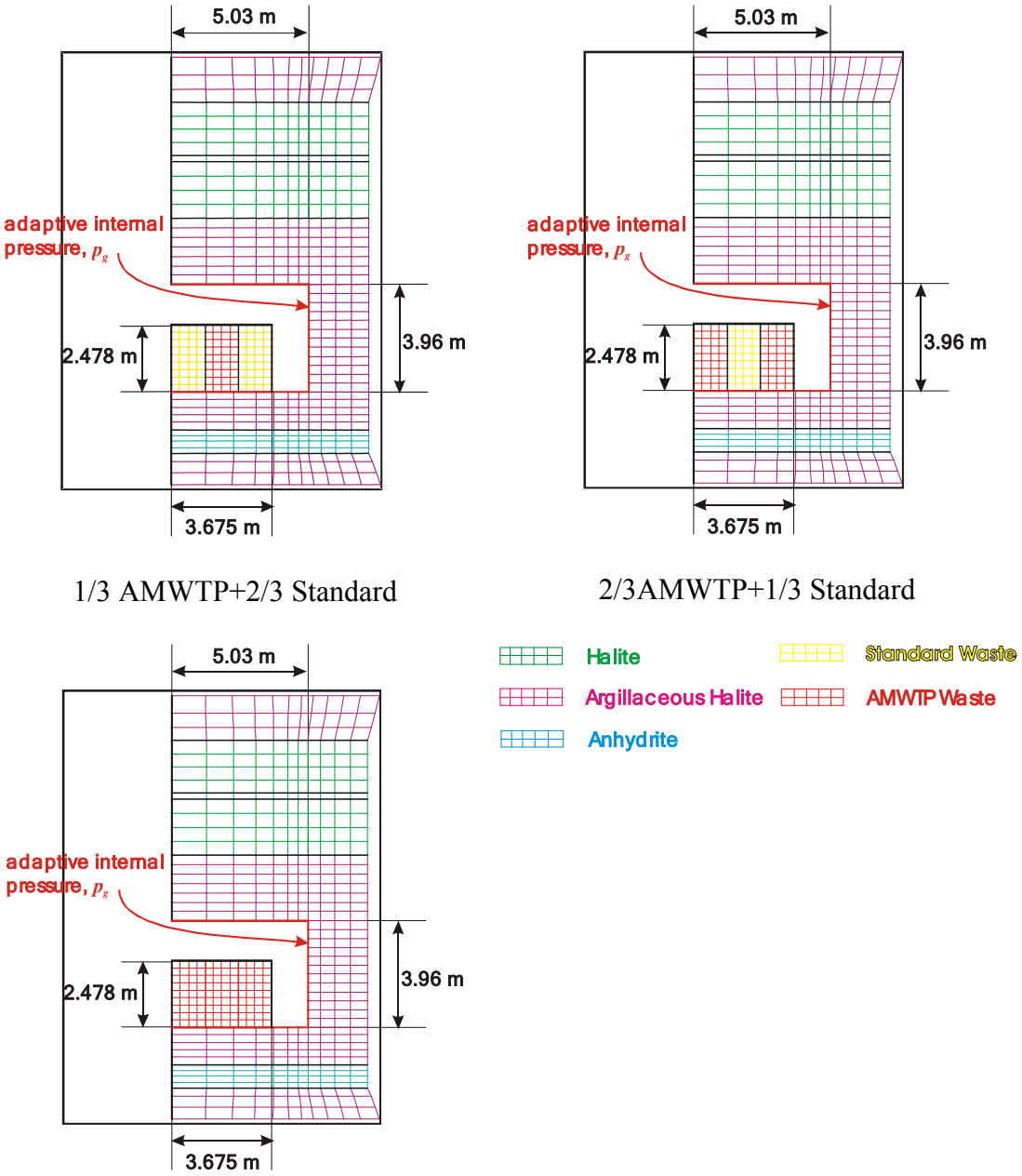

Figure L-1: Meshes for cases including AMWTP waste.

Table L-1: Initial porosities of the disposal room containing AMWTP waste.

	1/3 AMWTP	2/3 AMWTP	All AMWTP
The calculations described in App. L	0.808	0.773	0.743
The later calculations described in Section 5.0	0.802	0.766	0.739

L-2 File Naming Convention

The earlier calculations described in this appendix were conducted using the same codes and computational procedures identified in Section 4.0 of this report. The general path for any of these subdirectories is: /…/poro/. All of the files related to the analyses are existed as mentioned in Section 4. In addition, the earlier files used by Hansen et al. (2003a) are existed in the subdirectories /NoLateral/ under AMWTP waste directories, i.e. /…/poro/1puck/NoLateral/, /…/poro/2puck /NoLateral/, and /…/poro/3puck/NoLateral. All of the files that remain within each subdirectory are the same as listed and described in Table 9.

L-3 Results

Figures L-2 through L-4 illustrate room closure for configurations 4 (1/3 AMWTP), 5 (2/3 AMWTP) and 6 (all AMWTP). Note the difference in mesh representation of the AMWTP waste (compared to Figures 25, 26 and 27). Figures L-5 through L-7 show pressure histories for these three waste configurations, using the mesh representation shown in Figures L-1. The conversion from SANTOS porosity to BRAGFLO porosity is given by Equation (3). Figures L-8 through L-10 show the porosity histories for the cases involving AMWTP waste that were used in Hansen et al. (2003a).

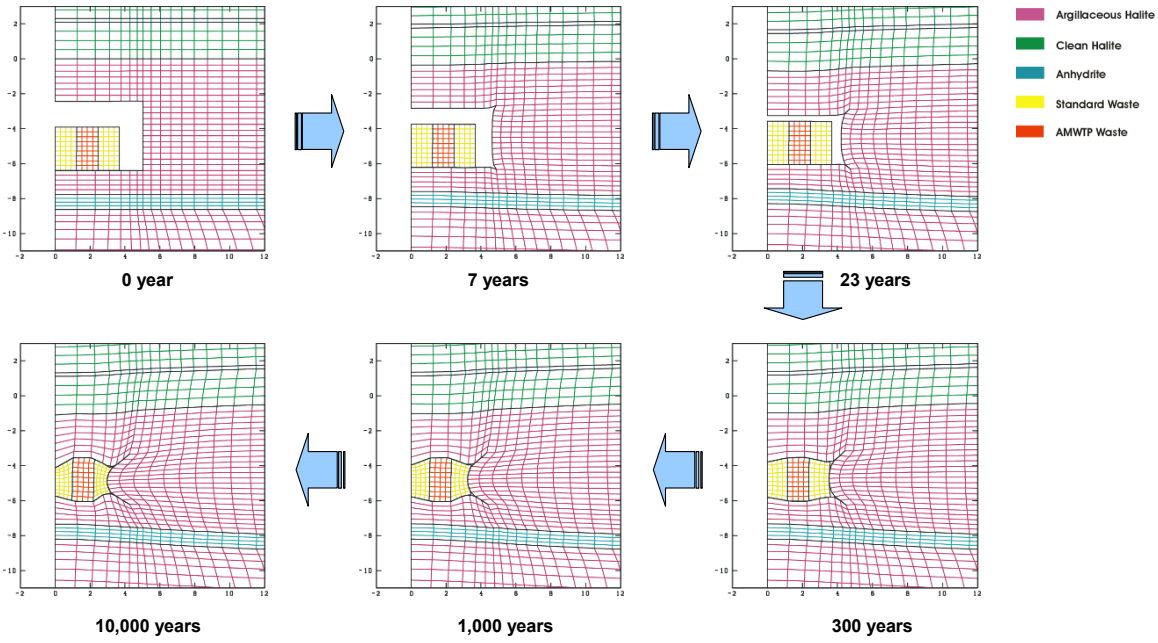

Figure L-2. Close-up view of the deformed disposal room containing the 1/3 AMWTP + 2/3 standard waste for *f*=0.0 (earlier calculations).

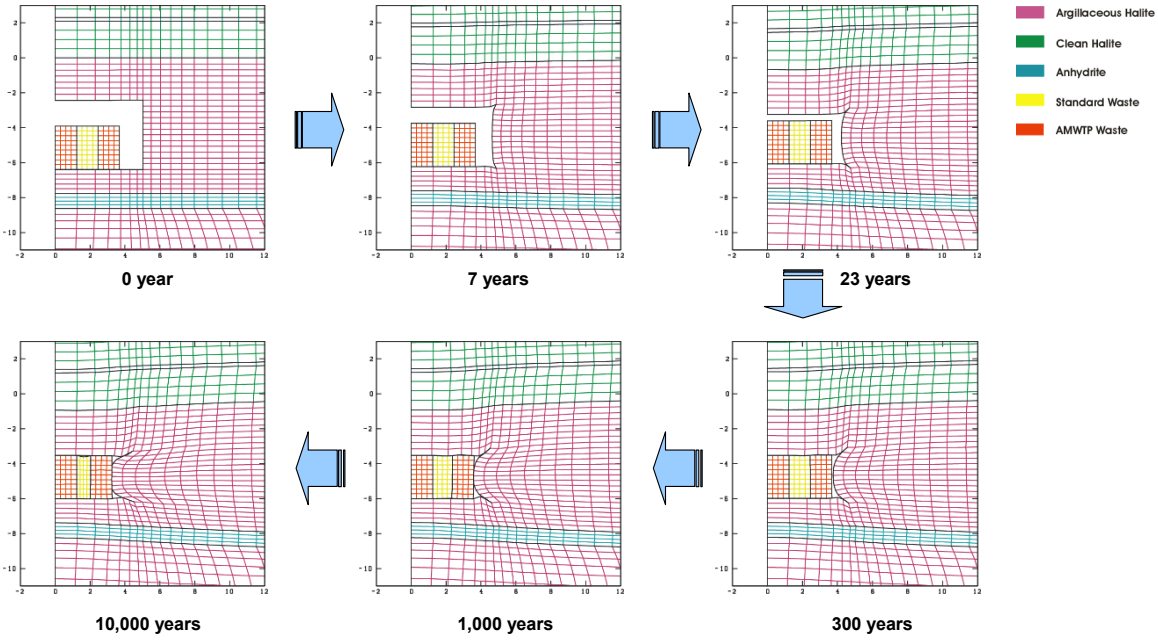

Figure L-3. Close-up view of the deformed disposal room containing the 2/3 AMWTP + 1/3 standard waste at 10,000 years for *f*=0.0 (earlier calculations).

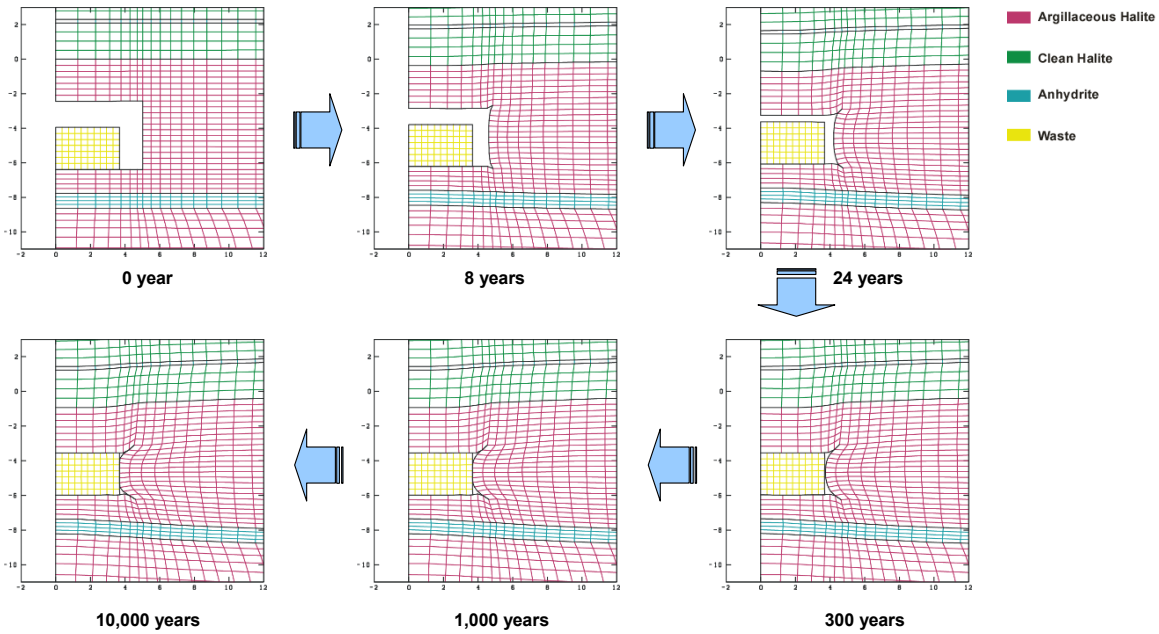

Figure L-4. Close-up view of the deformed disposal room containing all AMWTP waste for *f*=0.0 (earlier calculations).

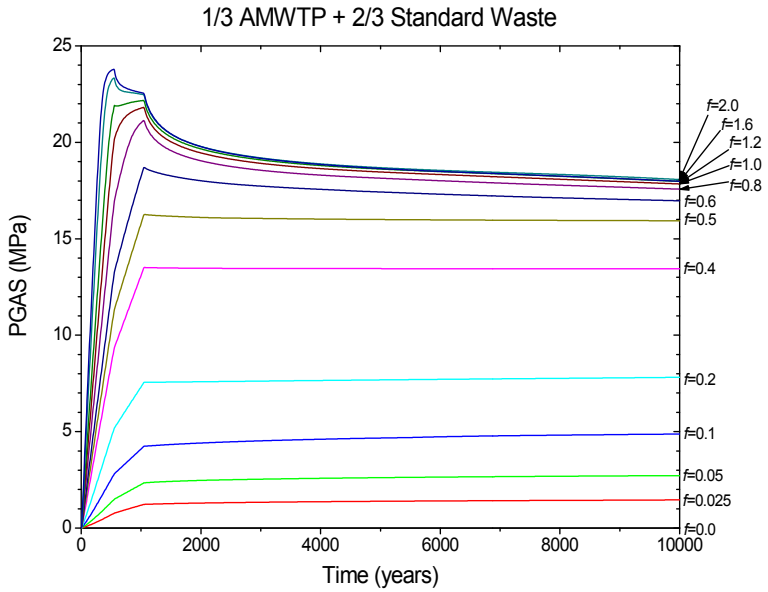

Figure L-5. Pressure histories for a disposal room containing 1/3 AMWTP + 2/3 standard waste used by Hansen et al., (2003a)

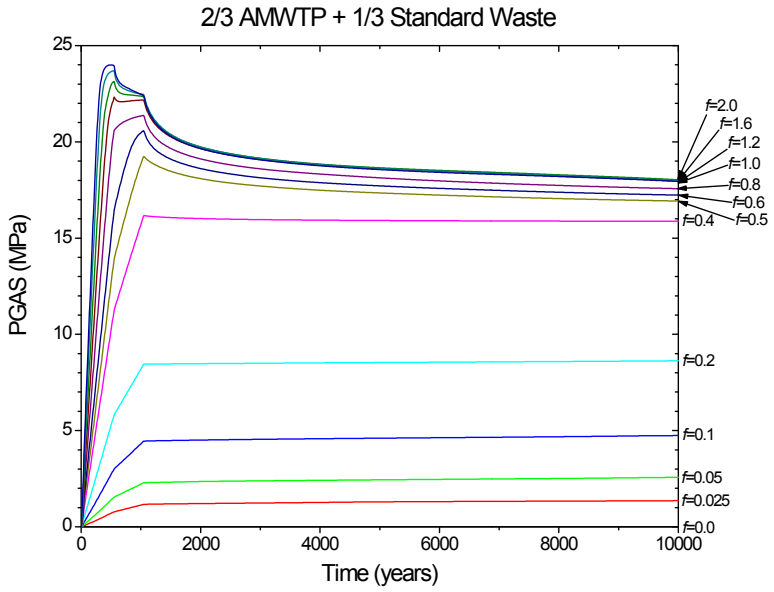

Figure L-6. Pressure histories for a disposal room containing 2/3 AMWTP + 1/3 standard waste used by Hansen et al., (2003a)

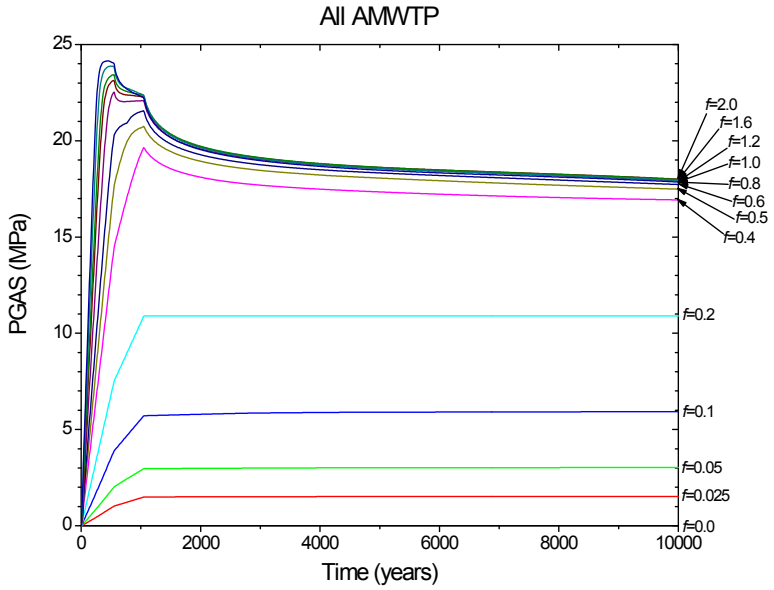

Figure L-7. Pressure histories for a disposal room containing all AMWTP waste used by Hansen et al., (2003a)

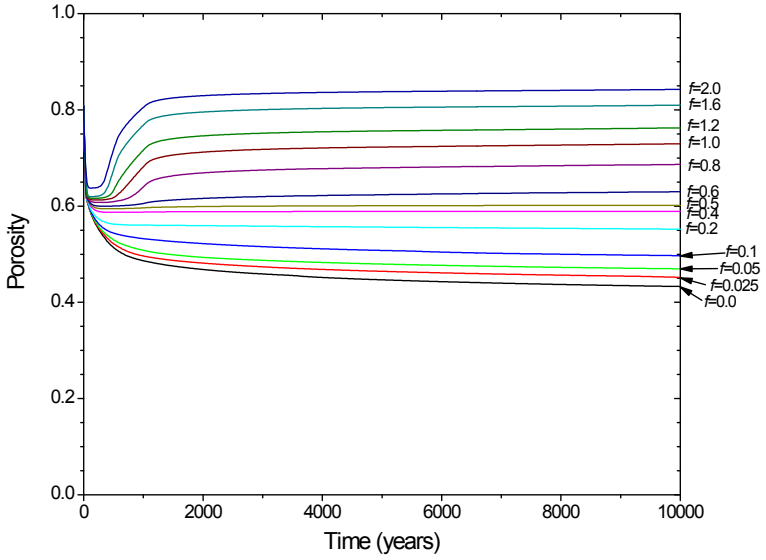

Figure L-8. Porosity histories for a disposal room containing 1/3 AMWTP + 2/3 standard waste used by Hansen et al., (2003a)

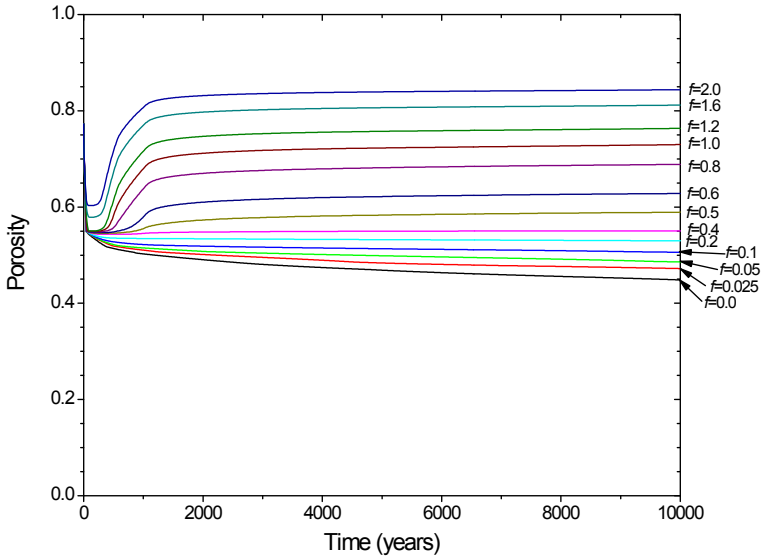

Figure L-9. Porosity histories for a disposal room containing 2/3 AMWTP + 1/3 standard waste used by Hansen et al., (2003a)

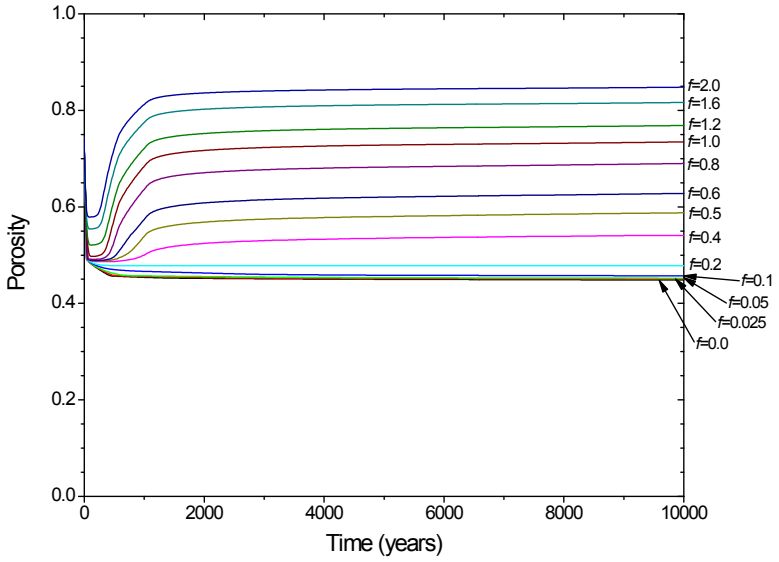

Figure L-10. Porosity histories for a disposal room containing all AMWTP waste used by Hansen et al., (2003a)

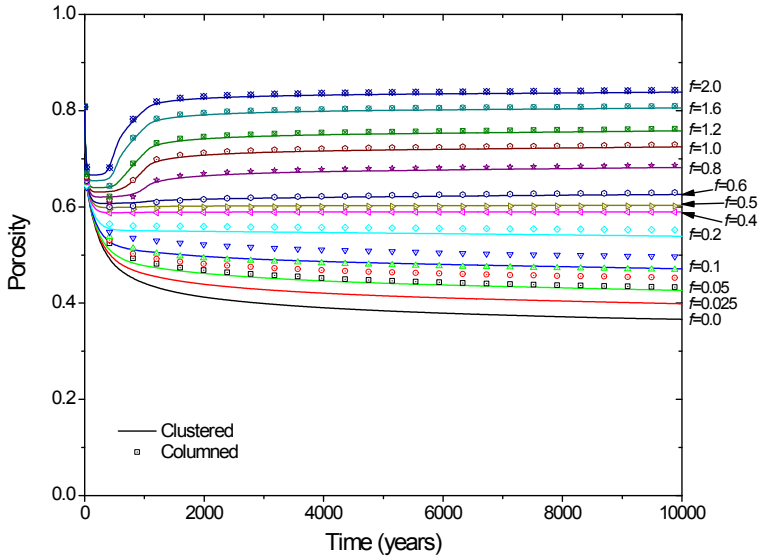

Figure L-11: Porosity histories for a disposal room containing 1/3 AMWTP + 2/3 standard waste: Solid lines are for the results from the clustered model in Section 5.3 and symbols are for the results from the columned model used by Hansen et al., (2003a)

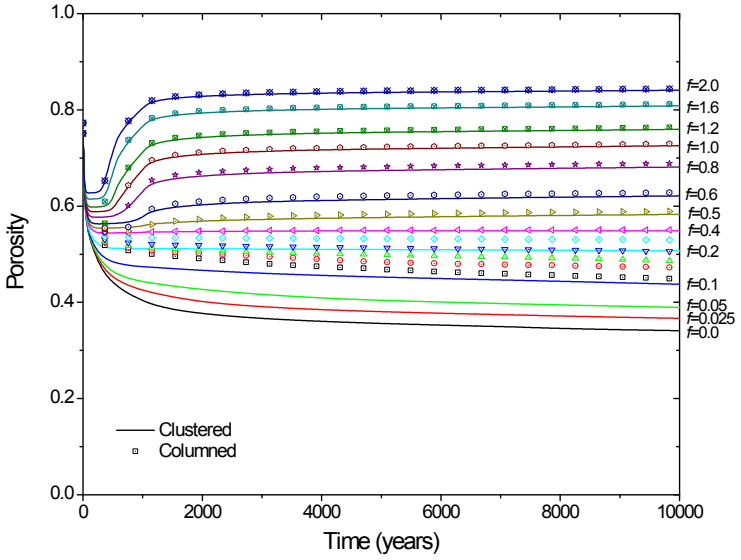

Figure L-12: Porosity histories for a disposal room containing 2/3 AMWTP + 1/3 standard waste: Solid lines are for the results from the clustered model in Section 5.3 and symbols are for the results from the columned model used by Hansen et al., (2003a)

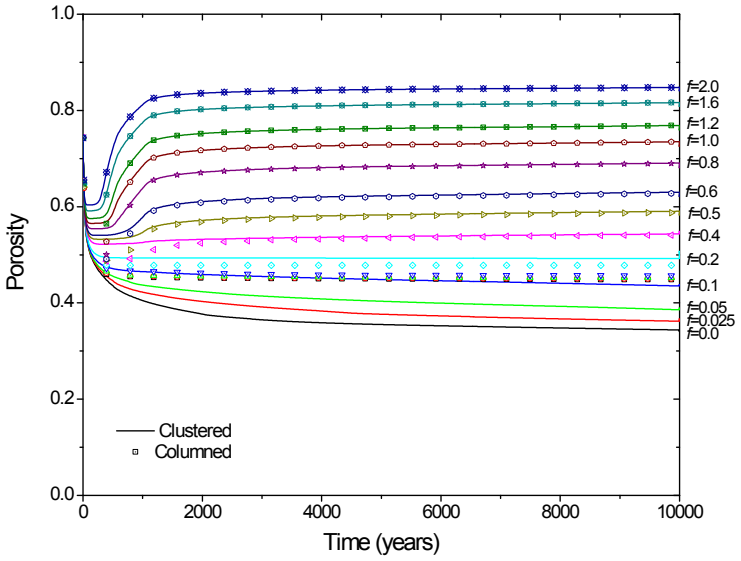

Figure L-13: Porosity histories for a disposal room containing all AMWTP waste: Solid lines are for the results from the clustered model in Section 5.3 and symbols are for the results from the columned model used by Hansen et al., (2003a)

Figures L-11 through L-13 compare the porosity histories for the earlier calculations (used by Hansen et al., 2003a) with the results of the calculations described in Section 5.3 of this report.

For the values of *f* less than 0.4, the porosities from the early calculations are higher than the porosities shown in Section 5.0, because the lateral deformation of the AMWTP waste was not considered in the earlier analyses. This is because the AMWTP wastes in those earlier calculations impede the inward movement of the wall: in other words, the AMWTP container stacks are fixed after the roof contacts the top of the stacks. In contrast, the movement of the AMWTP containers due to room closure is considered in later calculations, leading to smaller room volume and lower porosity.

For values of *f* greater than 0.4, the room is inflated by generated gas pressure, the lateral deformation of the AMWTP is less of a factor, and the porosity histories of earlier calculations are almost the same as the later calculations.

References

Hansen, C.W., L.H. Brush, M.B. Gross, F.D. Hansen, B.Y. Park, J.S. Stein and T.W. Thompson. 2003a, *Effects of Supercompacted Waste and Heterogeneous Waste Emplacement on Repository Performance*, Revision 1, ERMS#532475, Sandia National Laboratories, Carlsbad NM.

Hansen, C.W., L.H. Brush, F.D. Hansen, J.S. Stein. 2003b, *Analysis Plan for Evaluating Assumptions of Waste Homogeneity in WIPP Performance Assessment (AP-107),* Revision 1. Sandia National Laboratories, Carlsbad, NM., ERMS 531067.

NOTICE: This document was prepared as an account of work sponsored by an agency of the United States Government. Neither the United States Government nor any agency thereof, nor any of their employees, nor any of their contractors, subcontractors, or their employees, makes any warranty, express or implied, or assumes any legal liability or responsibility for the accuracy, completeness, or usefulness or any information, apparatus, product or process disclosed, or represents that its use would not infringe privately owned rights. Reference herein to any specific commercial product, process or service by trade name, trademark, manufacturer, or otherwise, does not necessarily constitute or imply its endorsement, recommendation, or favoring by the United States Government, any agency thereof or any of their contractors or subcontractors. The views and opinions expressed herein do not necessarily state or reflect those of the United States Government, any agency thereof or any of their contractors. This document was authored by Sandia Corporation under Contract No. DE-AC04-94AL85000 with the United States Department of Energy. Parties are allowed to download copies at no cost for internal use within your organization only provided that any copies made are true and accurate. Copies must include a statement acknowledging Sandia Corporation's authorship of the subject matter.

WASTE ISOLATION PILOT PLANT (WIPP)
Distribution List
(Revised 7/7/2005)

Federal Agencies

1 US Department of Energy
Office of Civilian Radioactive Waste Mgmt.
Attn: Deputy Director, RW-2
Forrestal Building
Washington, DC 20585

8 US Department of Energy
Carlsbad Field Office
Attn: P. Detwiler
C. Wu
G. Basabilvazo
S. Casey
D. Mercer
R. Nelson
R. Patterson
Mailroom
P.O. Box 3090
Carlsbad, NM 88221-3090

1 US Department of Energy
Office of Environmental Restoration and Waste Management
Attn: P. Bubar, EM-20
Forrestal Building
Washington, DC 20585-0002

1 US Department of Energy
Office of Environmental Restoration and Waste Management
Attn: Mary Bisesi/Lynne Smith, EM-23
Washington, DC 20585-0002

1 US Environmental Protection Agency
Radiation Protection Programs
Attn: B. Forinash
ANR-460
Washington, DC 20460

Boards

1 Defense Nuclear Facilities Safety Board
Attn: D. Winters
625 Indiana Ave. NW, Suite 700
Washington, DC 20004

State Agencies

1 Attorney General of New Mexico
P.O. Drawer 1508
Santa Fe, NM 87504-1508

2 Environmental Evaluation Group
Attn: Library
7007 Wyoming NE
Suite F-2
Albuquerque, NM 87109

1 NMED Hazardous Waste Bureau
WIPP Project Leader
2905 Rodeo Park Dr E., Bldg 1
Santa Fe, NM 87505-6303

1 NM Bureau of Geology & Mineral Resources
801 Leroy Place
Socorro, NM 87801

Laboratories/Corporations

1 Battelle Pacific Northwest Laboratories
Battelle Blvd.
Richland, WA 99352

1 Los Alamos National Laboratory
Attn: B. Erdal, INC-12
P.O. Box 1663
Los Alamos, NM 87544

3 Washington TRU Solutions
Attn: Library, GSA-214
P.O. Box 2078
Carlsbad, NM 88221

1 Golder Associates, Inc.
Attn: Bill Thompson
44 Union Blvd., Suite 300
Lakewood, CO 80228

1 John F. Schatz Research & Consulting
Attn: John F. Schatz
4636 South Lane
Del Mar, CA 92014

1 GRAM
Attn: Krishan Wahi
8500 Menaul Blvd., NE
Albuquerque, NM 87112

1 Mike Gross
415 Riviera Drive
San Rafael, CA 94901-1530

National Academy of Sciences
WIPP Panel

1 National Academies
Attn: Barbara Pastina
Committee on WIPP
Board on Radioactive Waste Management
500 Fifth Ave NW; Keck 634
Washington, DC 20001

Universities

1 University of New Mexico
Geology Department
Attn: Library
141 Northrop Hall
Albuquerque, NM 87131

Libraries

1 Government Information Department
Zimmerman Library
University of New Mexico
MSCO5 3020
Albuquerque, NM 87131-0001

1 New Mexico Junior College
Pannell Library
Attn: Earl Dye
5317 Lovington Highway
Hobbs, NM 88240

1 New Mexico State Library
Attn: L. Canepa
1209 Camino Carlos Rey
Santa Fe, NM 87507

1 New Mexico Tech
Joseph R. Skeen Library
801 Leroy Place
Socorro, NM 87801

Foreign Addresses

2 Francois Chenevier
ANDRA
Parc de la Croix Blanche
1-7 rue Jean Monnet
92298 Chatenay-Malabry Cedex
FRANCE

1 Commissariat a L'Energie Atomique
Attn: D. Alexandre
Centre d'Etudes de Cadarache
13108 Saint Paul Lez Durance Cedex
FRANCE

1 Bundesanstalt fur Geowissenschaften und Rohstoffe
Attn: M. Wallner
Postfach 510 153
D-30631 Hannover
GERMANY

1 Bundesministerium fur Forschung und Technologie
Postfach 200 706
5300 Bonn 2
GERMANY

1 Gesellschaft fur Anlagen und Reaktorsicherheit (GRS)
Attn: B. Baltes
Schwertnergasse 1
D-50667 Cologne
GERMANY

1 Dr.-Ing. Klaus Kuhn
TU Clausthal Institut fur Bergbau
Erzstr. 20
D-38678 Clausthal-Zellerfeld
GERMANY

1 Dr. Susumu Muraoka
Nuclear Material Control Center
Tokai-Mura, Ibaraki-Ken, 319-11
JAPAN

2 Nationale Genossenschaft furdie Lagerung Radioaktiver Abfalle
Attn: NAGRA Library
Hardstrasse 73
CH-5430 Wettingen
SWITZERLAND

1 AEA Technology
Attn: W. R. Rodwell
424-4 Harwell
Didcot, Oxfordshire OX11 OQJ
UNITED KINGDOM

1 Dr. Myung-Jae Song
Nuclear Environment Technology Institute
Korea Hydro & Nuclear Power Co., Ltd (KHNP)
150 Duckjin-dong, Yusong-ku, Taejon, 305-600, Republic of KOREA

4 Korea Atomic Energy Research Institute
Attn: Dr. Chang-kyu Park
Dr. Young-Jin Kim
Dr. Pil-Soo Hahn
Dr. Chunsoo Kim
150 Duckjin-dong, Yusong-ku, Taejon, 305-600, Republic of KOREA

1 Prof. Chang Sun Kang
Seoul National University
Shillim-dong, Kwanak-gu, Seoul, 151-742
Republic of KOREA

1 Prof. Chung In Lee
Seoul National University
School of Civil, Urban and Geosystem Engineering
Shillim-dong, Kwanak-gu, Seoul, 151-742
Republic of KOREA

1 Prof. Jooho Whang, Ph.D.
Kyung Hee University
College of Advanced Technology
Dept. of Nuclear Engineering
1, Seochun-Ri, Kihung-Eup, Yongin-City, Gyeonggi-Do, 499-701
Republic of KOREA

Internal

	MS	Org.	
1	0136	0216	M. K. Knowles
1	0372	9127	J. Jung
1	0372	9127	J. F. Holland
1	0701	6100	P. B. Davies
1	0706	6113	D. J. Borns
1	0706	6113	B. L. Ehgartner
2	0731	6034	823 Library
1	0751	6117	T. W. Pfeifle
1	0751	6117	M. Lee
1	0771	6800	D. Berry
10	0771	6853	F. D. Hansen
1	0776	6842	J. S. Stein
2	0899	9616	Technical Library
1	1395	6820	S. A. Orrell
1	1395	6821	D. Kessel
1	1395	6822	M. Rigali
1	1395	6822	L. H. Brush
8	1395	6034	WIPP Library
1	1395	6820	M. J. Chavez
1	1395	6822	C. G. Herrick
10	1395	6821	B. Y. Park
2	1395	6820	WIPP Records Center
1	9018	8945-1	Central Technical Files